Optimization of the skidded load-out process

N.L.M. Verhoef

Delft University of Technology

Sponsored by Heerema Marine Contractors

Optimization of the skidded load-out process

By

N.L.M. Verhoef

in partial fulfilment of the requirements for the degree of

Master of Science

in Offshore and dredging engineering

at the Delft University of Technology,

to be defended on 14th of June 2017

Supervisor:	Prof. dr. ir. M. Kaminski	TU Delft
Thesis committee:	Ir. M. Van Kester	HMC
	Ir. R.Bos	TU Delft
	Dr.Ir. P. Van Woerkom	TU Delft

An electronic version of this thesis is available at http://repository.tudelft.nl/.

TU Delft Delft University of Technology

Abstract

The structures which HMC installs offshore are fabricated onshore and subsequently moved onto a barge or ship, seafastened and then transported to the offshore location. The process of moving a structure from the onshore quayside to the barge or ship is called the load-out. This load-out can be performed by lifting, skidding or using a trailer (SPMT). This thesis research focused only on a skidded load-out onto a barge.

During the load-out the weight of the jacket or topside is gradually transferred from the quay to the barge. The barge gradually takes more of the load so ballast water needs to be continuously pumped or discharged depending on the location of the structure and the location of the ballast tank concerned. Improper ballasting during this process will cause the alignment between the quay and the barge to be disrupted which in turn causes peak loads in the topside or jacket and the barge. It is questioned if there are more suitable ballasting methods or a structural solution in order to lower these peak loads? It is also modeled what the effects are of quayside stiffness and the best method to model this stiffness.

Therefore a 2-D representation of the entire load-out is made. This model will be made using the finite element method, via a numerical model, in MATLAB. A base case load-out of a topside will be applied to this model. Using this model, optimizing the ballast configuration will be researched. Several different criteria for the optimization were tested and its different effects on the forces during the load-out were researched and quantified. The structural solution of relocating the skidbeams to an area of lower deck stiffness was also tested and the results studied. The effects of the quayside stiffness and modelling methods were also quantified using the 2-D MATLAB model.

The conclusion derived from the optimizations is that there are other ballast configurations which perform better in reducing the peak forces experienced during the load-out. The key to these optimizations is that they keep the barge-quay alignment as perfect as possible. If a critical element is present in the load-out the ballast configuration can be adjusted to lower the forces in this specific element. The results of the simulation in which the skidbeams were relocated show that this approach has no beneficial effects in reducing the forces during the load-out, mainly due to the presence of the transverse bulkheads in het barge. Furthermore for the modelling of the quayside it was proven that especially when using a low stiffness quayside, modelling the quayside without taking into account the foundation layer stiffness is inaccurate and can lead to lower forces in the model than which occur in reality.

Acknowledgement

For the fulfilment of my thesis I am indebted to many people. I am very thankful for the continuing support and understanding of my thesis professor, Dr. Mirek Kaminski. Because of my illness during the completion of this thesis it was hard to keep high spirits. Therefore it was nice to know I had the support of Dr. Kaminski. I would also like to thank the other members of my committee; Reinier Bos and Paul van Woerkom.

This thesis was made possible by Heerema Marine Contractors, Leiden. They made it possible for me to complete my master thesis. I would like to thank Maurice van Kester and Peter Schoenmaekers in particular. Despite the fact that it took me almost two and a half years to complete my research due to illness, HMC kept supporting me and providing me with the tools necessary. This was primarily due to the support of ir. Van Kester and ir. Schoennmaekers. I would also like to thank my fellow students at HMC which made graduating just that bit more fun, especially lunch. Thanks to all the other colleagues at HMC who helped me with the issues throughout my research.

Graduating wasn't easy for me so it was nice that I had the full support of the people close to me. Special thanks to my parents, Cor and Inge, for supporting me with my health issues and for uplifting my spirits throughout the graduating process. I would also like to thank my girlfriend, Anouk, for her continuing support and encouragement.

Table of Contents

Table of figures

1 Introduction

1.1 General introduction

This thesis is performed for Heerema Marine Contractors hereafter named HMC. HMC is a world leading marine contractor with a track-record of over 50 years of successful projects in the oil and gas industry. HMCs core business is the transportation, installation and removal of all sort of offshore structures linked to the oil and gas sector. To complete these projects HMC owns some of the world's biggest semi-submersible crane vessels. The SSCVs Thialf and Hermod and the DCV Balder. These vessels have very large deck areas and unique capacities in heavy lifting and motion behaviour which has earned HMC a superior reputation when it comes to station keeping and workability. In recent years HMC has also become a big player in the instalment of subsea pipelines and subsea structures reaching ultra-deep water depths. Especially since the addition of the deep-water construction vessel, the Aegir, this monohull vessel can install subsea pipelines and perform complex infrastructure projects in ultra-deep water. Besides these vessels HMC operates several supporting barges. Some are only suitable as cargo barges but HMC also owns several launch barges (for launching a jacket offshore) and float-over barges (for placing the topside onto the jacket offshore). These barges are involved in a lot of HMC projects. One of these barges, the H-851 barge , will return in more depth later on in this thesis.

The installation of almost all bottom founded offshore production platforms occurs in the same 2 steps. These two steps are the installation of the substructure, which carries the weight of the topside, and the installation of the topside, which houses the production capabilities and the personnel. See Figure 1-1 for the distinction between topside and substructure.

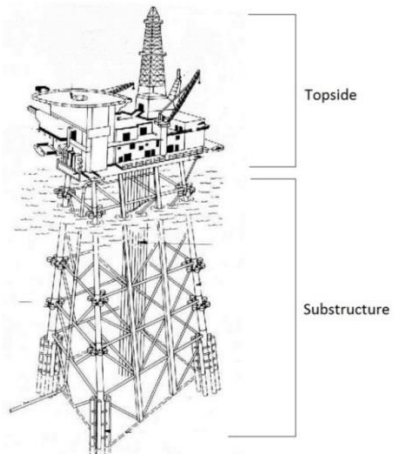

Figure 1-1 Topside and Substructure

Often the topside and the substructure are transported to the offshore location by barge. For this to be possible the topside as well as the substructure first needs to be transported from the onshore production facility or yard onto the barge. This process is called the load-out and will be topic of this thesis.

The load-out process is more complex than simply sliding it off the quay onto the barge. Since most structures in the offshore industry are of a very large scale and weight, the weight of the structure to be transported will affect the draft, structural integrity of the barge and the stability of the barge.

Once arrived at the offshore location the substructure can be slid of the barge by ballasting the barge in such a way that the angle which the barge makes with the sea level is sufficient enough for the interface between substructure and barge to overcome the friction force. Once the substructure is floating in the water it can then be upended by an SSCV and placed on the ocean floor.

In case of a topside, it can be lifted onto the substructure at the offshore location by an SSCV or, and this is the case for more heavy topsides, it is placed onto the substructure by the float-over method. This method enthrals ballasting the barge with the topside on it between the substructure legs gradually transferring the load from barge to substructure.

1.2 Problem statement

The structures which HMC installs are fabricated onshore and subsequently loaded-out onto a barge, seafastened and then transported to the offshore location. The load-out can be performed by lifting, skidding or using a trailer (SPMT) however this research will only focus on a skidded load-out. Transferring a topside from the quay to the barge poses several problems. During the load-out the weight of the jacket or topside is gradually transferred from the quay to the barge. The barge gradually takes more of the load so ballast water needs to be continuously pumped or discharged depending on the location of the structure and the location of the ballast tank concerned.

Improper ballasting during this process will cause the alignment between the quay and the barge to be disrupted. Misalignment of the barge and the quay in turn can cause peak loads in the barge and via the skidbox and the deck support frame throughout the entire topside. These peak loads during the load-out can overstress certain elements of the barge and the topside plus the skidbox and it is imperative therefore that the loads which occur during the load-out are reduced as much as possible be it either by adjusting the ballasting methods or by using a structural solution.

How the weight of the topside during the load-out is exactly distributed also is dependent on the quayside stiffness. There is a need to know what the effects are of the quayside stiffness on the loads exerted on the barge and topside during the load-out. The effects of the quayside stiffness on the earlier mentioned methods to reduce the loads also need to be modelled.

1.3 Thesis approach

The approach taken in this thesis in order to attack the problems stated in the problem statement is as follows. First a 2-D representational model of the entire load-out process will be constructed. This model will be made using the finite element method in the software program called MATLAB. Every element which is off influence to the load-out shall be modelled. The quay, barge and topside including the skidbox and deck support frame shall be modelled by using Timoshenko beam elements. The model is then applied to a base case scenario of a topside load-out. The properties such as stiffness and weights of all structures are loaded into the model from external sources. The entire load-out shall be modelled using 113 steps from the topside being fully on the quay until its final position on the barge. The model can't be verified with a real world situation so in order to verify its results the results of an extensive 3-d model of a load-out are used.

Using the model for the base case scenario, several options are undertaken in order to see how the peak forces during the load-out can be reduced. The forces will first be optimized by creating new ballasting methods with the help of the model. Several of these methods will be proposed each with different criteria for optimization. The effects of these new optimizations on the barge and topside structures will be compared with the standard ballast configuration and with each other.

Structural optimizations which hope to achieve the same goal as the ballast optimizations are also tested using the MATLAB model. The effect of these structural changes will also be monitored and compared to the original structural configuration.

The influence of uncertainties in quayside stiffness and its effects on the loads during the load-out will also be monitored. The effects this has on the optimizations are yet unknown and also need to be accounted for.

1.4 Structure of this report

In chapter 1 a general introduction to this thesis report is given. The problem statement and thesis objective was given. The structure of the report is also given in this chapter.

In chapter 2 a step back is taken. The process of the load-out is looked at as a whole. All the facets of the load-out will be looked at in this chapter. A look is also taken at the various ways a structure can be loaded-out onto a transport barge and the applicability and benefits of each method.

Chapter 3 will give a detailed description of the base case load-out used in this research. A description of the Heerema barge H-851 will be given. This is HMCs biggest load-out barge. It has been used successfully in the past for various projects. The H-851 is used for the heaviest structures so the load-outs in which this barge is involved are the most critical and challenging load-outs. The structural details of the barge which are relevant for the model will be given. This especially means the location and capacity of the longitudinal bulkheads as well as the transverse web frames. The location and size of the ballast tanks will also be presented as well as the capacity of the pumps. The Wheatstone topside and its aspects will also be presented in this chapter.

In chapter 4 the core of this thesis report Since the load-out process has been described and the structural details of the barge involved are known, the model can be made using MATLAB. This is done in chapter 4. In this chapter a detailed description of the MATLAB model is given. Furthermore the theoretical background of the model will be extensively explained in this chapter. At the end of this chapter verification of the model is given.

In chapter 5 the model will be used to investigate new ballasting configurations. The goal of these new configurations will be to reduce the forces exerted on the barge and topside during the load-out. Several optimizations will be presented each having different base criteria. The results of these optimizations shall be compared with each other and with the standard ballast configuration used in the base case.

Chapter 6 will be a continuation of the same goals as which were set in chapter 5. Reducing the loads on the topside and on the barge. However in this chapter the possibilities of another method to reach this goal are researched. The main question is, is there a structural solution which reduces the loads during the load-out? Relocating the skidbeam in order to make the connection between skidbox and barge less stiff might be this solution. These effects are researched in chapter 6.

In chapter 7 the effects of the quayside stiffness on the displacements and forces of/on the topside, skidboxes and barge will be researched. These effects aren't properly quantified yet and with the help of the MATLAB model this will be achieved.

Finally in chapter 8 we will talk about the conclusions which can be drawn from this thesis research Also recommendations for future research is given as well in chapter 9 for future load-outs. Possible improvements to the MATLAB model will also be discussed.

2 Load-out procedure

As mentioned earlier this thesis focuses on the load-out procedure. In this chapter a look shall be taken at the various load-out possibilities and methods. A more in depth look will be taken at the skidded load-out since this method is the focus of this thesis.

2.1 Alternative Load-out methods

A load-out can be performed in multiple ways. First 2 distinctly different methods are looked at. These are a lifted load-out and a trailered load-out. All two of these methods pose different challenges and offer different solutions. The focus of this thesis lies mainly with the skidded load-out. The lifted load-out and trailered load-out will only briefly be looked at but will not be incorporated into the model.

2.1.1 Lifted load-out

With this method cranes positioned on the quayside or cranes positioned on the barge or ship itself will lift the structure to be loaded-out and place it onto the transportation barge or ship as can be seen in Figure 2-1.

Figure 2-1 Lifted load-out

This method can only be used for structures with a low weight or is used for structures which are cut up in several pieces and which are then assembled offshore. This method of load-out poses different challenges compared to the other two methods. For example a failure in the cables of the lifting crane can have enormous consequences. This is can result in a complete loss of the structure and in case of a floating crane also of this crane. The ballasting procedure in this method is also completely different.

There is no need any more for the barge to be aligned with the quayside. The barge will however take the full load in a shorter time span since the full structure is placed on it at once contrary to the other methods where the structure gradually moves onto the barge. . In the case where the cranes are on the barge or ship itself a big roll moment is exerted on the ship, which needs to be countered by the ballast configuration. Cable failure in this situation would cause the ship to roll to the other side due to the loss of load on the quay side. Usually buoyancy cans are attached to the other side of the ship in order to counter this event.

This method isn't used for large offshore structures like a single topside although for smaller objects this method is a proved and successful method for load-outs.

2.1.2 Trailered load-out

A trailered load-out is a load-out method by which the structure is placed onto a platform vehicle with a large array of wheels. Almost always, the trailers used are so called self-propelled modular transporters or for short SPMT. These SPMTs have a grid of several computer controlled wheels, each individually controlled. Each wheel is also adjustable in ride height via a cylinder attached to each wheel. This allows for the platform on which the structure is positioned to remain flat which allows an evenly weight distribution even when moving on an unevenly train. For example the "step" between the quayside and a barge during a load-out.

The trailered load-out is used very often in the offshore industry. It is a method which can be easily scaled up for larger constructions just by using more SPMTs. In Figure 2-2 the load-out of a petrochemical module with the help of SPMTs can be seen.

Figure 2-2 Trailered load-out

Though the trailered load-out is often used in the offshore industry to transport large structures from quay to barge it has its limitations up to a certain weight class. The very high weight topsides aren't suited for a SPMT load-out. These require a different method. In these cases a skidded load-out is used which is the topic of this thesis research.

2.2 Skidded load-out

For structures in the very high weight range (+ 25000mT) the skidded load-out is the preferred method. With a skidded load-out the structure is placed on skidshoes or a skidbox. Usually jackets are placed on skidshoes and a topside is placed on a skidbox, which is a long box shaped beam which transfers the weight from the DSF to the barge and quay. This box shape, usually there are two, is skidded from the quay onto the barge over so called skidbeams, seen in Figure 2-3. These skidbeams introduce the forces into the barge in an appropriate way not damaging the deck. Since the skidded load-out involves overcoming a lot of friction the skidbeam is lined with Teflon plating in order to reduce the friction coefficient. These Teflon plates can be seen in Figure 2-3 on the right. Usually extra grease is added to reduce the friction coefficient even further.

Figure 2-3 Skidbeams on a barge

The pulling power generated to move a 40.000mT construction against the friction comes from hydraulic strand jacks. These strand jacks are attached to the front of the skidbox, as can be seen in Figure 2-4. Steel cables which run through these strand jacks run towards the bow of the barge where they are attached to the so called deadman anchor. This anchor, seen in Figure 2-5 is fixed firmly to the deck of the barge. The steel cables are first tensioned to see whether or not all cables receive the same amount of tension.

Figure 2-4 Strand jack attachment front skidbox

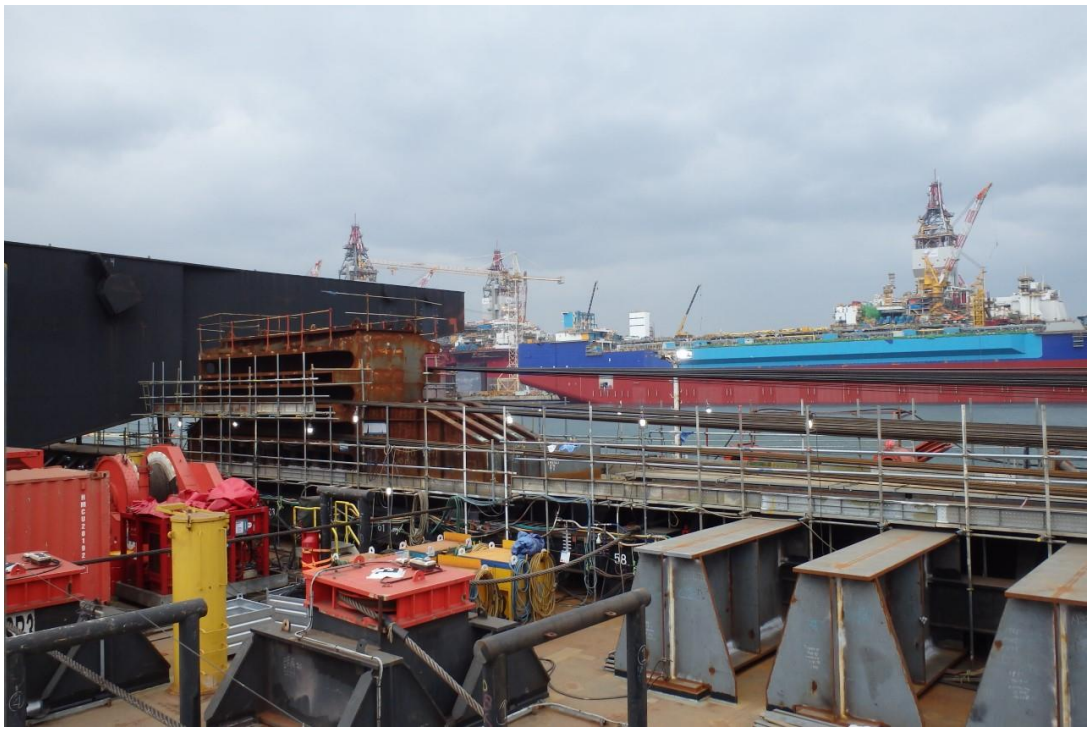

Figure 2-5 Deadman anchor

Once the barge has been cleared of any obstacles the skidding can commence. The strand jacks at the front of the skidbox start pulling the cable through the strand jacks towards the back. Like a rope climber the topside slowly starts to move onto the barge. Meanwhile the ballast has to be constantly monitored by an operator. This is done via a computer keeping a close watch to the barge heel and trim. As the topside inches towards the final destination on the barge, ballast water has to constantly discharged via discharge pipes, seen in Figure 2-6, in order to keep the draft of the barge stable

Figure 2-6 Ballast discharge pipes

When the topside arrives on its final position on the barge, preparations have to be taken to prepare it for transportation to the offshore location. The topside is fixed into positions and other constructions are welded into place.

3 Base Case scenario

In this chapter the base case to which the load-out model will be applied is described. The context in which this operation is carried out will also be explained. The tested load-out will be a load-out which was performed at the DSME yard in Okpo, South Korea.

3.1 Base case field

The base case field will be the Wheatstone development. The Wheatstone development consists of the Wheatstone and WA-16R/17R (Iago) offshore gas fields. Production from these fields is transported to a Central Processing platform where the gas is dehydrated and the condensate dewatered, from there it is transported through a pipeline to an onshore LNG plant in Western Australia. The field is located on the north western shelf offshore Western Australia in 70m to 80m of water depth. The operator of the field is Chevron Australia Pty Ltd.

Daewoo Shipbuilding and Marine Engineering (DSME) have awarded HMC with the contract to install and transport the Steel gravity structure and the topside. The topside was fabricated at the DSME yard in Okpo, South Korea and after the load-out which will be analyzed in this report, transported to Western Australia on the HMC barge H-851.The offshore installation of the topside was done by float-over in the 4th quarter of 2014. The H-851 was maneuvered between the SGS columns and by deballasting the barge to a lower draft the topside was placed on the SGS.

3.2 HMC barge H-851

The load-out at the DSME yard in Okpo is performed onto the HMC barge H-851. This barge plays a major role in this report since it is the only barge to which the model will be applied.

3.2.1 H-851 history and function

The H-851 launch barge was built by Daewoo shipbuilding and Heavy Machinery in South-Korea. It was designed and built for HMC. The barge is named after its length, being 851 feet. The barge was launched on 25th of July 1987. At the time of its launch it was the largest barge in the world and it remains till this day.

The first project for which the barge was used was the transportation and launch of the Bullwinkle jacket in 1988. This was a record breaking project. It was installed at a water depth of 412 meter and with a weight of 49375 mT it still is the heaviest jacket in the world.

Figure 3-1 Bullwinkle on H-851 at Corpus Christi

After the Bullwinkle launch the H-851 was used on various other jacket launches. It was also used for the dismantling of the Brent Spar. It has also launched several compliant towers. The H-851 was initially built as a launch barge. The tilting beams at the aft of the barge are a testimony to this.

However in 2011 HMC decided it wanted to expand the functions of the H-851. Rising sea level and increasing awareness of environmental risks caused designers to increase the required platform air gap. Increasing air gaps and increasing topsides weight required larger barges for transport and installation. So a large barge with ample stability and a large deck would fulfill these needs. HMC decided to use the H-851 for the float-over operation of North Rankin B. This 23600mT topside with an air gap of 28 meter required a barge with the dimensions of the H-851. The large width of the H-851 makes it perfect for transportation however the barge needed to be sufficiently narrow to fit into the jacket slot. The barge was therefore modified with the following set of goals: optimizing float-over capability, maximizing the launch and transport capacity and minimizing the effect on tow speed and behavior. The first 100 meters were made narrower from 63 meter to 42 meters in width. Now smaller topsides can be position on the narrow bow for installation at jackets with smaller slots. The narrowing of the barge led to a minor reduction in transport and launch capacity but it was concluded that the pros outweighed the cons.

The new modified H-851has the following capabilities:

- Install ultra-heavy weight topsides of at least 23,600mT with its center of gravity 50mabove the barge keel, while being exposed to transport wave heights of Hs = 8.5m.
- Install topsides up to 30,000mT
- Launch and transport large jackets over 35,000mT.
- Transport multiple facilities at the same, saving the multiple transports to remote areas.
- Carry huge amount of installation equipment on its large deck area.
- Reach transit speeds between 6-8 knots.

The H-851 can transport ultra-heavy weight structure with a high center of gravity due to its sheer size which causes to have sufficient stability during transport. It also has sufficient margin for any future increases in weight or in the center of gravity height of the topside of a project. The use of a large barge is also useful not only during transport but also for the installation. A lot of float-overs are tide dependent due to the limits in barge depth which can limit the window of installation due to not having enough freeboard after load-transfer. The H-851 with its depth of 15 meters won't encounter this problem.

The deck of a barge which is performing a float-over operation can be very crowded with equipment. Another advantage of the H-851 is the very large deck space. The experience from float-over operations is that sufficient deck space is required for the complex mooring systems. During the float-over mooring wires are connected to the substructure to minimize the loads on the substructure.

The aft of the H-851 is built very strong due to the forces which are exerted upon it during a jacket launch.

A problem during load-out with the H-851 is the huge tilting beam at the stern. The solution to this is that the rocker arms are removed and in its place infill pieces are placed. They fill the gap between the skidbeams at the level side of the barge and the skidbeams at the quayside. So for every load-out of a topside the rocker beams have to be cut off and infill pieces are welded into place.

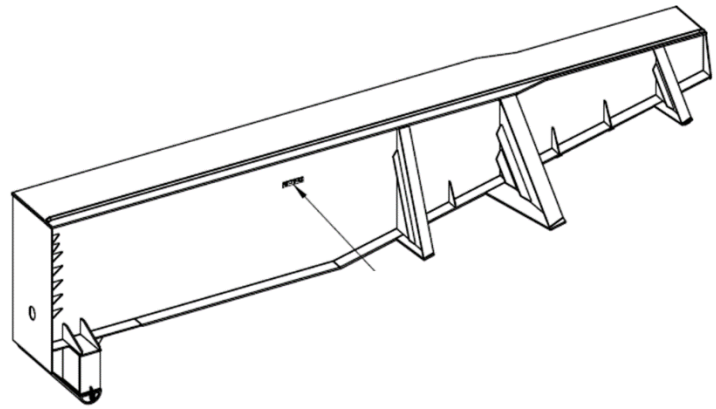

Figure 3-2 Infill pieces

The general dimensions of the barge can be seen in Figure 3-3. Here the tilting beams can be seen on the top left whilst they are still in place. During the load-out they are removed. It can also be seen that the bow of the H-851 is narrower than the stern making it ideal for float-over operations at narrower jacket slots.

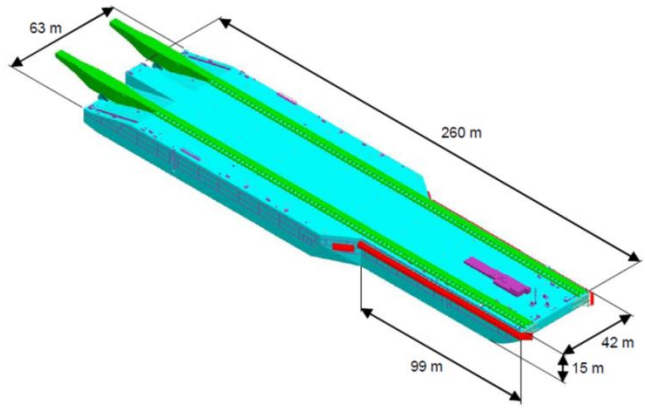

Figure 3-3 General dimensions H-851

3.2.2 HMC barge H-851 weight

An important aspect of the barge in order to model its behavior is the weight distribution of the barge. The basic weight of the barge without any project specific material on it is known to be 35081 mT. The weight of the project material is also known and so is its location. The tilting beams are also included because in this project the tilting beams are also transported together with the topside. In Table 3-1 an overview is given on how much the major weight components contribute to the total weight. As can be seen the project specific material weight totals 10519 mT so it is an important factor to take into account. This will be used in the model described in chapter 4.

Table 3-1 Weight overview of H-851 during Wheatstone load-out

Item	Weight	C.o.G.		
	(mT)	X (m)	Y (m)	Z (m)
H-851	35081	142.89	0.07	8.14
Skid beams	2352	115.53	0.00	16.19
Diesel Oil Storage tank	117	32.43	-2.70	2.09
Fresh water tank	463	18.75	-15.75	11.25
New Fuel Oil tank	440	31.88	-14.33	11.25
Rubber sway fenders	880	61.25	0.00	12.00
Float-over equipment	2629	131.20	-0.40	15.60
Infill Piece (Stern wedge) SB	420	248.09	-16.80	14.16
Infill Piece (Stern wedge) PS	420	248.09	16.80	14.16
Tilting Beams	2798	88.75	0.00	20.00
Total (excl. Bilge)	**45600**	**135.23**	**-0.29**	9.95

3.2.3 Barge longitudinal strength

The second important property of the barge is its stiffness. As was mentioned earlier, the model, which will be described in chapter B, will be a 2-D representation of the load-out seen from the side of the barge (perpendicular to the length direction of the barge). Therefore to exactly know the longitudinal stiffness of the barge is paramount to get accurate results. The barge is divided into 105 sections with a length of 2.5 meters for all sections except the first and the last which are 1.25 meters in length. This is chosen because as can be seen in Figure 3-4 the barge has 106 web frames and each web frame divides the barge into a section with a different profile and thus a different strength.

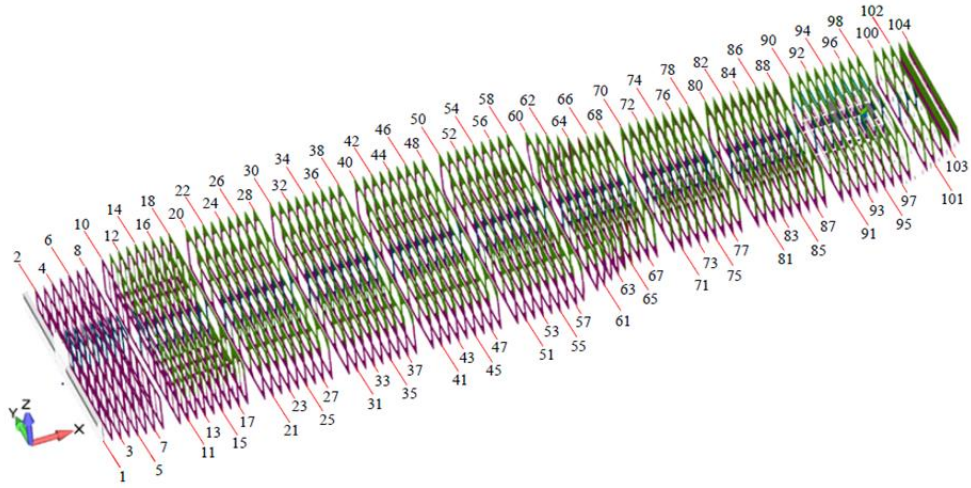

Figure 3-4 Web frame numbering in the barge

Although the web frames are taken as to decide how to divide the barge, they aren't important for the longitudinal strength of the barge. The web frames are simply too narrow to really contribute significantly to the longitudinal strength. Their function is mainly to withstand torsional forces around the x-axes.

In calculating the longitudinal stiffness of the barge a look is only taken at the major structural components which contribute to the longitudinal stiffness. The effects of other components in the barge such as piping are neglected. Also holes in the plating for piping and ballast flow are neglected.

The major structural components can be divided into two classes: plating and stiffening. The major plating forms the outsides of the barge, so the deck, bottom and side shells. Other important major plating are the longitudinal bulkheads inside the barge which can be seen in Figure 3-5. From these bulkheads the barge gains a significant portion of its longitudinal stiffness. From the figure one can also see that the stern of the bow is relatively stiff despite the fact that it is less deep.

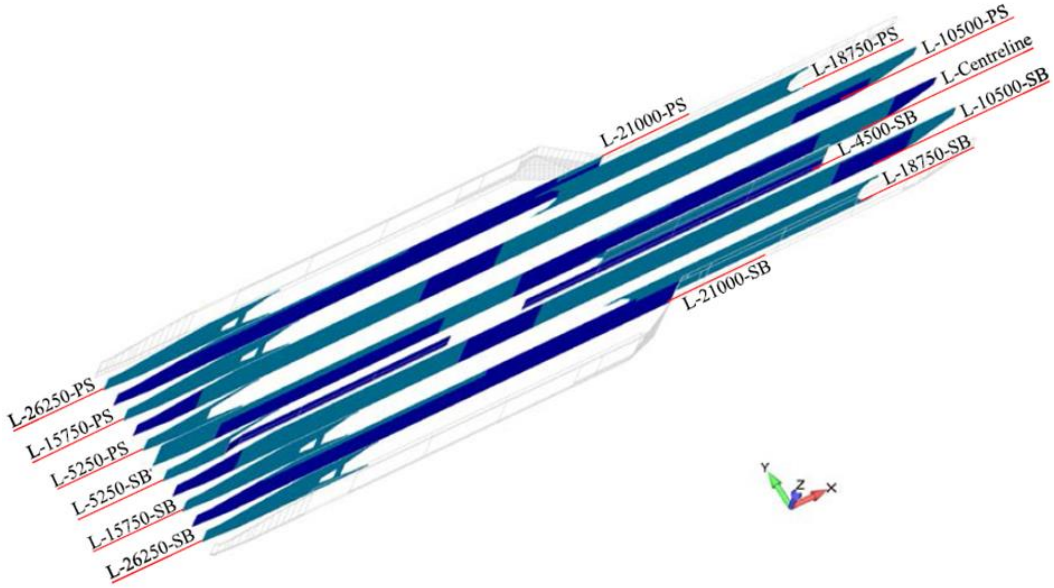

Figure 3-5 Longitudinal Bulkheads

Stiffening is also added at the deck and the bottom and also contributes to the longitudinal strength of the barge. Below the calculation for one section of the barge is given as an example of the method used for all sections of the barge.

The method of calculating the longitudinal stiffness per section is using simple structural mechanics. In Figure 3-6 a schematized version of a barge section is given. In it one can see the side shells (ss), the deck, the bottom plate and the longitudinal bulkheads (lbh), all parts are considered to be rectangular.

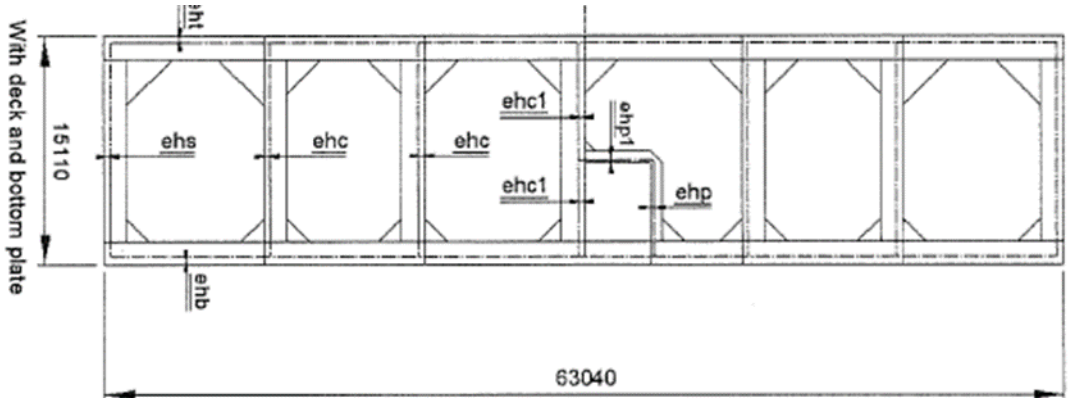

Figure 3-6 Schematized version of barge cross section

Then the moment of inertia of each part is calculated plus adding Steiner's rule

Equation 3-1

$$I_z = \frac{1}{12} bh^3 + A * a^2$$

In which *b* is the width, *h* the height and *a* the distance in the vertical plane from the c.o.g. of the part to the c.o.g. of the entire section. There are 72 stiffeners on the deck and bottom plates at the stern section of the barge and 54 at the bow section of the barge. These also need to be added to the total moment of inertia of each section.

This has been done for all sections, giving the longitudinal strength over the barge. The resulting maximum allowable bending moment and shear force can be seen in Figure 3-7 and Figure 3-8.

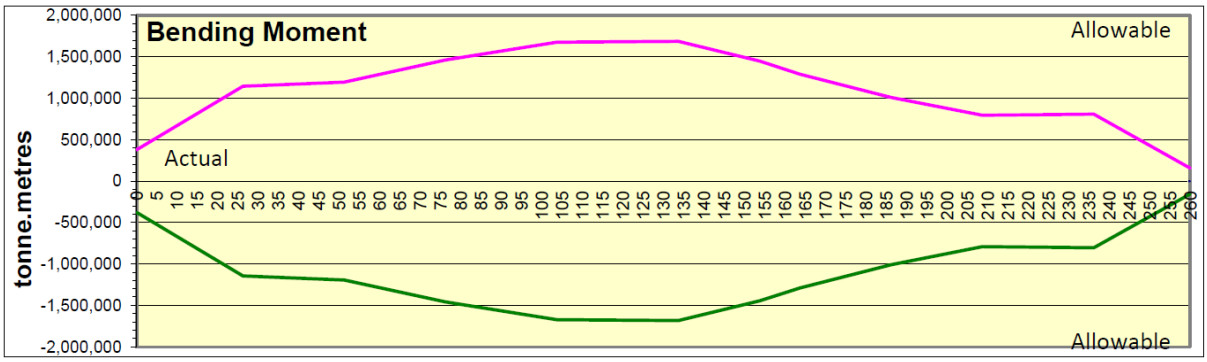

Figure 3-7 Maximum bending moment

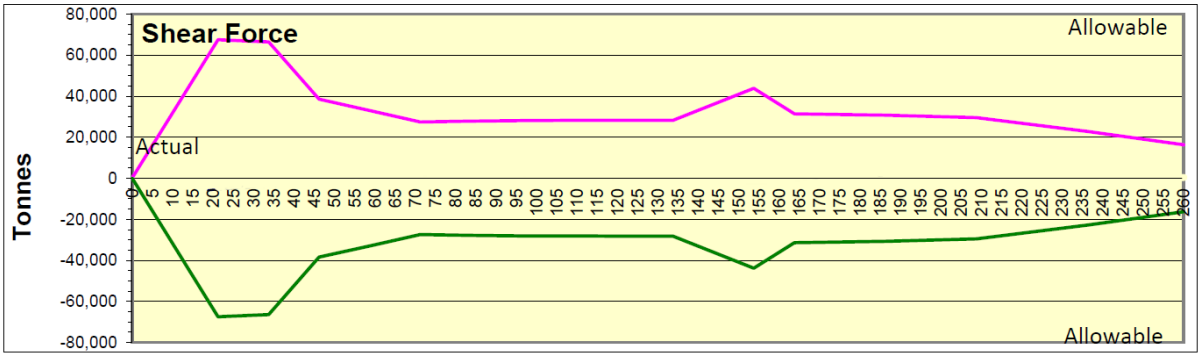

Figure 3-8 Maximum shear force

As can be seen in the previous figures the maximum allowed bending moment and shear force have the same allowable tolerances in both directions. A negative bending moment has the same maximum value as a positive bending moment for each section; same applies to the shear force. Therefore in this thesis, especially in chapter 5 where optimizations are performed, no preference is given for the barge either being loaded in a negative or positive moment or shear force.

3.2.4 Ballast system of the H-851

One of the most important factors during the load-out is the ballasting of the barge. The ballasting needs to make sure that the correct draft is maintained as to keep the barge and quay as much aligned as possible. Also the heel and trim of the barge need to stay within certain limits.

The barge is equipped with an internal ballast system consisting of four ballast pumps capable of ballasting at a rate of 2000cu.m per hour will be used as contingency. Two pumps are located in the main pump room, and two pumps are located in the auxiliary pump room. The combined maximum ballast rate will be 8200 tons per hour. However, under MWS guidelines for redundancy purposes, the total flowrate at any one stage will be limited to 4100 tons per hour.

Both ballast systems are controlled and monitored from a control station on the barge deck with 100% redundancy in the barge's integrated control room. The lay-out of the ballast system can be seen in Figure 3-9. From the central pump room in the bow of the barge a main pipeline runs through the center of the barge towards all ballast tanks.

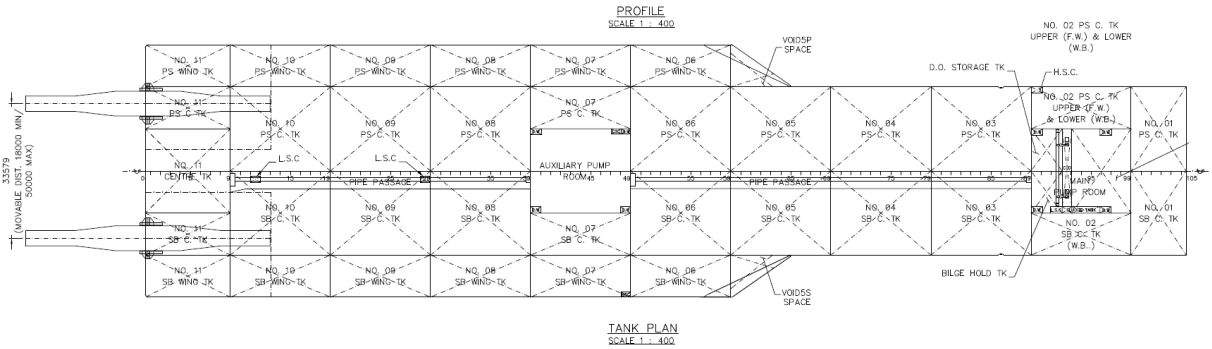

Figure 3-9 Ballast tanks lay-out

The capacity of each tank can be seen in Table 3-2.

Table 3-2 Capacity of water ballast tanks

CAPACITY OF WATER BALAST TANKS S.G. =1.025								
TANKS	DESCRIPTION	LOCATION (FRAMES)	VOLUME(m³) 100%	WEIGHT (TONNES)	CENTER OF GRAVITY(m)			MAX. FREE-SURFACE MOMENT(tm)
					L.C.G	V.C.G	T.C.G	
1SBC	NO 1 STARBOARD SIDE CENTER	99 – 105	2813.5	2883.9	252.16	9.73	−10.61	10575.2
1PSC	NO 1 PORT SIDE CENTER	99 – 105	2846.5	2917.7	252.13	9.72	10.50	10876.9
2SBC	NO 2 STARBOARD CENTER	89 – 99	3472.8	3559.6	233.64	6.81	−15.75	2267.0
2PSC	NO 2 PORT. CENTER. LOWER TK	89 – 99	1913.5	1961.3	233.56	3.81	15.75	2267.0
3SBC	NO 3 STARBOARD SIDE CENTER	79 – 89	6987.5	7162.2	208.75	7.94	−11.38	19776.1
3PSC	NO 3 PORT SIDE CENTER	79 – 89	7733.9	7927.3	208.75	7.50	10.50	19776.1
4SBC	NO 4 STARBOARD SIDE CENTER	69 – 79	6982.4	7157.0	183.75	7.94	−11.38	19776.1
4PSC	NO 4 PORT SIDE CENTER	69 – 79	7741.3	7934.8	183.75	7.50	10.50	19776.1
5SBC	NO 5 STARBOARD SIDE CENTER	59 – 69	7001.8	7176.9	158.75	7.94	−11.38	19776.1
5PSC	NO 5 PORT SIDE CENTER	59 – 69	7748.9	7942.6	158.75	7.50	10.50	19776.1
6SBW	NO 6 STARBOARD WING	49 – 59	3820.1	3915.6	133.65	7.54	−26.21	2443.4
6SBC	NO 6 STARBOARD SIDE CENTER	49 – 59	7009.0	7184.3	133.75	7.94	−11.38	19776.1
6PSW	NO 6 PORT SIDE WING	49 – 59	3820.1	3915.6	133.65	7.54	26.21	2443.4
6PSC	NO 6 PORT SIDE CENTER	49 – 59	7756.9	7950.8	133.75	7.50	10.50	19776.1
7SBW	NO 7 STARBOARD WING	39 – 49	3873.7	3970.5	108.75	7.50	−26.24	2472.0
7SBC	NO 7 STARBOARD SIDE CENTER	39 – 49	3882.4	3979.5	108.75	7.50	−15.75	2472.0
7PSW	NO 7 PORT SIDE WING	39 – 49	3873.7	3970.5	108.75	7.50	26.24	2472.0
7PSC	NO 7 PORT SIDE CENTER	39 – 49	3882.4	3979.5	108.75	7.50	15.75	2472.0
8SBW	NO 8 STARBOARD WING	29 – 39	3877.6	3974.5	83.75	7.50	−26.24	2472.0
8SBC	NO 8 STARBOARD SIDE CENTER	29 – 39	7023.9	7199.5	83.75	7.94	−11.38	19776.1
8PSW	NO 8 PORT SIDE WING	29 – 39	3877.6	3974.5	83.75	7.50	26.24	2472.0
8PSC	NO 8 PORT SIDE CENTER	29 – 39	7772.8	7967.1	83.75	7.50	10.50	19776.1
9SBW	NO 9 STARBOARD WING	19 – 29	3881.4	3978.4	58.75	7.50	−26.24	2472.0
9SBC	NO 9 STARBOARD SIDE CENTER	19 – 29	7030.3	7206.1	58.75	7.94	−11.38	19776.1
9PSW	NO 9 PORT SIDE WING	19 – 29	3881.4	3978.4	58.75	7.50	26.24	2472.0
9PSC	NO 9 PORT SIDE CENTER	19 – 29	7780.4	7974.9	58.75	7.50	10.50	19776.1
10SBW	NO 10 STARBOARD WING	9 – 19	3759.7	3853.7	34.02	7.30	−26.24	2472.0
10SBC	NO 10 STARBOARD SIDE CENTER	9 – 19	6853.4	7024.8	33.98	7.79	−11.34	19776.1
10PSW	NO 10 PORT SIDE WING	9 – 19	3759.7	3853.7	34.02	7.30	26.24	2472.0
10PSC	NO 10 PORT SIDE CENTER	9 – 19	7629.3	7820.0	33.95	7.35	10.44	19776.1
11SBW	NO 11 STARBOARD WING	0 – 9	2174.2	2228.6	11.72	5.59	−26.24	2092.6
11SBC	NO 11 STARBOARD SIDE CENTER	0 – 9	2227.4	2283.1	11.71	5.58	−15.75	2101.2
11PSW	NO 11 PORT SIDE WING	0 – 9	2174.2	2228.6	11.72	5.59	26.24	2092.6
11PSC	NO 11 PORT SIDE CENTER	0 – 9	2227.4	2283.1	11.71	5.58	15.75	2101.2
11C	NO 11 CENTER	0 – 9	5472.1	5608.9	11.19	6.83	0.00	16809.7
TOTAL BALAST WATER			174563.2	178927.5	112.37	7.50	0.07	357655.6

The procedure when ballasting for the load-out is to assume the ballast tanks can be at least 3% full and up to a maximum of 97%. The model which will be described later on will be 2-D, therefore how the ballast is distributed over the width of the barge is unimportant in the model. Seen in 2-D there are 11 ballast tanks. All are the summations of the ballast tanks over their respective number of frames, thus ballast tank 1 is the summation of all the ballast tanks in section frames 0-9, so ballast tanks 11C, 11PSC, 11PSW, 11SBC and 11SBW. Doing this for all the ballast tanks we get the possible load by meter for each section of barge, keeping in mind the range in which between the ballast tanks can be filled. This is summarized in Figure 3-10

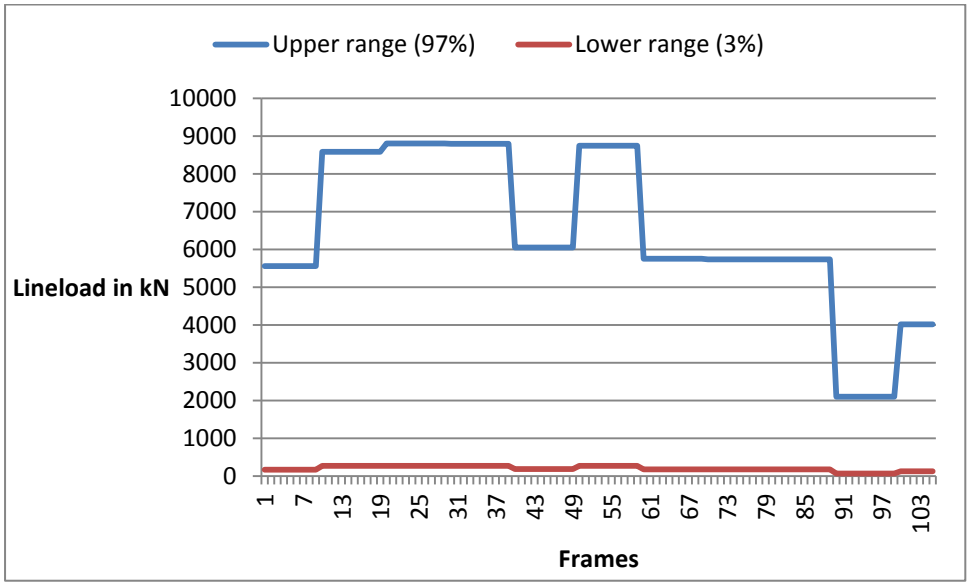

Figure 3-10 Ballast range line load

For each load-out a new ballast plan needs to be calculated. In this plan, the ballast configuration is given for each load-out step. The amount of steps is also project dependent. For the base case scenario

the ballast configuration wasn't determined by HMC themselves. This was outsourced to another company called ALE. The ALE ballast plan is seen as the standard ballast configuration in this thesis. The summary for the ALE ballast plan can be seen in Figure 3-11.

TANK PERCENTAGE FULL SUMMARY

TANK REF	STAGE NUMBER																					
	00	01	02	03	04	05	06	07	08	09	10	11	12	13	14	15	16	17	18	19	20	21	22
1PSC	11%	15%	18%	24%	29%	38%	48%	56%	64%	70%	77%	82%	86%	89%	89%	89%	89%	89%	89%	89%	77%	62%	62%
1SBC	11%	15%	18%	24%	30%	39%	49%	57%	64%	71%	78%	83%	87%	90%	90%	90%	90%	90%	90%	90%	78%	62%	62%
2PSC	97%	97%	97%	97%	97%	97%	97%	97%	97%	97%	97%	97%	97%	97%	97%	97%	97%	97%	97%	97%	97%	97%	97%
2SBC	96%	96%	96%	96%	96%	96%	96%	96%	96%	96%	96%	96%	96%	96%	96%	96%	96%	96%	96%	96%	96%	96%	96%
3PSC	52%	54%	57%	61%	64%	66%	68%	71%	74%	77%	79%	81%	83%	84%	84%	84%	84%	81%	72%	62%	58%	50%	44%
3SBC	47%	49%	53%	57%	60%	62%	65%	69%	72%	75%	78%	80%	81%	83%	83%	83%	83%	79%	69%	58%	53%	46%	39%
4PSC	97%	97%	97%	97%	97%	97%	97%	97%	97%	97%	97%	97%	97%	97%	97%	92%	88%	81%	72%	62%	57%	50%	44%
4SBC	97%	97%	97%	97%	97%	97%	97%	97%	97%	97%	97%	97%	97%	97%	97%	92%	87%	79%	69%	58%	53%	45%	38%
5PSC	97%	97%	97%	97%	97%	97%	97%	97%	97%	97%	97%	97%	97%	97%	97%	91%	88%	81%	72%	62%	57%	51%	44%
5SBC	97%	97%	97%	97%	97%	97%	97%	97%	97%	97%	97%	97%	97%	97%	97%	91%	87%	79%	69%	58%	53%	46%	39%
6PSW	84%	84%	84%	84%	84%	84%	84%	84%	84%	84%	84%	84%	84%	84%	84%	84%	84%	84%	84%	84%	84%	84%	84%
6PSC	97%	97%	97%	97%	97%	97%	97%	97%	97%	97%	97%	97%	97%	97%	97%	97%	97%	97%	97%	97%	97%	97%	97%
6SBC	55%	55%	55%	55%	55%	55%	55%	55%	55%	55%	55%	55%	55%	55%	55%	55%	55%	55%	55%	55%	55%	55%	55%
6SBW	47%	47%	47%	47%	47%	47%	47%	47%	47%	47%	47%	47%	47%	47%	47%	47%	47%	47%	47%	47%	47%	47%	47%
7PSW	12%	16%	20%	25%	30%	34%	39%	43%	47%	52%	56%	63%	70%	78%	85%	92%	95%	97%	97%	97%	97%	97%	97%
7PSC	97%	97%	97%	97%	97%	97%	97%	97%	97%	97%	97%	97%	97%	97%	97%	97%	97%	97%	97%	97%	97%	97%	97%
7SBC	97%	97%	97%	97%	97%	97%	97%	97%	97%	97%	97%	97%	97%	97%	97%	97%	97%	97%	97%	97%	97%	97%	97%
7SBW	55%	52%	47%	42%	38%	33%	29%	24%	20%	16%	11%	10%	8%	8%	8%	8%	8%	8%	8%	8%	8%	8%	8%
8PSW	8%	8%	8%	8%	8%	8%	8%	8%	8%	8%	8%	8%	8%	8%	8%	8%	8%	8%	8%	8%	8%	8%	8%
8PSC	75%	72%	68%	64%	61%	58%	54%	52%	49%	46%	44%	41%	38%	36%	32%	26%	31%	35%	40%	44%	44%	44%	44%
8SBC	83%	79%	75%	71%	68%	64%	60%	57%	54%	51%	49%	46%	42%	39%	36%	29%	35%	39%	44%	49%	49%	49%	49%
8SBW	8%	8%	8%	8%	8%	8%	8%	8%	8%	8%	8%	8%	8%	8%	8%	8%	8%	8%	8%	8%	8%	8%	8%
9PSW	3%	3%	3%	3%	3%	3%	3%	3%	3%	3%	3%	3%	3%	3%	3%	3%	3%	3%	3%	3%	3%	3%	3%
9PSC	75%	72%	68%	64%	61%	58%	54%	52%	49%	46%	44%	41%	38%	36%	32%	26%	31%	35%	40%	44%	44%	44%	44%
9SBC	83%	79%	75%	71%	68%	64%	60%	57%	54%	51%	48%	46%	42%	39%	36%	29%	35%	39%	44%	49%	49%	49%	49%
9SBW	3%	3%	3%	3%	3%	3%	3%	3%	3%	3%	3%	3%	3%	3%	3%	3%	3%	3%	3%	3%	3%	3%	3%
10PSW	3%	3%	3%	3%	3%	3%	3%	3%	3%	3%	3%	3%	3%	3%	3%	3%	3%	3%	3%	3%	3%	3%	3%
10PSC	76%	73%	69%	65%	62%	59%	56%	53%	50%	47%	45%	42%	39%	36%	33%	27%	32%	36%	41%	45%	45%	45%	45%
10SBC	85%	81%	77%	73%	69%	66%	62%	59%	56%	52%	50%	47%	43%	40%	37%	30%	36%	40%	46%	50%	50%	50%	50%
10SBW	3%	3%	3%	3%	3%	3%	3%	3%	3%	3%	3%	3%	3%	3%	3%	3%	3%	3%	3%	3%	3%	3%	3%
11PSW	97%	85%	71%	58%	47%	39%	35%	30%	25%	21%	18%	15%	12%	9%	7%	7%	18%	32%	35%	40%	59%	66%	72%
11PSC	95%	83%	70%	57%	46%	38%	34%	29%	25%	21%	17%	14%	11%	9%	7%	7%	18%	31%	35%	39%	58%	64%	70%
11C	88%	83%	77%	72%	66%	61%	54%	49%	43%	38%	33%	28%	24%	20%	15%	7%	11%	17%	18%	20%	27%	38%	48%
11SBC	95%	83%	70%	57%	46%	38%	34%	29%	25%	21%	17%	14%	11%	9%	7%	7%	18%	31%	35%	39%	58%	64%	70%
11SBW	97%	85%	71%	58%	47%	39%	35%	30%	25%	21%	18%	15%	12%	9%	7%	7%	18%	31%	35%	40%	59%	65%	72%
Start Time :	03:24	04:00	04:20	04:40	05:00	05:20	05:40	06:00	06:20	06:40	07:00	07:20	07:40	08:00	08:20	08:40	09:10	09:45	10:25	11:05	11:45	12:25	13:05
Stop Time :	04:00	04:20	04:40	05:00	05:20	05:40	06:00	06:20	06:40	07:00	07:20	07:40	08:00	08:20	08:40	09:10	09:45	10:25	11:05	11:45	12:25	13:05	13:32
Duration :	00:36	00:20	00:20	00:20	00:20	00:20	00:20	00:20	00:20	00:20	00:20	00:20	00:20	00:20	00:20	00:30	00:35	00:40	00:40	00:40	00:40	00:40	00:27
Tide Height	0.36	0.38	0.41	0.47	0.55	0.65	0.77	0.90	1.04	1.18	1.32	1.46	1.59	1.71	1.81	1.92	1.99	1.98	1.87	1.69	1.44	1.17	0.99
Dist. Pulled	0.00	5.00	10.00	15.00	20.00	25.00	30.00	35.00	40.00	45.00	50.00	55.00	60.00	65.00	70.00	77.00	85.00	95.00	105.00	115.00	125.00	135.00	141.63

Figure 3-11 Ballast plan base case load-out

As can be seen the standard ballast plan distinguishes 22 steps for the load-out. The MATLAB model consists of 113 steps. The steps which correspond with a step from the standard ballast configuration are matched and given the same ballast value. For the steps in between, interpolation with the help of MATLAB for the ballast values is used. What also needs to be taken into account is that for each stage the tide height is different and thus the draft of the barge is different. Same as with the ballast values, this too is interpolated in order to get the tide height and thus the draft for all the 113 steps.

3.3 Base case topside

The base case platform will be the largest offshore gas processing platform ever installed in Australia, with a topside weight of about 37,000 tons. The topside is located 28m above sea level and is designed to withstand 12-storey waves.

Figure 3-12 Wheatstone topside at its final offshore location

For the load-out the topside will be supported by a deck support frame. The DSF supports the deck at the deck support units of which there are 8 in this set-up. The DSF can be seen in Figure 3-13,

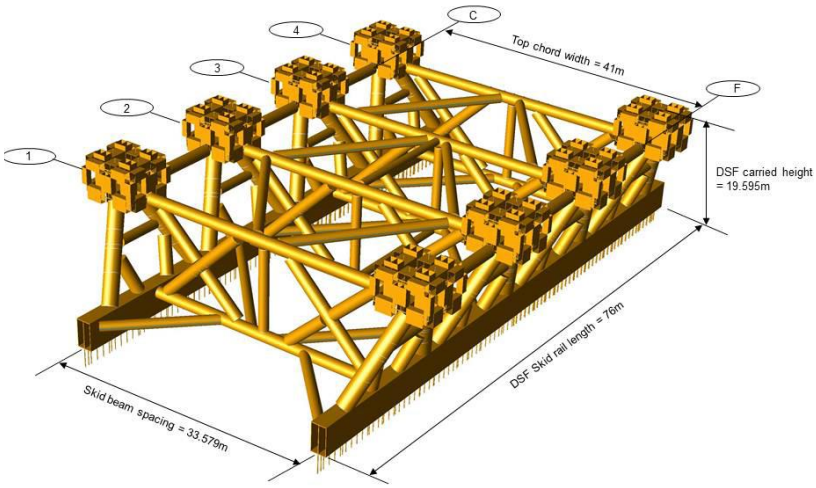

Figure 3-13 Deck support frame

More technical background for the base case topside shall be given in chapter 4 where the MATLAB model is described. How the stiffness of the topside is implemented into the model is explained in Appendix B.

4 FEM-Model

In this chapter the model which was built of the load-out is explained. First a short description of the used theory is given. This is then applied to the model. The software which is used for this model is MATLAB which is ideal for numerical simulations. At the end of the chapter a verification of the model is provided.

4.1 FEM theory

Finite Element Analysis, hereafter named FEA is method which can be used for a variety of field problems using a numerical solution. Field problems require that we determine the spatial distribution of one or more dependent variables. In this case displacements and stresses over a barge or skidbox. A field problem can be described by differential equations or by integral expressions. The FEM is named after the finite elements which can be seen as very small pieces of a structure. In each of these elements a field quantity has a simple spatial variation described by a polynomial term. The actual variation is more complex so the FEA provides an approximation of the exact solution. The finite elements are connected at so called nodes. Connecting all these elements together and a structure is formed. The arrangement of these elements over the structure is called the "mesh". This mesh is represented numerically by a system of equations who's unknown can be solved at the nodes. These nodal values are values of the field quantities and depending on the type of field also its first derivatives. The solution for nodal quantities in combination with the assumed field quantities in any given element completely determines the spatial variation of the field in that element. Thus the field quantity over the entire structure is approximated element by element in piecewise fashion. An FEA doesn't provide an exact solution however by increasing the number of elements the solution can be improved until it almost resembles the exact solution.

The solution to a static structure equation is $[K]\{D\} = \{R\}$. In which D represents the nodal degrees of freedom, R represents the nodal forces and K represents the combination of all the element matrices. This can also be seen as $[K]^{-1}\{R\} = \{D\}$. In order to solve these structure equations first the element matrix K needs to be determined.

The type of element chosen for the model will be a 2D beam element. This type of element has a node at both ends. Both nodes have 3 degrees of freedom being vertical displacement, horizontal displacement and rotation, u,v and θ. The nodal rotations are normal to the xy-plane. An example of such an element can be seen in See Figure 4-1

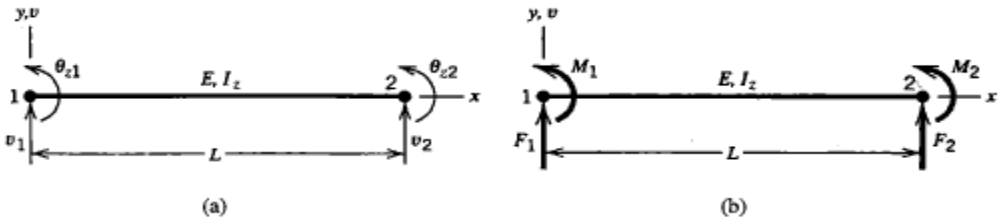

Figure 4-1Beam element in xy plane

Forming the correct element matrix is of the utmost importance. The method of forming the element matrix will now be explained in detail

Interpolation forms a continuous function that is correct at a certain number of points and satisfies prescribed conditions. In FEA these points are the nodes of elements and the conditions are nodal values of a field quantity. The nodal values often aren't exact and even if they are the interpolation results provide an approximation at the inter laying locations. The interpolating functions in FEA are almost always polynomials.

Using a generalized degree of freedom a_i, the interpolating polynomial with a dependent variable ϕ and independent variable x can be written as:

$$\phi = \sum_{i=0}^{n} a_i x^i \quad or \quad \phi = [\mathbf{X}]\,\{\mathbf{a}\}$$

In which

$$[X] = [1 \quad x \quad x^2 \quad x^n] \quad \text{and} \quad \{a\} = [a_0 \quad a_1 \quad a_2 \quad a_n]^T$$

In which n is dependent on the level of interpolation. So $n=1$ for linear, 2 for quadratic and 3 for cubic. The relation between nodal values $\{\boldsymbol{\phi_e}\}$ and the a_i can be seen as.

$$\{\boldsymbol{\phi_e}\} = [\mathbf{A}]\{\mathbf{a}\}$$

In which $[\mathbf{A}]$ is $[\mathbf{X}]$ evaluated at the appropriate nodal location.

$$\{\phi\} = [\mathbf{N}]\{\boldsymbol{\phi_e}\} \; where \; [\mathbf{N}] = [\mathbf{X}][\mathbf{A}]^{-1}$$

Each N_i in the matrix **N** is a so called shape function. Each shape function gives the interpolated $\phi = \phi(x)$ when the corresponding ϕ_i has the value unity and all the others are zero. In a complete structure the values of $\boldsymbol{\phi_e}$ will be in matrix $\{\mathbf{D}\}$. So solving for $\{\mathbf{D}\}$ gives the nodal values in each element.

Now the formulas for the element stiffness matrix and for load vectors can be derived using the principle of virtual work, other methods can also be used but for cases with structural mechanics the principle of virtual work will be sufficient.

The principle of virtual work is stated in the form:

$$\int \{\delta\boldsymbol{\varepsilon}\}\{\sigma\}\,dV = \int \{\delta\mathbf{u}\}^T\{\mathbf{F}\}\,dV + \int \{\delta\mathbf{u}\}^T\{\Phi\}\,dS$$

The displacements $\{u\}$ can be interpolated using the following form:

$$\{\mathbf{u}\} = [\mathbf{N}]\{\mathbf{d}\}$$

And so the strains $\{u\}$ can be written as:

$$\{\boldsymbol{\varepsilon}\} = [\delta][\mathbf{N}]\{\mathbf{d}\}$$

The matrix which is formed by $[\delta][\mathbf{N}]$ is called the strain displacement matrix. Hereafter symbolized by $[\mathbf{B}]$. From the previous equations we get.

$$\{\delta\mathbf{u}\}^T = \{\delta\mathbf{d}\}^T[\mathbf{N}]^T \quad and \quad \{\delta\boldsymbol{\varepsilon}\}^T = \{\delta\mathbf{d}\}^T[\mathbf{B}]^T$$

Combining these with the known stress-strain relation we get:

$$\{\delta\mathbf{d}\}^T\left(\int[\mathbf{B}]^T[\mathbf{E}][\mathbf{B}]\,dV\{\mathbf{d}\} - \int[\mathbf{B}]^T[\mathbf{E}]\{\boldsymbol{\varepsilon_0}\}dV + \int[\mathbf{B}]^T\{\boldsymbol{\sigma_0}\}dV - \int[\mathbf{N}]^T\{\mathbf{F}\}dV - \int[\mathbf{N}]^T\{\boldsymbol{\Phi}\}dV\right) = 0$$

d isn't a function of coordinates and so isn't included in the integrals. Equation has to be correct for any value $\{\delta\mathbf{d}\}$ of the equilibrium configuration so we can say

$$[\mathbf{k}]\{\mathbf{d}\} = \{\mathbf{r}_e\}$$

With the element stiffness matrix being:

$$[\mathbf{k}] = \int[\mathbf{B}]^T[\mathbf{E}][\mathbf{B}]\,dV$$

And the load vector applied to the structure nodes including all sources except element deformation is:

$$\{\mathbf{r}_e\} = \int[\mathbf{N}]^T\{\mathbf{F}\}\,dV + \int[\mathbf{N}]^T\{\boldsymbol{\Phi}\}dV + \int[\mathbf{B}]^T[\mathbf{E}]\{\boldsymbol{\varepsilon_0}\}\,dV - \int[\mathbf{B}]^T\{\boldsymbol{\sigma_0}\}dV$$

If the previous equations are applied to a beam element somethings change. Now stress and strain are replaced with bending moment M and curvature κ. In the previous equation the integrand of the first integral becomes $(\delta\kappa)^T M\,dx$. The other characteristics of a beam element are:

$$M = EI_z\kappa \;, \quad \kappa = \frac{d^2v}{d^2x} \;, \quad v = [\mathbf{N}]\{\mathbf{d}\} \;, \quad \kappa = [\mathbf{B}]\{\mathbf{d}\}$$

Where v is the vertical displacement or lateral displacement of the beam. To form the element matrix first the shape functions need to be found. The degrees of freedom at the nodes for a beam element are the lateral displacement of each node and the rotation at each node. So $\{\mathbf{d}\}$ becomes:

$$\{\mathbf{d}\} = \begin{pmatrix} v_1 \\ \theta_1 \\ v_2 \\ \theta_2 \end{pmatrix}$$

As mentioned earlier the 4 shape functions can be determined by choosing each degree of freedom with value unity and the remaining d.o.f. zero. The corresponding 4 equations are the 4 shape functions. See Figure 4-2 for the shape functions

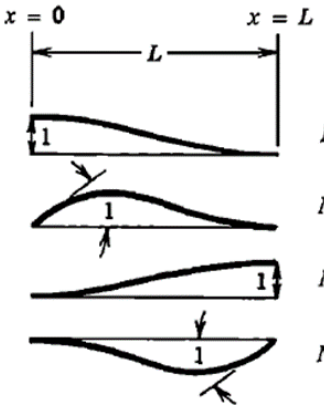

		At $x = 0$		At $x = L$	
		N_i	$N_{i,x}$	N_i	$N_{i,x}$
N_1	$= 1 - \frac{3x^2}{L^2} + \frac{2x^3}{L^3}$	1	0	0	0
N_2	$= x - \frac{2x^2}{L} + \frac{x^3}{L^2}$	0	1	0	0
N_3	$= \frac{3x^2}{L^2} - \frac{2x^3}{L^3}$	0	0	1	0
N_4	$= -\frac{x^2}{L} + \frac{x^3}{L^2}$	0	0	0	1

Figure 4-2 shape functions for a beam

Now that the shape functions are know the strain displacement matrix can be formed ,keeping in mind that $[\mathbf{B}] = \frac{d^2}{dx^2}[\mathbf{N}]$ since we are looking at a bending beam.

$$[\mathbf{B}] = \frac{d^2}{dx^2}[\mathbf{N}] = \left[-\frac{6}{L^2} + \frac{12x}{L^3} \quad -\frac{4}{L} + \frac{6x}{L^2} \quad \frac{6}{L^2} - \frac{12x}{L^3} \quad -\frac{2}{L} + \frac{6x}{L^2} \right]$$

To form the element stiffness matrix equation mentioned earlier is used replacing *E* with *EI*.

$$[\mathbf{k}] = \int_0^L [\mathbf{B}]^T [\mathbf{EI}][\mathbf{B}]\, dx$$

Assuming that *EI* is constant over one element the element stiffness matrix for a beam element is:

$$[\mathbf{k}] = \begin{pmatrix} \frac{12EI}{L^3} & \frac{6EI}{L^2} & \frac{-12EI}{L^3} & \frac{6EI}{L^2} \\ \frac{6EI}{L^2} & \frac{4EI}{L} & \frac{-6EI}{L^2} & \frac{2EI}{L} \\ \frac{-12EI}{L^3} & \frac{-6EI}{L^2} & \frac{12EI}{L^3} & \frac{-6EI}{L^2} \\ \frac{6EI}{L^2} & \frac{2EI}{L} & \frac{-6EI}{L^2} & \frac{4EI}{L} \end{pmatrix}$$

The nodal loads are:

$$\{\boldsymbol{r_e}\} = \begin{pmatrix} F_1 \\ M_1 \\ F_2 \\ M_2 \end{pmatrix}$$

A quick verification of the element matrix can be given by using the forget-me-nots. This is done below for v_1 and only $\mathbf{k}(1,1)$ and $\mathbf{k}(2,1)$. v_1 is assumed to be unity in this example and the other d.o.f. zero.

$$v_1 = 1: \quad \frac{\mathbf{k}(1,1)L^3}{3EI} - \frac{\mathbf{k}(2,1)L^2}{2EI} = 1 \;\; and \;\; \theta_1 = 0: \quad \frac{\mathbf{k}(1,1)L^2}{2EI} - \frac{\mathbf{k}(2,1)L}{EI} = 0$$

To satisfy both equations we get:

$$\mathbf{k}(1,1) = \frac{12EI}{L^3} \quad and \quad \mathbf{k}(2,1) = \frac{6EI}{L^2}$$

To obtain the nodal loads for a uniform downward load q over the length of the barge we can use the direct method, so the forces are ql/2 and ql2/2 however we can also use the second integral in equation BB, in which {Φ}=-q and dS=ds. Both give the same results as one would expect.

In order to allow the beam to stretch as well as bend axial translations at both nodes still needs to be added to the model. Therefore stiffness matrix [**k**] is expanded to a 6x6 matrix. Looking at a bar under an axial force at both nodes, see Figure 4-3, the following equations are derived.

$$\frac{AE}{L}(u_1 - u_2) = F_1 \;\; and \;\; \frac{AE}{L}(u_2 - u_1) = F_2$$

Figure 4-3 Bar under axial forces

The bending stiffness terms are also adjusted to take into account the transverse shear deformation thus creating a Timoshenko beam element. The final matrix received can be seen in Figure 4-4.[1]

$$[\mathbf{k}] = \begin{bmatrix} X & 0 & 0 & -X & 0 & 0 \\ 0 & Y_1 & Y_2 & 0 & -Y_1 & Y_2 \\ 0 & Y_2 & Y_3 & 0 & -Y_2 & Y_4 \\ -X & 0 & 0 & X & 0 & 0 \\ 0 & -Y_1 & -Y_2 & 0 & Y_1 & -Y_2 \\ 0 & Y_2 & Y_4 & 0 & -Y_2 & Y_3 \end{bmatrix} \begin{matrix} u_1 \\ v_1 \\ \theta_{z1} \\ u_2 \\ v_2 \\ \theta_{z2} \end{matrix}$$

where

$$X = \frac{AE}{L} \qquad Y_1 = \frac{12EI_z}{(1+\phi_y)L^3} \qquad Y_2 = \frac{6EI_z}{(1+\phi_y)L^2}$$

$$Y_3 = \frac{(4+\phi_y)EI_z}{(1+\phi_y)L} \qquad Y_4 = \frac{(2-\phi_y)EI_z}{(1+\phi_y)L} \qquad \phi_y = \frac{12EI_z k_y}{AGL^2}$$

Figure 4-4 Final Beam element matrix

4.2 MATLAB model of the load-out process

The knowledge from the previous paragraph will now be applied to the load-out of the topside onto the barge H-851. To be able to put a complex process like the load-out into a numerical model in MATLAB several assumptions have to be made:

- The model is made to be a 2-D presentation of the load out. Seen from the side view of the barge
- Yaw, sway and roll of the barge are not taken into account.
- All components are Timoshenko beam-models

The model of the load out is composed of three main structures; the barge H-851, the topside Wheatstone and the quay. Each will be independently formed and have its own structure stiffness matrix, d.o.f. and force vector. These three components will then be combined to form one large system with one system stiffness matrix K_{sys}.

4.2.1 Barge model

The model of the barge will form the base of the entire model. The barge is modeled as a beam which is supported on springs, see Figure 4-5

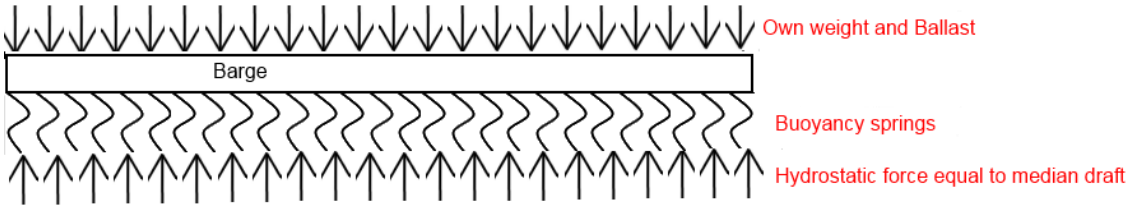

Figure 4-5 Barge model continuous

The springs represent the buoyancy force exerted by the water onto the barge. The deeper the draft the higher the buoyant force will be. The current is also taken to be a constant. The required draft is therefore known. To set the barge deck at zero the hydrostatic force equal to the median draft is also applied onto the barge, this force isn't constant over the entire length of the barge due to a difference in width of the barge and due to the bow being slightly "rounded" upwards. The only forces which are exerted in a downward direction on the barge are the barge's own weight and the ballast water in each tank. The height of the quay is taken to be the zero point.

The model seen in Figure 4-5 needs to be discretized to be able to use in the numerical model. The barge is there for subdivided into beam elements, see Figure 4-6.

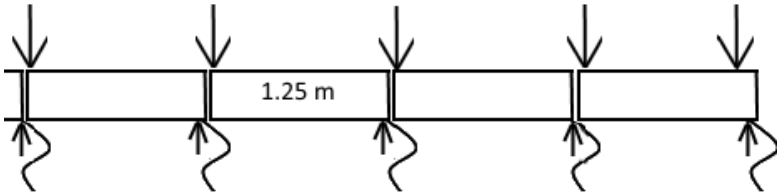

Figure 4-6 Barge model discrete

The barge is divided into 208 beam elements. This division is chosen because as was shown in chapter 3 the barge consists of 105 frame sections with varying *EI* with the first and last element with a length of 1.25 meters.. Thus each element has a length of 1,25 meter. Except for the first and the last

element, each of the 105 frame sections is thus represented by 2 beam elements. Since the total barge length is 260 meters this is deemed to be a fine enough meshing to be accurate.

After the discretization the buoyancy springs are now attached at each node, a node being the connection between each beam element. Each spring represents the buoyancy force exerted on the barge over a length of 1.25 meters, except for the first and last spring attached to the barge, these represent only half an element and thus represent 0.625 meters. The spring stiffness is represented by $k_{Buoyancy}$.

$$k_{Buoyancy} = buoyancy\ stifness = \rho * g * w * 1.25$$

In which
ρ= Density of water
g= Gravitational constant
w= Width of the barge at section

The mean draft force is analogous to the buoyancy force described above. It too represents 1.25 meters of hydrostatic force exerted on the barge in the positive direction except for the first and the last nodal force which represent 0.625 meters. However because the previous equation referred to a stiffness and this refers to a force, this equation is multiplied by the mean draft to get the hydrostatic force exerted on the barge by the mean draft.

The force at the nodes which represents the own weight of the barge plus the ballast is discretized differently than the buoyancy force. The weight of the barge and ballast differ per element as was seen in chapter 3. The force at each node represents half of the distributed load on the beam to the left and half of the beam to the right, with the buoyancy this didn't matter because both were the same, now however this distinction needs to be made.

$$F_{W+B} = \left(\frac{q_{left} + q_{right}}{2}\right) * 1.25$$

In which
$q_{left} + q_{right}$ = distributed load on beam left and right of node
F_{W+B} = Nodal load for weight of barge plus ballast.

For the horizontal forces at the nodes the same method is used as for the vertical forces. So the distributed load on half of each neighboring element is added. The only horizontal forces which are directly applied onto the barge itself will be the friction loads at the Deadman anchor caused by the skidding force of the topside onto the barge. As explained in chapter BBB the load-out is a quasi-static process thus the topside isn't always skidding and so friction forces aren't always present.

Now that the model is complete the discretized beam on springs can be expressed in a matrix. The standard 2-D beam element matrix was given in Figure 4-4. The springs at each node still need to be incorporated into this matrix. The springs can also be seen as a vertical force acting on the node. Since $F_v = k * u_v$ the springs for $k_{buoyancy}$ need to be inserted in the stiffness matrix at the elements (2,2) and (5,5) since these describe the direct relationship between the vertical force at the nodes and the vertical displacement just like the springs. See Equation 4-1 for the beam matrix equation.

Equation 4-1 Matrix including springs

$$\begin{bmatrix}
\frac{AE}{L} & 0 & 0 & -\frac{AE}{L} & 0 & 0 \\
0 & \frac{12EI}{(1+\Phi)L^3} + k_{buoyancy} & \frac{6EI}{(1+\Phi)L^2} & 0 & -\frac{12EI}{(1+\Phi)L^3} & \frac{6EI}{(1+\Phi)L^2} \\
0 & \frac{6EI}{(1+\Phi)L^2} & \frac{(4+\Phi)EI}{(1+\Phi)L} & 0 & -\frac{6EI}{(1+\Phi)L^2} & \frac{(2-\Phi)EI}{(1+\Phi)L} \\
-\frac{AE}{L} & 0 & 0 & \frac{AE}{L} & 0 & 0 \\
0 & -\frac{12EI}{(1+\Phi)L^3} & -\frac{6EI}{(1+\Phi)L^2} & 0 & \frac{12EI}{(1+\Phi)L^3} + k_{buoyancy} & -\frac{6EI}{(1+\Phi)L^2} \\
0 & \frac{6EI}{(1+\Phi)L^2} & \frac{(2-\Phi)EI}{(1+\Phi)L} & 0 & -\frac{6EI}{(1+\Phi)L^2} & \frac{(4+\Phi)EI}{(1+\Phi)L}
\end{bmatrix}$$

The next beam element expands the matrix to a 9x9 matrix because only one node gets add. The matrix of the new beam element is added to the previous causing element (1,1) to be added to element (4,4) of the previous.

Repeating this process for all the 208 beam elements that make up the barge model and thus a stiffness matrix for the whole barge is received. See matrix Equation 4-2 for the matrix with a size of 209*3 rows by 209*3 columns. This matrix will be used in the rest of model when more structures are added. The color shading is added because later on multiple matrices will be added so the color is to clarify which is which. The numbers in the corners are to clarify matrix size.

Equation 4-2

$$\begin{bmatrix}
1 & & 727 \\
 & K_{Barge} & \\
727 & &
\end{bmatrix} \bullet \begin{bmatrix} U_{x1} \\ U_{y1} \\ U_{\Phi 1} \\ \vdots \\ \vdots \\ \vdots \\ U_{x209} \\ U_{y209} \\ U_{\Phi 209} \end{bmatrix} = \begin{bmatrix} F_{x1} \\ F_{y1} \\ M_{z1} \\ \vdots \\ \vdots \\ \vdots \\ F_{x209} \\ F_{y209} \\ M_{z209} \end{bmatrix}$$

4.2.2 DSF + Topside + Skidbox

The next addition to the model of the barge will be the topside plus the deck support frame including the skidboxes. The topside and deck support frame will also be a beam model. The construction of this model however is much more complex since these aren't just beams attached to each other in one

direction all in the same way. Here we have nodes which are connected to multiple beams thus making it more complex.

The topside is supported by the deck support frame during the entire load-out. The deck support frame transfers the weight of the topside onto the skidboxes which in turn transfer the weight via the skidbeams onto the barge and quay.

The construction of the DSF + topside + skidboxes needs to be made applicable in this model. The main thing that needs to be done is to turn this 3-d construction into a 2-D beam model. In the transition from 3-d to 2-d several assumptions will be made, which will be explained per section. These assumptions cause the model to be less of a representation of reality. The goal is to still stay as accurate as possible.

The topside forms a complex 3-D structural model. The forces caused by the weight are guided through smaller structural members towards the main structural frame. In Figure 4-7 and Figure 4-8 what is deemed to be the main structural frame is highlighted in red. Clearly distinguishable are the three deck level; the lower deck level, the intermediate deck level and the upper deck level. In the front view 3 different "cells" can be seen, in the side view 6 cells are taken to be a part of the main structural frame. This main structural frame will be used in the MATLAB model, the smaller structural members will be neglected. All the forces will be directly applied onto the main structural frame.

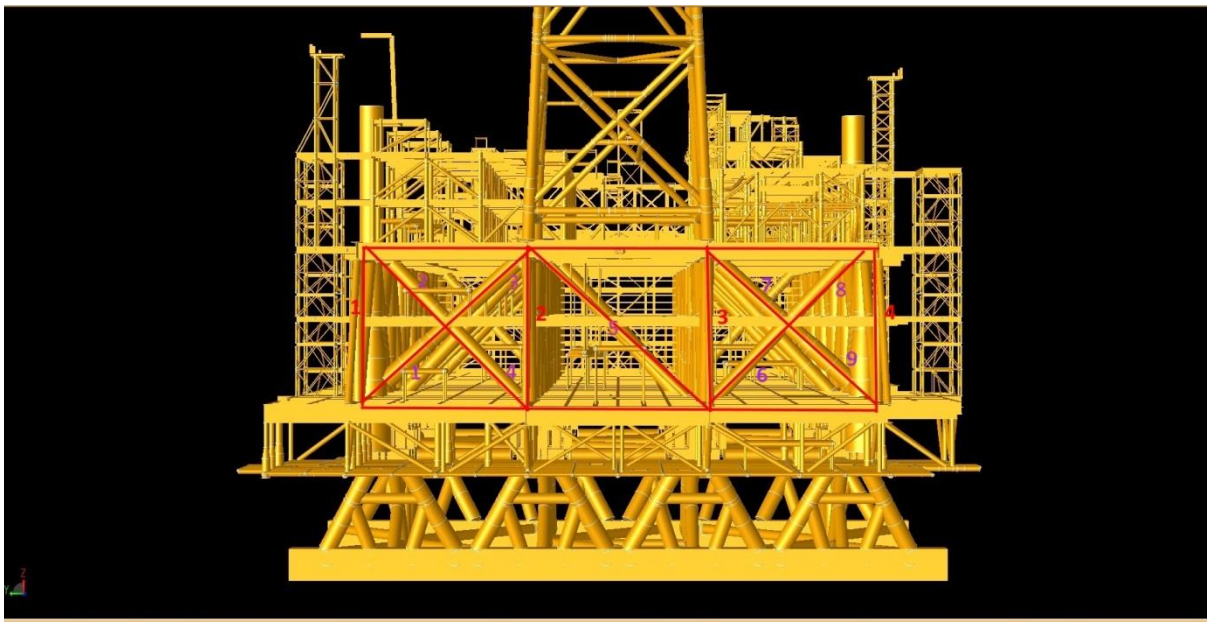

Figure 4-7 Front view topside+DSF

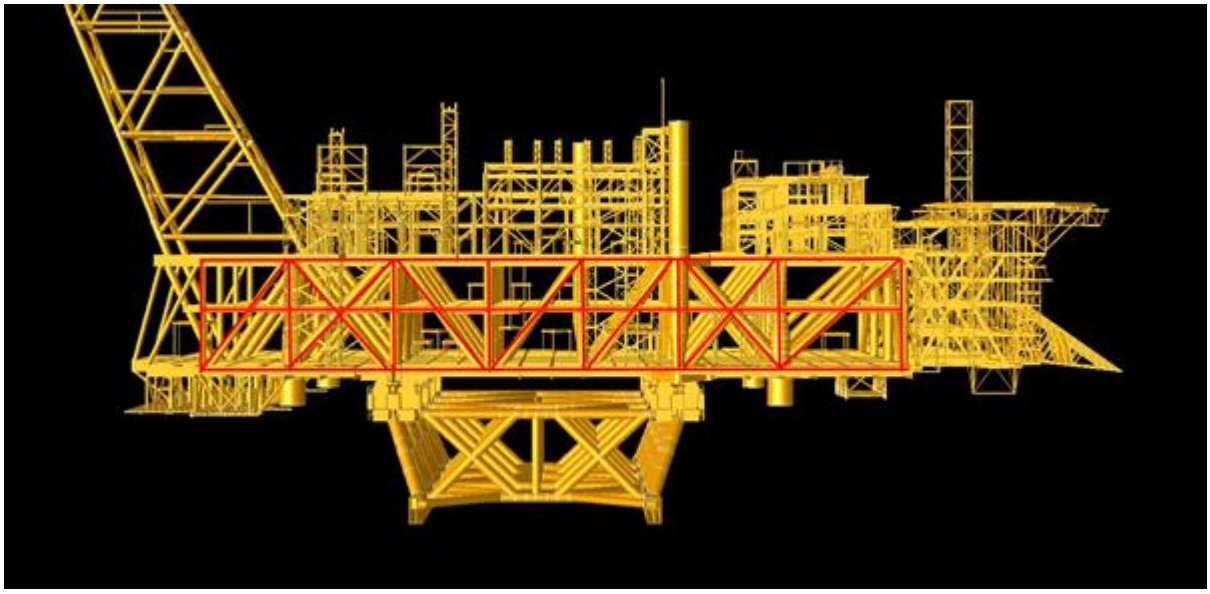

Figure 4-8 Sideview Topside+DSF

The 3-D main structural frame now needs to be made into 2-D. Therefore the front view from Figure 4-7 is used. The forces as well as the stiffness of the structural members seen in the side view are superimposed onto each other to get an accurate representation. The transformation from the 3-D model to the 2-D model including the stiffness calculations for all the members, the superposition of the forces and the weight distribution can be seen in Appendix B: Topside configuration**.**

Via the DSU's the weight of the topside is guided to the deck support frame. Just like the topside the deck support frame needs to transform into a 2-D representation. For the deck support frame all members are taken into account as they are all part of the main load bearing structure. The side view shown in Figure 4-9 forms a correct presentation of a part of the deck support frame model used.

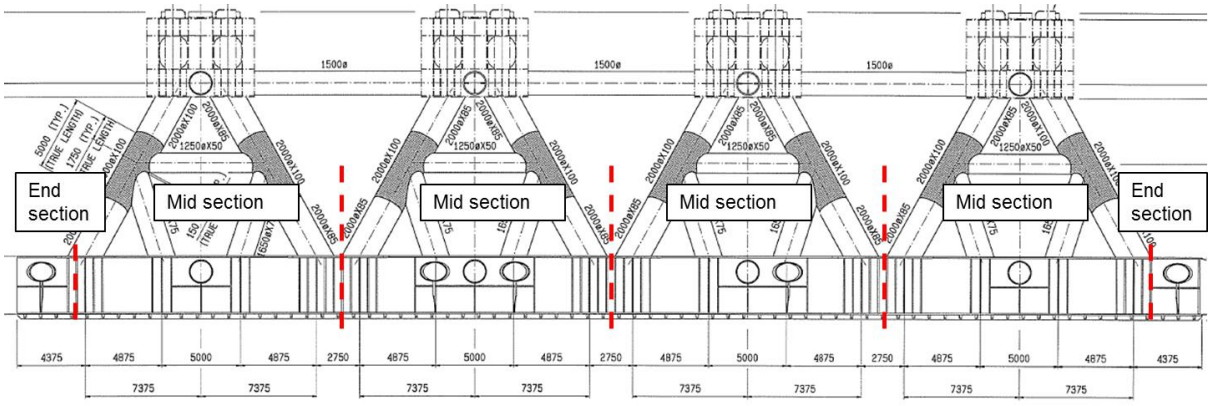

Figure 4-9 DSF dimensions, front view

However as can be seen in Figure 4-8 there is also a frame section connecting the two sides of deck support frame. So a vertical member is added in the center each mid-section connecting the DSU to the skidbox. In the actual DSF the members enter the skidboxes at an angle introducing forces in the z-direction, this is neglected in the 2-d representation. The transformation from 3-D to 2-D and the superposition of the elements is explained more elaborate in Appendix B: Topside configuration**.**

Finally the skidboxes need to be added to the DSF and topside. The skidboxes are responsible for the final transfer of weight of the topside onto the timber in the skidbeams. In the model the skidbox is

assumed to be homogenous throughout. As can be seen in Figure 4-9 this isn't the case in reality as there are several vertical flanges inside the boxes, however these do not contribute significantly for the longitudinal stiffness.

Bothe skidboxes have the exact same lay-out, since the model in M is 2-D the *EI* value of one skidbox is multiplied by two to get the representation of both skidboxes in the model. To calculate the stiffness of the skidbox a simple hand calculation is performed. The profile of the skidbox can be seen in Figure 4-10. Using the equation below, the stiffness of the skidbox can be easily found using the values seen in Figure 4-10.

Equation 4-3

$$moment\ of\ inertia = \frac{1}{12} * b * h^3 + A^2 * z$$

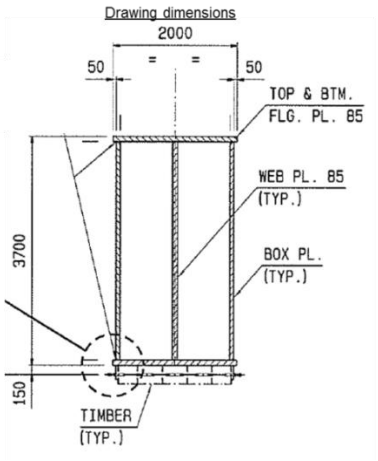

Figure 4-10 Profile of the skidbox

Since the skidboxes play in important role in the model later on when the effects of optimizations will be discussed, their allowed shear forces and moments are calculated too.

Allowable shear force

The stresses resulting from shear force can be calculated using the equation below. The maximum allowed stress is known so with the help of Figure 4-10 the maximum allowed shear force can be calculated.

Equation 4-4

$$\sigma_{max,shear} = \frac{V * S_z}{b * I}$$

In which:

$\sigma_{max,shear}$	$=0.4*f_y=0.4*340=136$ N/mm^2
V	= Shear force
S_z	= Static moment sliding element
b	= width at cross section halfway
I	= moment of inertia of skidbox

Using the values which can be derived from Figure 4-10 the maximum allowed shear force over the skidbox is calculated to be: 8.1*10^4 kN.

Allowable bending moment

The same as was done for the shear force is repeated for the maximum allowed bending moment [2]:

Equation 4-5

$$\sigma_{max,bending} = \frac{M * z}{I}$$

In which:

$\sigma_{max,bending}$ = $0.66*f_y=0.66*340=224.4$ N/mm^2
M = bending moment on skidbox
z = half the height of the skidbox
I = moment of inertia of skidbox

Using Equation 4-5 and with the values derived from Figure 4-10 the maximum allowed bending moment is found to be; 159.74 MNm.

Care should be taken that these forces aren't exceeded. A special note will be made in this report in the occasion that it does.

With the skidbox added the structure of topside, DSF and skidbox is now complete. The topside, DSF and skidbox are later on combined with the barge and the quay. Therefore the nodes of the skidbox need to align with the nodes of the barge. Both structures are beam elements and since the barge consists of beam elements with the size of 1.25 meters it is only logical that the skidbox will have beam elements with a size of 1.25 meters too. This way all the nodes of the skidbox will always align with a node on the barge. See Figure 4-11. Every step in which the skidbox moves further up the barge equals one node further along the barge thus every step is 1.25 meters.

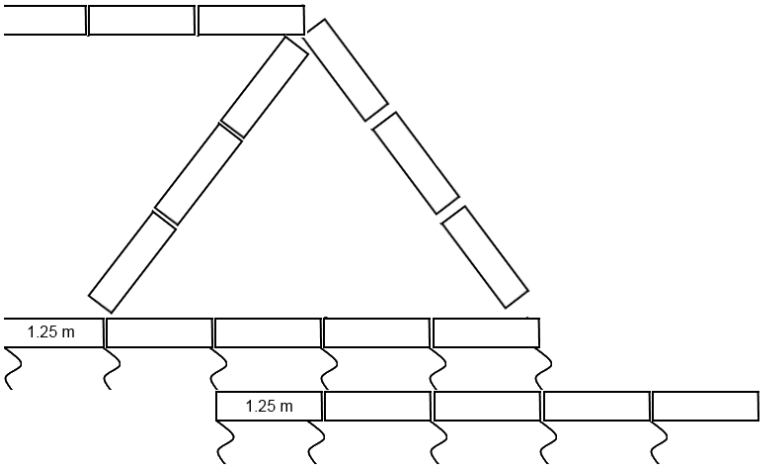

Figure 4-11 skidbox - barge connection

The connection between the skidbox and the barge is formed by springs at every overlapping node. These springs resemble the stiffness of the deck in combination with the timber in the skidbeams. The value for this spring stiffness will be the topic of chapter 7, here the deck stiffness will be further clarified. For now it suffices to mention that the stiffness of the wood is calculated using the following formula:

$$k_{wood} = \frac{N}{\Delta t} = \frac{EA}{t} = \frac{1430 * 10^6 * 4}{0.3} = 1.9 * 10^{10} N/m$$

In which:
E = Young's modulus of wood
A = Area over which force is applied
t = thickness of wood layer

The deck stiffness is given for now to be 1.8*10^9 N/m (received using SACS analysis) and at the transverse bulkheads to be 3.354*10^9, however a deeper analysis of the deck will be performed in chapter 6. For combining this with the wood stiffness to form the springs connecting the skidbox and the barge the following equation is used:

$$\left(\frac{1}{k_{wood}} + \frac{1}{k_{deck}}\right)^{-1} = k_{con} = 1.644 * 10^9$$

In which:
k_{wood} = Stiffness wood
k_{deck} = Stiffness barge deck
k_{con} = Stiffness connecting spring barge-skidbox

When combining the topside and the barge another force factor comes into play which needs to be added into the model. As could be seen in chapter 3 a skidded load-out works by attaching cables from an anchor at the front of the barge to the skidboxes. If the strand jacks are engaged a normal force and moment is applied at the deadman anchor. This force is constant over the entire load-out since the pulling force required stays the same. This pulling force is equal to the friction coefficient times the weight of the whole topside structure. The friction coefficient was determined to be 0.10 so the pulling force at the deadman anchor is 0.10*$weight\ topside+DSF$. The created moment's arm is equal to the distance from the center of the barge to the point where the cables attach at the deadman anchor, seen in Figure 4-12

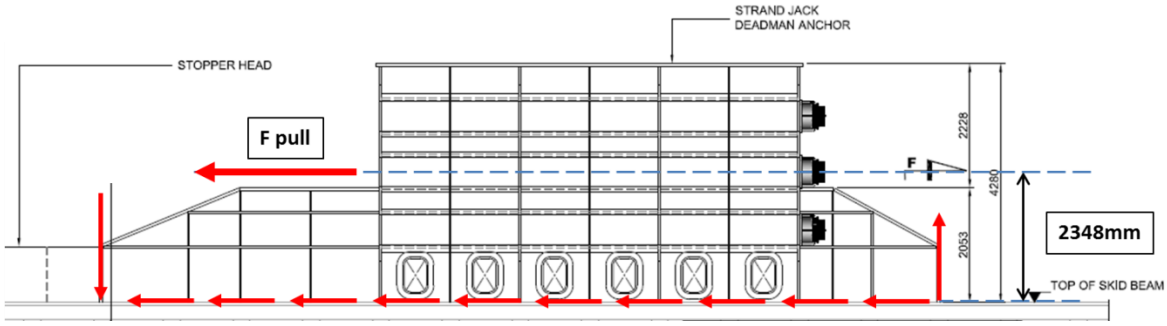

Figure 4-12 Deadman Anchor connection to barge

This same amount of friction force is also applied to the interaction between the bottom of the skidbox and the skidbeams. The total friction force is distributed evenly over the length of skidbox. However the location of the skidbox, as in how much of it is on the quay and how much is on the barge, changes for each step of the load-out. Thus the normal force and moment which are applied onto the barge and quay also change for each step. The arm of the moment due to the friction of the skidbox onto the barge is equal to the distance from the center of the barge to the deck.

For combining both structures, the barge and the whole topside system, Equation 4-2 is expanded with the stiffness matrix equation of the topside system. Both are structures are beam models so they can be simply combined in the same matrix. In matrix Equation 4-6 the approach for this is shown.

Equation 4-6 Stiffness matrix equation topside and barge

$$\begin{bmatrix} K_{Topside} & \\ & K_{Barge} \end{bmatrix} \bullet \begin{bmatrix} U_{Topside} \\ U_{Barge} \end{bmatrix} = \begin{bmatrix} F_{Topside} \\ U_{Barge} \end{bmatrix}$$

Both matrices are now still uncoupled. The springs which were seen in Figure 4-11 connecting the skidbox to the barge still need to be incorporated inside the matrix. The springs actually couple the displacements of the barge with the forces on the topside and vice versa. For example if the barge would move in a positive y-direction the springs would compress and so exert a force on the topside system. In the matrix they would be in the position which was previously empty, see

Equation 4-7 Stiffness matrix incl. connection springs

$$\begin{bmatrix} K_{Topside} & K_{T\text{-}B} \\ K_{T\text{-}B} & K_{Barge} \end{bmatrix} \bullet \begin{bmatrix} U_{Topside} \\ U_{Barge} \end{bmatrix} = \begin{bmatrix} F_{Topside} \\ U_{Barge} \end{bmatrix}$$

The matrix which represents the connecting springs $K_{T\text{-}B}$ changes for each step of the load-out since the amount of nodes as well as which nodes are connected change for each step. See Equation 4-8 for the above right connection matrix.

Equation 4-8 Connection stiffness matrix per step

	K_{spring}							
	↑							
	↑							
	K_{spring}			K_{spring}				
	↑							
	↑							
	K_{spring}	→	→	K_{spring}	→	→	K_{spring}	

In the first step only the last node of the skidbox and the first node of the barge are connected, which is in the bottom left of the matrix. As the skidbox travels further up the barge more nodes are connected. The matrix seen above covers only the first three steps in this process. For the lower left connecting matrix the transpose of this matrix is formed.

4.2.3 Quayside

The final structure that needs to be added to the model is the quayside. The quay will also be modeled as a beam supported on springs. See Figure 4-13.

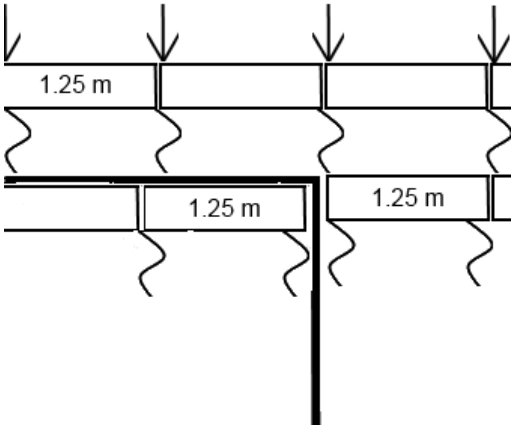

Figure 4-13 Quay modeled as beam elements

The beam itself will represent the concrete foundation slab of the quay. The springs represent the characteristics of the ground below. The stiffness matrix for the quay will look identical to the stiffness matrix for the barge and the skidbox, with a spring support on every node. The beam element size will also be 1.25 meters, analogous to the skidbox beam element size because of node alignment. Further characteristics for the quay will be the topic of chapter 7. Until chapter 7 the HMC method will be used which means that the stiffness of the foundation slab is set to zero and the value for the stiffness of the soil below set to 26579mT/m/m, which is the assumed stiffness by HMC at the DSME yard.

Incorporating the quay into the total system gives the final system seen in Figure 4-14

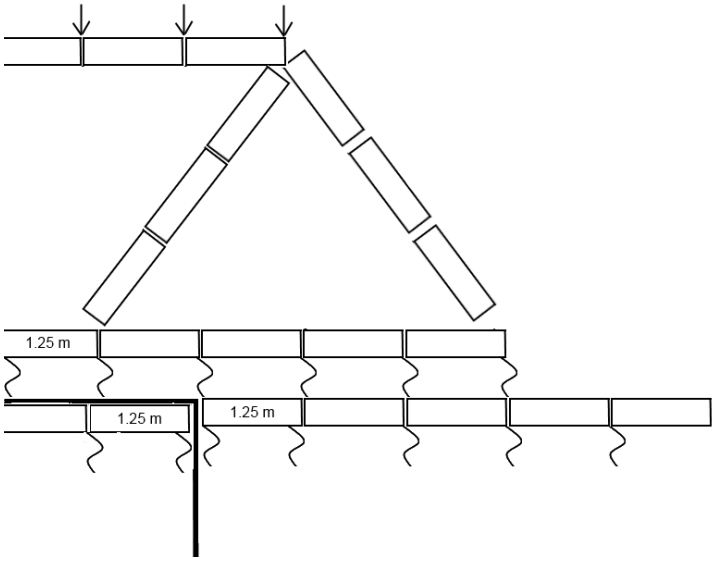

Figure 4-14 Total system including topside, barge and quay

The connection between the skidbox and the quay is formed by springs at every overlapping node. These springs represent the wood inside the skidbeam.

Integrating the quay into the total system is done analogous to the method used in incorporating the topside into the barge. Giving the following matrix equation:

Equation 4-9

$$\begin{bmatrix} K_{quay} & K_{q\text{-}t} & 0 \\ K_{q\text{-}t} & K_{topside} & K_{t\text{-}b} \\ 0 & K_{t\text{-}b} & K_{Barge} \end{bmatrix} \bullet \begin{bmatrix} U_{Quay} \\ U_{Topside} \\ U_{Barge} \end{bmatrix} = \begin{bmatrix} F_{Quay} \\ F_{Topside} \\ F_{Barge} \end{bmatrix}$$

In which the matrix $K_{q\text{-}t}$ form the connection matrix between the quay and the skidbox, this matrix differs per load-out step similar to the matrix in Equation 4-8.

4.2.4 Springs iteration

The springs connecting the skidbox to the quay and the barge still need to be adjusted. Normal springs work in tension and compression but the springs in this model only act in compression. If for example there is a gap between the surface of the skidbox and the barge the springs would still exert a tension force on the skidbox and the barge. Therefore the springs which are in tension need to be removed. This is an iterative process. Removing springs in one location might cause the springs in another location to transform from being in compression to being in tension. The method of incorporating this into the model is described in Figure 4-15

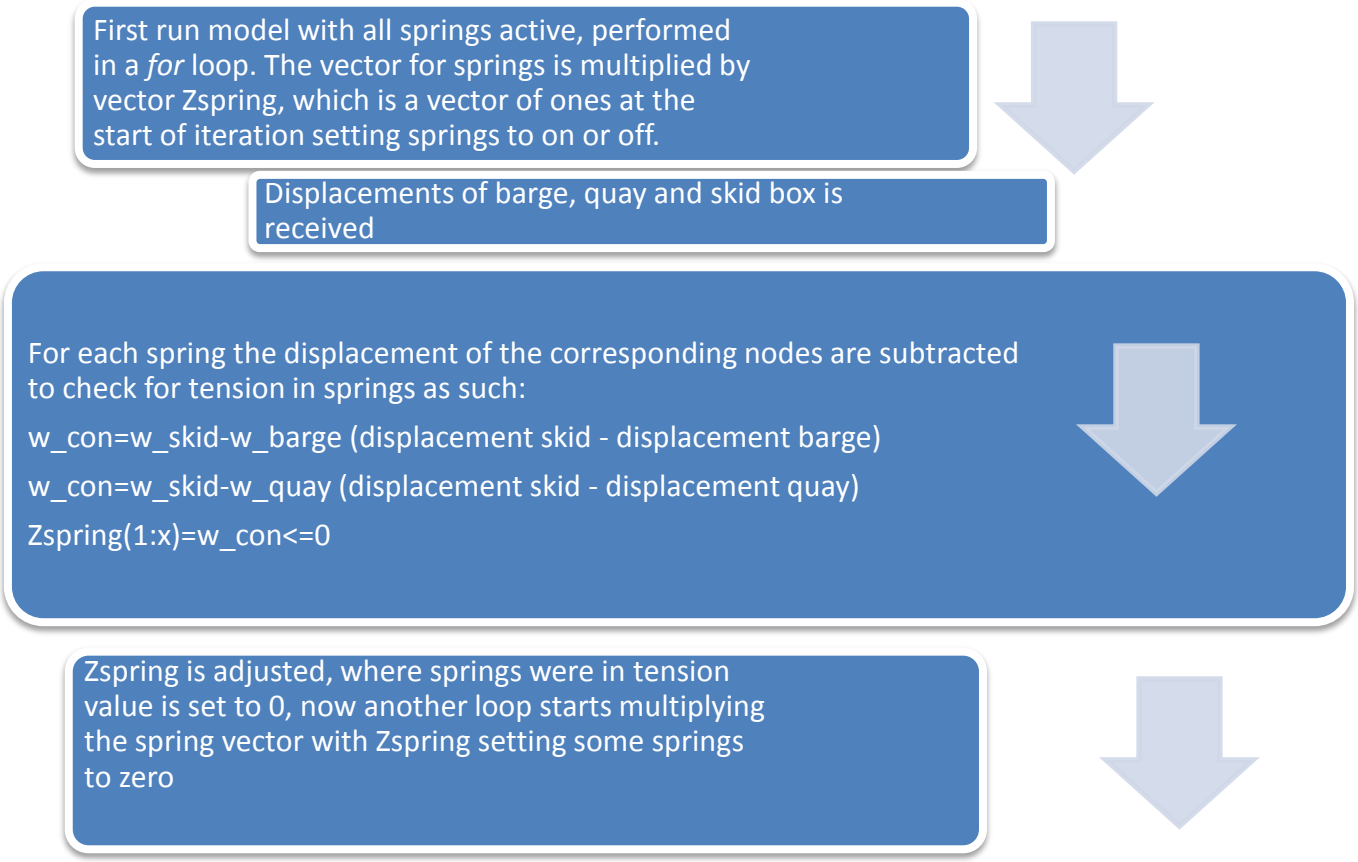

Figure 4-15 For-loop spring iteration

The first run is performed with all the springs being active. From this the displacements of the barge, quay and skidbox is received. Depending on the location of the spring the displacement of the skidbox and the displacement of the quay and barge respectively is compared. If the displacement of the barge or quay is larger than the displacement of the skidbox in a downwards direction the spring is turned off.

The script for setting the springs to zero was tested by using an upper bar connected to a lower bar via the connection springs, same as in the model with the barge and the skidbox. The lower bar has a force on it causing a certain displacement and the upper bar has no forces on it. In Figure 4-16 the upper graph shows the displacement of both bars without the script which sets the springs in tension to zero and the lower graph shows the displacement of the bars while using the script.

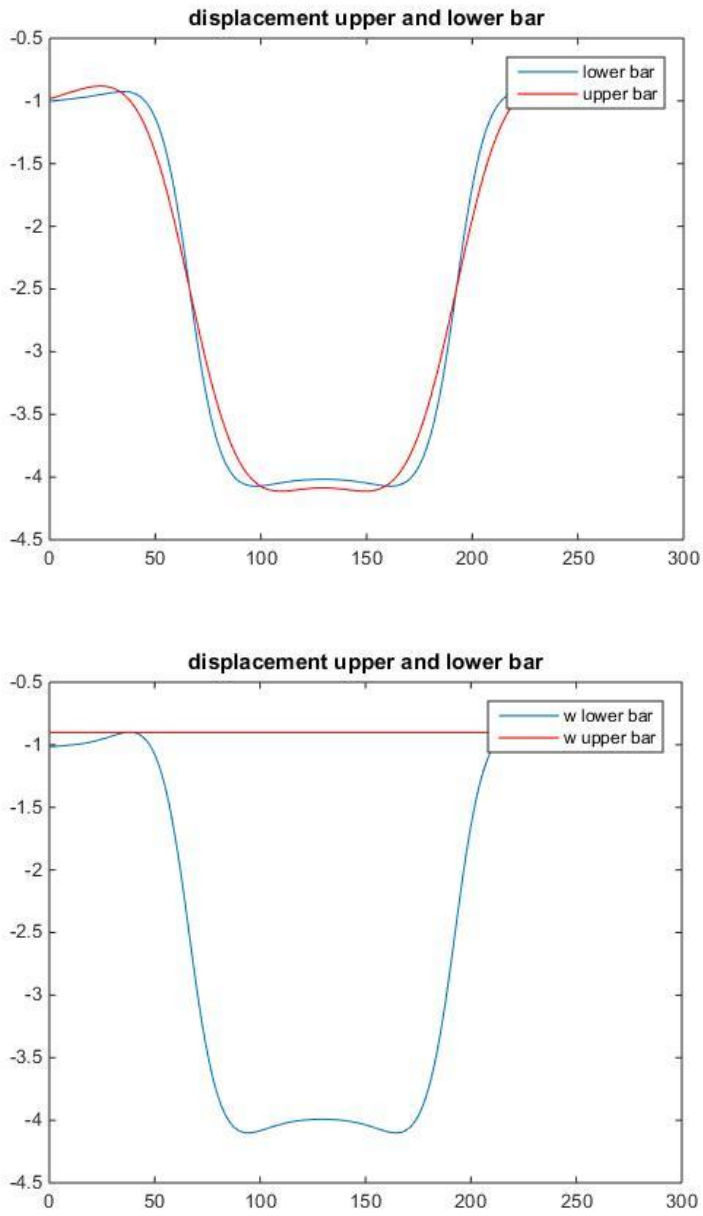

Figure 4-16 Spring iteration example

4.3 Method of verification of the model

To test whether or not the model is an accurate representation of the real life situation described in chapter 3 the model needs to be verified. Unfortunately however HMC has no data available on barge displacements or measured forces during the load-out of the base case topside or any other topside load-out for that matter. So verifying the model with the actual situation wasn't possible.

However the base case load-out was analyzed extensively and a complete 3-D model has been made, see fig. This model was made using FEMAP.

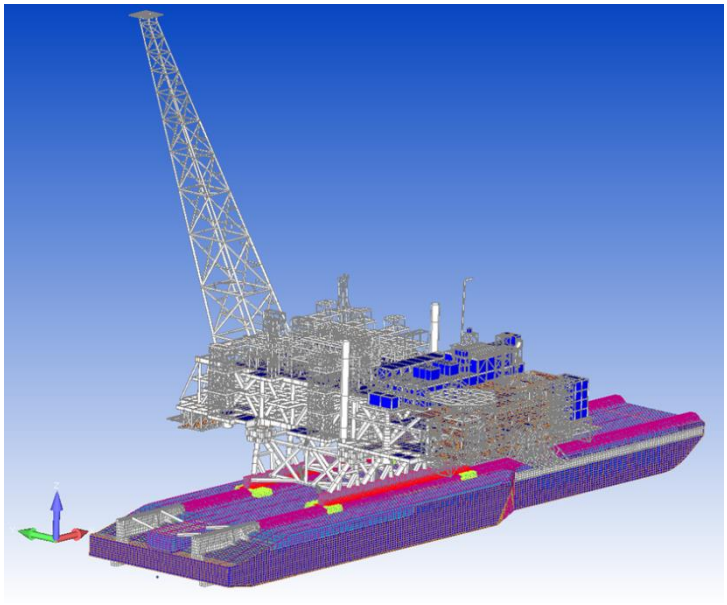

Figure 4-17 3-D FEM model

This model was made for 9 load out steps, each of these steps will also be used to verify the MATLAB model by comparing the displacement of the barge in the FEM model to the displacements of the barge in the MATLAB model. Unfortunately due to this model not being accessible anymore due to HMC changing FEM software this is the only method to verify the model. The 9 load-out steps which were used for this model are:

- Step 1, front DSF at x = 6.125m* (at frame 2, 9% on barge)
- Step 2, front DSF at x = 16.125m* (at frame 7, first intermediate stern wedge support)
- Step 3, front DSF at x = 31.125m (section break stern wedge/skid way fore of DSF)
- Step 4, front DSF at x = 49.250m (section break in skid way fore of DSF)
- Step 5, front DSF at x = 56.125m (75% on barge)
- Step 6, front DSF at x = 74.875m (100% on barge)
- Step 7, front DSF at x = 94.250m (section break in skid way fore of DSF)
- Step 8, front DSF at x = 106.750m (section break stern wedge/skid way aft of DSF)
- Step 9, front DSF at x = 140.500m (final position on barge)

The results which the model gave for these stresses have actually been verified with the actual load-out. Several strain gauges were in place during the base case load-out and the results predicted by the model proved to be quit close to the measured values. In Figure 4-18 an example is given for the resemblance in the values between the model and the strain gauge measurements in ballast tank PS6 for all the 9 steps.

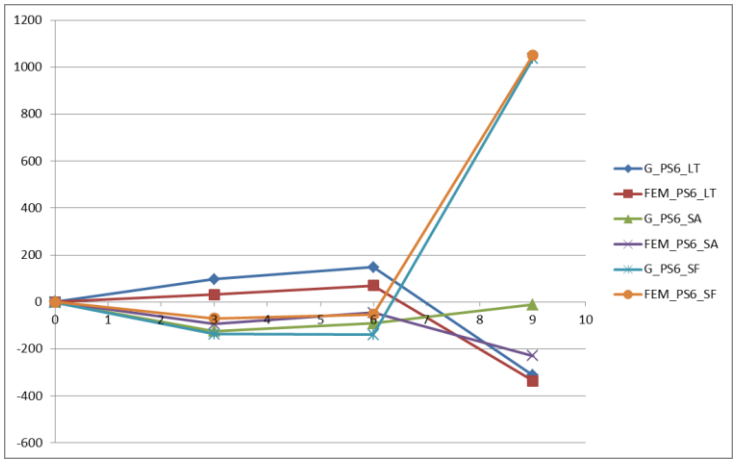

Figure 4-18 Verification of 3-D model with reality

"The strain gauge data and the FEM results match very well at higher strain levels for both linear and shear strains, but the rosette gauge output appears to give significant differences with respect to the FEM results." [2]

These local stresses aren't included in the MATLAB model so can't be used as verification since the MATLAB model mostly focuses on global forces and displacements. That is why the barge displacements is used. These displacements do not match the displacement during the actual load-out due to the fact that another ballast configuration is used for the FEM model. For verifying the MATLAB model this ballast configuration is also used. The results for the barge displacements for each of the 9 steps can be seen in Figure 4-19

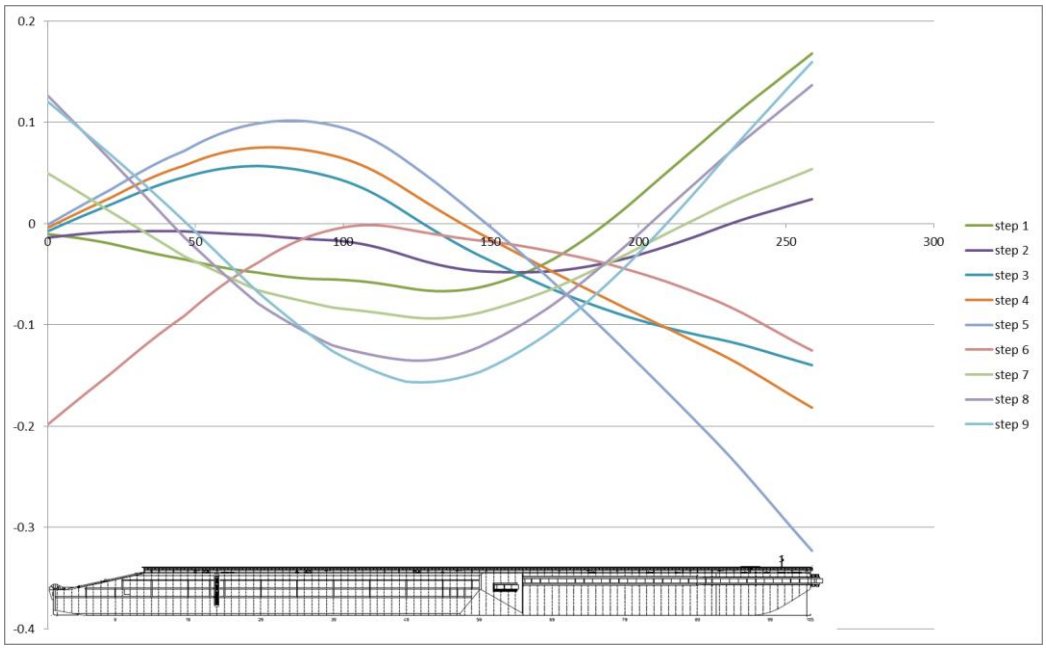

Figure 4-19 Results 3-D model

It shows the displacement of the barge CL longitudinal BKHD at deck level for each load-out step. This location was chosen to make the rotational effects as little as possible since there is no rotation of the barge in the MATLAB model. It is clear that the stern shows no vertical displacement during step 1 to 5, when there is still a part of the DSF on the quayside. Next for step 6 to 9 the deformation

transforms from a hogging to a sagging shape as can be expected when the DSF travels from stern to mid-ship position.

The MATLAB model consists of 113 steps, of these 113 steps the corresponding 9 steps are extracted and the barge deformation for those steps is shown in the graph below.

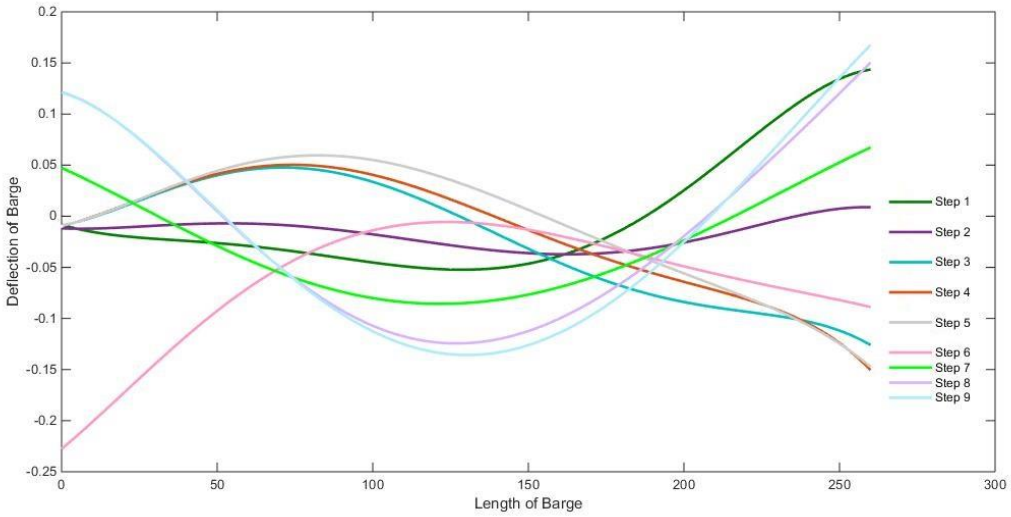

Figure 4-20 Verification of displacement for model

As can be seen the results from the FEM model and the MATLAB model resemble each other. However the results aren't exactly the same. There are several causes for this problem. The major difference is the fact that the FEM-model is a 3-D model and the MATLAB model is a 2-D model. The second big difference is that the MATLAB model will neglect local effects and local stiffness's and focuses on the global stiffness and displacements. The MATLAB model is much less complex compared to the FEM model.

5 Ballast optimization

In order to reduce the forces during the load-out on the topside as well as on the barge, the ballast configuration during each step of the load-out is calculated with the help of the MATLAB-model. It is believed that an optimization of the ballast configuration can lead to lower displacements of the barge and thus lower forces compared to the standard ballast plan. The methods used to achieve this ballast configuration optimization are described in this chapter.

5.1 Least squared method

The goal of the optimization is to keep the barge as level as possible through optimization of the ballast configuration. The deflection from this level barge needs to be as low as possible over the length of the total barge. The level barge also needs to align with the quayside. Supposed the level quayside is taken to be zero, we then have the following least-squares problem:

$$min\|U_{Barge}\|^2$$

With the help of the MATLAB optimization toolbox this can be solved. The method to solve constrained linear least-squares problems is with the help of the "lsqlin" command. This command solves least-squares curve fitting problem of the form:

Equation 5-1

$$min_x\|C \cdot x - d\|^2 \; such\; that \begin{cases} A \cdot x \leq b, \\ Aeq \cdot x = beq, \\ lb \leq x \leq ub \end{cases}$$

The above two constraints aren't used in this situation but the constraint $lb \leq x \leq ub$ is used. The values for these constraints depend on the corresponding ballast tanks. The algorithm used to solve the above equation is the "trust-region-reflective" algorithm. This algorithm is ideally suited for a situation in which there are only upper and lower bounds and no linear inequalities or equalities.

5.2 Reconfiguring the matrix to least squares method

In order to optimize the ballast configuration for the displacements of the barge, the model needs to be rewritten. The model is all written in one matrix as was described in chapter 4. To optimize for the displacements of the barge by ballast adjustment these two factors need to be "isolated" from the model.

The whole system in short can be represented as mentioned in chapter 4:

Equation 5-2

$$\begin{vmatrix} K_{quay} & K_{q\text{-}t} & 0 \\ K_{q\text{-}t} & K_{topside} & K_{t\text{-}b} \\ 0 & K_{t\text{-}b} & K_{Barge} \end{vmatrix} \bullet \begin{vmatrix} U_{Quay} \\ U_{Topside} \\ U_{Barge} \end{vmatrix} = \begin{vmatrix} F_{Quay} \\ F_{Topside} \\ F_{Barge} \end{vmatrix}$$

Using the inverse of the stiffness matrix this is rewritten into:

Equation 5-3

$$\text{inv} \begin{vmatrix} (K_{quay})^{-1} & (K_{q\text{-}t})^{-1} & 0 \\ (K_{q\text{-}t})^{-1} & (K_{topside})^{-1} & (K_{t\text{-}b})^{-1} \\ 0 & (K_{t\text{-}b})^{-1} & (K_{Barge})^{-1} \end{vmatrix} \bullet \begin{vmatrix} F_{Quay} \\ F_{Topside} \\ F_{Barge} \end{vmatrix} = \begin{vmatrix} U_{Quay} \\ U_{Topside} \\ U_{Barge} \end{vmatrix}$$

Here it is very important to note that $(K_{Barge})^{-1}$ doesn't represent the inverse of only K_{Barge} by itself, it represents the cells in the inverse matrix which in the normal matrix are represented by K_{Barge}.

The first optimization is performed with the intention of keeping the displacements of the barge as low as possible, therefore we are only interested in the section U_{Barge}. On the forces side the only section which will change with the optimization is F_{Barge} since this section contains the ballast forces. These need to be isolated from the other forces so that the ballast forces can be optimized. The least squares problem is rewritten into:

$$min\left\|U_{Barge\ due\ to\ ballast} - U_{Barge\ due\ to\ Topside+Barge\ weight}\right\|^2$$

$U_{Barge\ Topside+Barge\ weight}$ is calculated taking the whole system with all the forces excluding the ballast forces. $U_{Barge\ ballast}$, the displacement of the barge due to ballast forces, requires rewriting the matrix in order to isolate the ballast forces. The least squares problem is:

$$min\left\|K * F_{Ballast} - U_{Barge\ due\ to\ Topside+Barge\ weight}\right\|^2$$

The problem is now of the same form as Equation 5-1. K is equal to C, $F_{Ballast}$ is equal to x and $U_{Barge\ due\ to\ topside+barge\ weight}$ is equal to d. In which K hasn't been determined yet and $F_{Ballast}$ is the unknown for the algorithm is trying to solve.

K needs to describe the direct relationship between F_{Barge} and U_{Barge} neglecting all other forces. This is given by the matrix which is formed by the K_{Barge} section of the inverse system matrix which is called $(K_{Barge})^{-1}$. By isolating the relevant sections of the total system matrix the following matrix equation is received.

Equation 5-4

$$(K_{Barge})^{-1} \bullet \begin{bmatrix} F_{x1} \\ F_{y1} \\ F_{M1} \\ \vdots \\ F_{x209} \\ F_{y209} \\ F_{M209} \end{bmatrix} = \begin{bmatrix} U_{Barge} \end{bmatrix}$$

The ballast forces act in one direction only in this model so the horizontal force F_y and the moment F_M can be removed from the equation. The matrix $(K_{Barge})^{-1}$ needs to be adjusted accordingly by erasing the corresponding columns and rows in the matrix. Thus the following equation is formed:

Equation 5-5

$$(K_{Barge,\ Vertical\ forces})^{-1} \bullet \begin{bmatrix} F_{y1} \\ F_{y2} \\ F_{y3} \\ \vdots \\ F_{y207} \\ F_{y208} \\ F_{y209} \end{bmatrix} = \begin{bmatrix} U_{y1} \\ U_{y2} \\ U_{y3} \\ \vdots \\ U_{y207} \\ U_{y208} \\ U_{y209} \end{bmatrix}$$

Equation 5-5 represents a direct relation between the ballast forces at all 208 elements of the barge and the displacement of these elements, so the vertical displacement of the barge and the ballast forces are now isolated from the total system. One more change needs to be made however. As was seen in chapter 4, there are 11 ballast tanks in our model which all extent for several elements. F_{y1} and F_{y2} for example therefore need to have the same value. The matrix equation is therefore adjusted in such a way that the forces on each element are replaced by ballast tanks 1 to 11. It is known which elements correspond with which ballast tank, this is summarized in Table 5-1

Table 5-1 Ballast tanks and the corresponding elements

Ballast 1	Element 1:17
Ballast 2	Element 28:37
Ballast 3	Element 38:57
Ballast 4	Element 58:77
Ballast 5	Element 78:97
Ballast 6	Element 98:117
Ballast 7	Element 118:137
Ballast 8	Element 138:157
Ballast 9	Element 158:177
Ballast 10	Element 178:197
Ballast 11	Element 197:208

To use these ballast tanks in the force vector the matrix equation needs to be adjusted, in particular the stiffness matrix used in Equation 5-5. Since in the force vector F_{y1} to F_{y17} are combined, the columns 1 to 17 from $(K_{\text{Barge, Vertical forces}})^{-1}$ are added together to form $(K_{\text{Barge, Ballast tank forces}})^{-1}$. The final formed stiffness matrix $(K_{\text{Barge, Ballast tank forces}})^{-1}$ is a 209x11 matrix and the matrix equation becomes:

Equation 5-6

$$(K_{\text{Barge, Ballast tank forces}})^{-1} \bullet \begin{bmatrix} \text{Ballast 1} \\ \text{Ballast 2} \\ \text{Ballast 3} \\ \vdots \\ \vdots \\ \vdots \\ \text{Ballast 9} \\ \text{Ballast 10} \\ \text{Ballast 11} \end{bmatrix} = \begin{bmatrix} U_{y1} \\ U_{y2} \\ U_{y3} \\ \vdots \\ \vdots \\ \vdots \\ U_{y207} \\ U_{y208} \\ U_{y209} \end{bmatrix}$$

The optimization is bounded by the values which the ballast tanks can assume. The line load per ballast section was already calculated in chapter 4. The guideline which says that the ballast tanks should be maximum 97% filled and lowest 3% filled is adhered to. The values for the upper and lower boundaries used in MATLAB can be seen in Table 5-2.

Table 5-2 Upper and lower boundaries of ballast tanks

	Lower boundary (lb)	Upper boundary (ub)
Ballast 1	-5727944*0.97	-5727944*0.03
Ballast 2	-8852240*0.97	-8852240*0.03
Ballast 3	-9075466*0.97	-9075466*0.03
Ballast 4	-9066618*0.97	-9066618*0.03
Ballast 5	-6236668*0.97	-6236668*0.03
Ballast 6	-9018353*0.97	-9018353*0.03
Ballast 7	-5930194*0.97	-5930194*0.03
Ballast 8	-5919325*0.97	-5919325*0.03
Ballast 9	-5918118*0.97	-5918118*0.03
Ballast 10	-2166705*0.97	-2166705*0.03
Ballast 11	-4136913*0.97	-4136913*0.03

As the current optimization is the first in a series it shall be denoted optimization A.

5.2.1 Optimization A "Barge level" results

The first optimization is the optimization in which the barge will remain as level as possible, it is expected that this optimization will be most beneficial for the forces in barge compared to the other optimizations. Step 40 is considered first as this is considered an important step during the load-out, although other could also have been chosen. In Figure 5-1 the barge deflection can be seen with the optimized ballast and the standard ballast. The optimization does what it is intended to do and that is keeping the barge as level as possible. Since the deflections aren't that steep in the optimized ballast situation the moment is also lower as can be seen in Figure 5-2. The highest moment in the optimized situation is -0.63 GNm where as in the standard situation the highest moment is -3.2 GNm. This leads to a peak moment reduction in the barge equal to 19% of the original value.

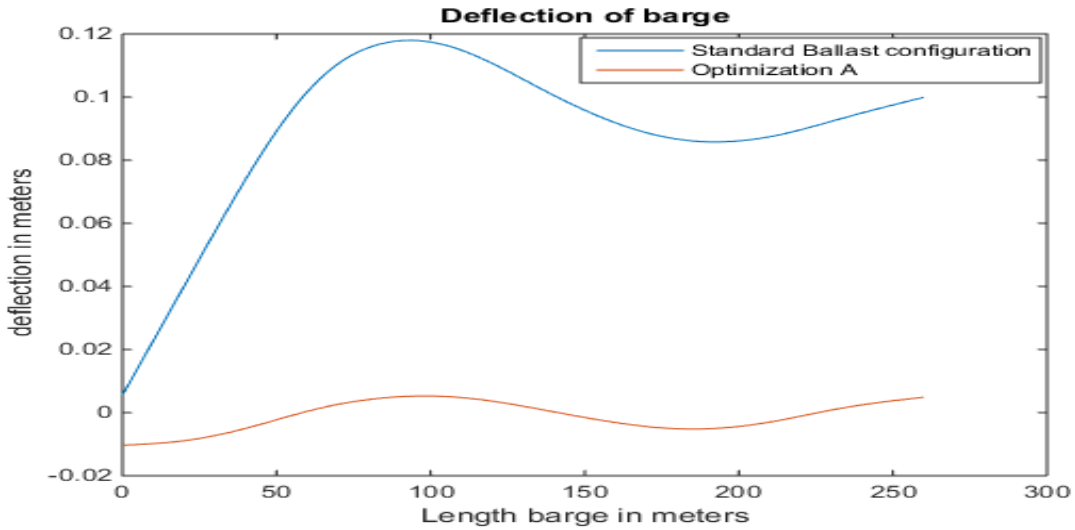

Figure 5-1 Barge deflection Standard vs Optimized

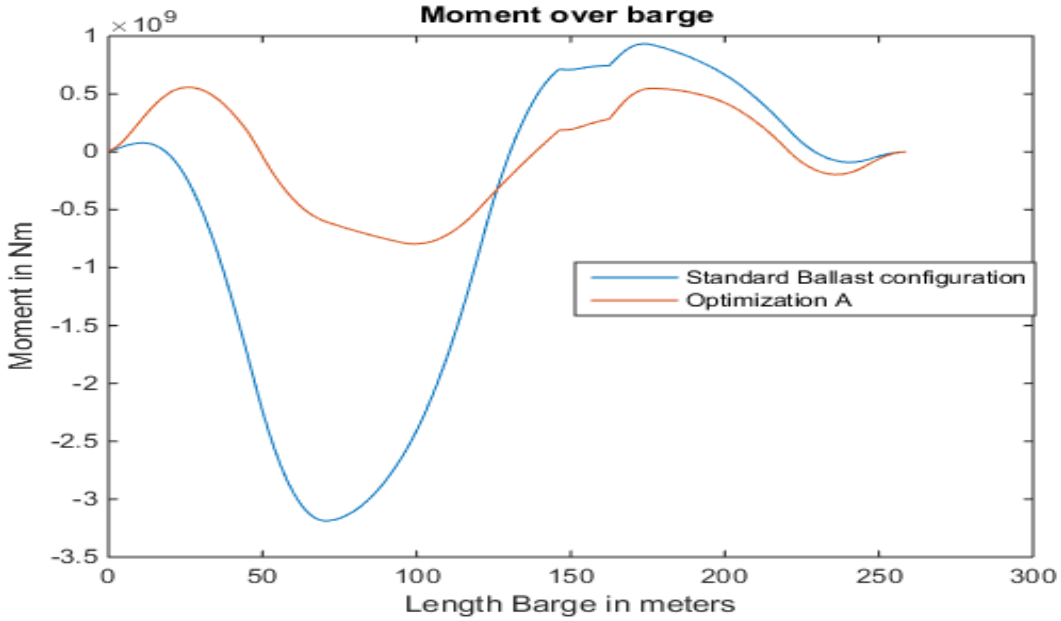

Figure 5-2 Moment over Barge Standard vs Optimized ballast configuration

The shear force in the barge is also reduced significantly as can be seen in Figure 5-3.

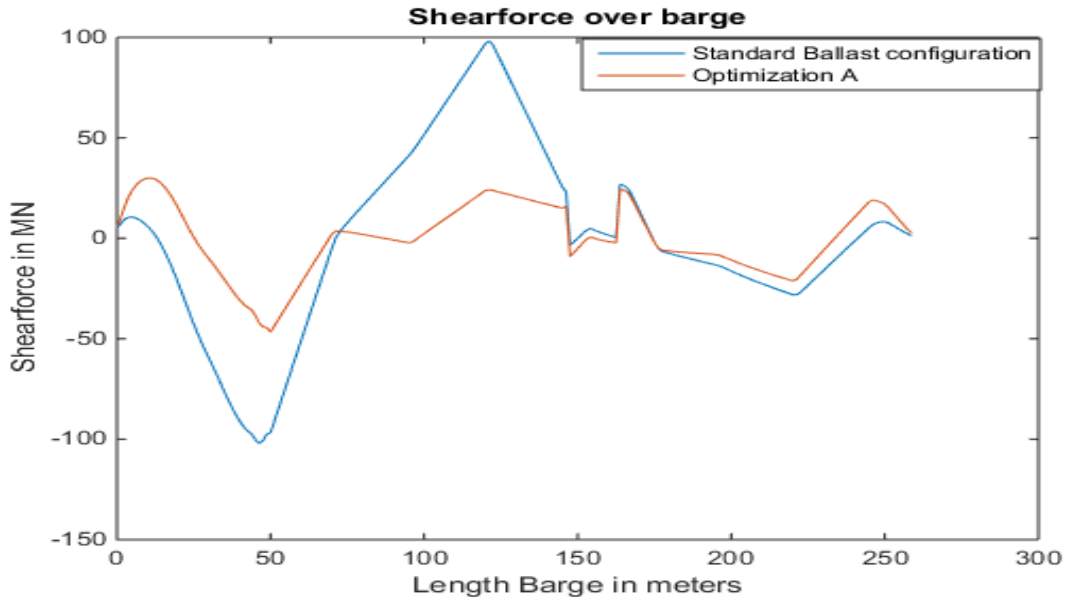

Figure 5-3 Shear force over Barge Standard vs Optimized ballast configuration

However what can also be seen is that with this optimization in this specific case, the barge level at the alignment with the quay drops below the quay level. This will cause the skidbox to lose support just past the quay. The skidbox will now deflect downwards, as can be seen in Figure 5-4

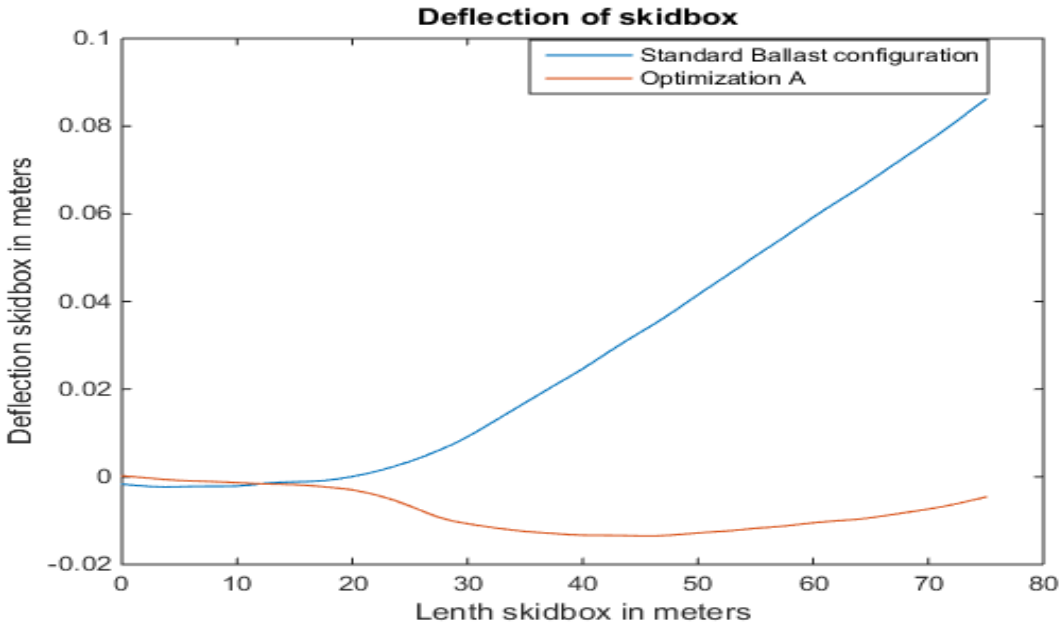

Figure 5-4 Skidbox deflection Standard vs Optimized ballast configuration

The effects of this on the moment over the skidbox can be seen in Figure 5-5.

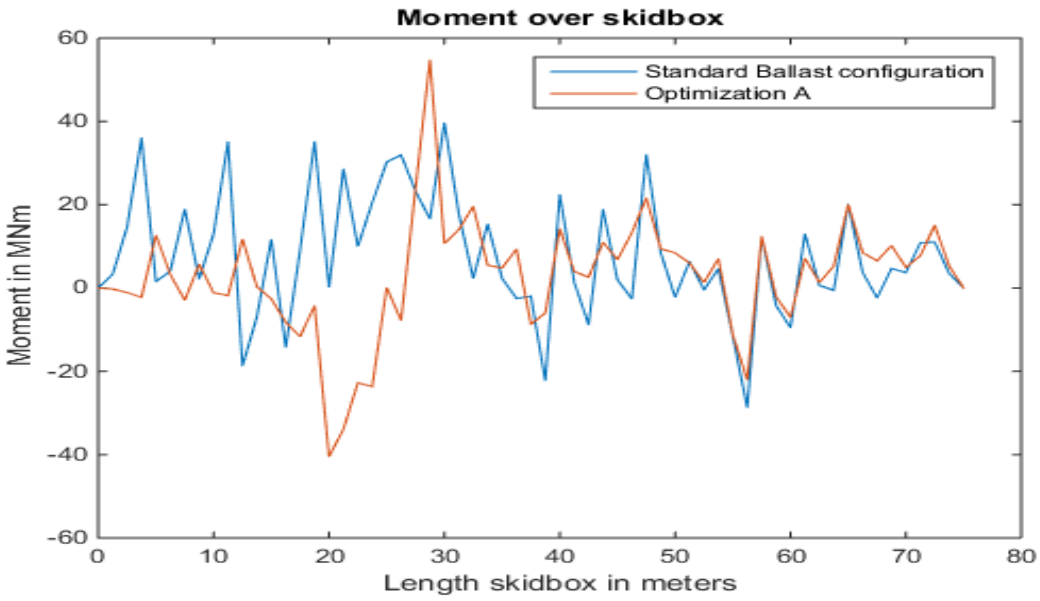

Figure 5-5 Moment distribution over skidbox Standard vs Optimized

Due to the skidbox in the optimized situation deflecting downwards first instead of upwards immediately, there is a distinct negative peak moment first followed by a positive peak moment where the skidbox slowly deflects upward. The positive peak moment increases with the optimization from 38 MNm to 55 MNm, which is an increase of 44%, so for step 40 the optimization forms no improvement for the moment over the skidbox. At other locations on the skidbox the moment however is reduced with the optimization.

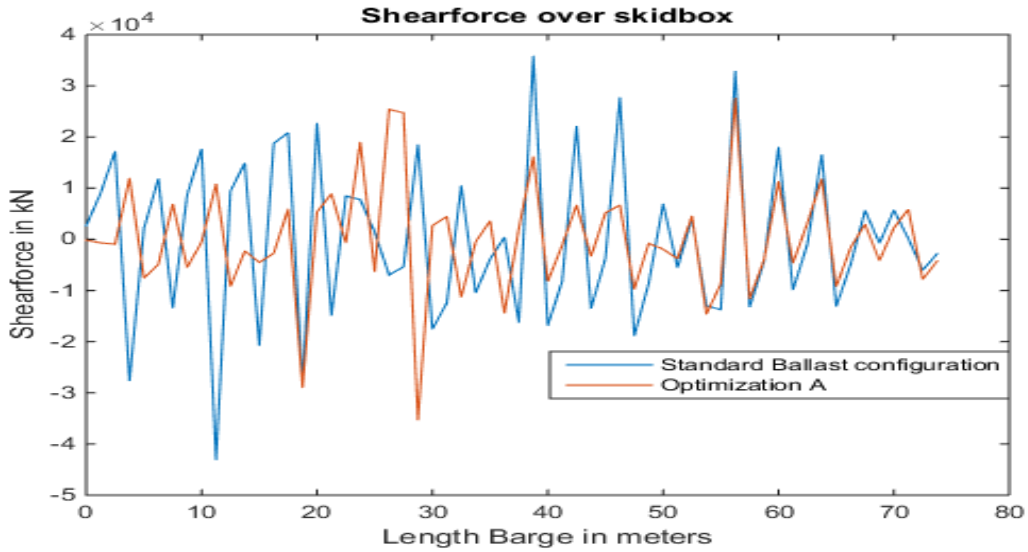

Figure 5-6 Shear force distribution over skidbox Standard vs Optimized

As can be expected from the moment distribution, the shear force also shows an increase at the barge-quay connection. However the peak shear force is reduced from -4.2*10^4 kN to-3.6*10^4 kN which is a reduction of 15%

Concluding it can be said that for step 40 in the load-out this optimization is beneficial to reduce the peak moment in the barge but not in the skidbox. However the goal wasn't to reduce the peak moment

of only the barge but also for the topside, represented here by the skidbox. Because the optimization isn't beneficial for step 40 doesn't mean that this is the case for every of the other load-out steps, in the MATLAB model there are 113 steps. Now a look is taken at the peak moment for the barge and skidbox for each section for all the load-out steps. This way it is possible to see what the effects of the optimization are for the overall load-out. Negative and positive moment is considered equally damaging so for the sake of drawing a conclusion from the following graphs only the absolute value for the moment is shown.

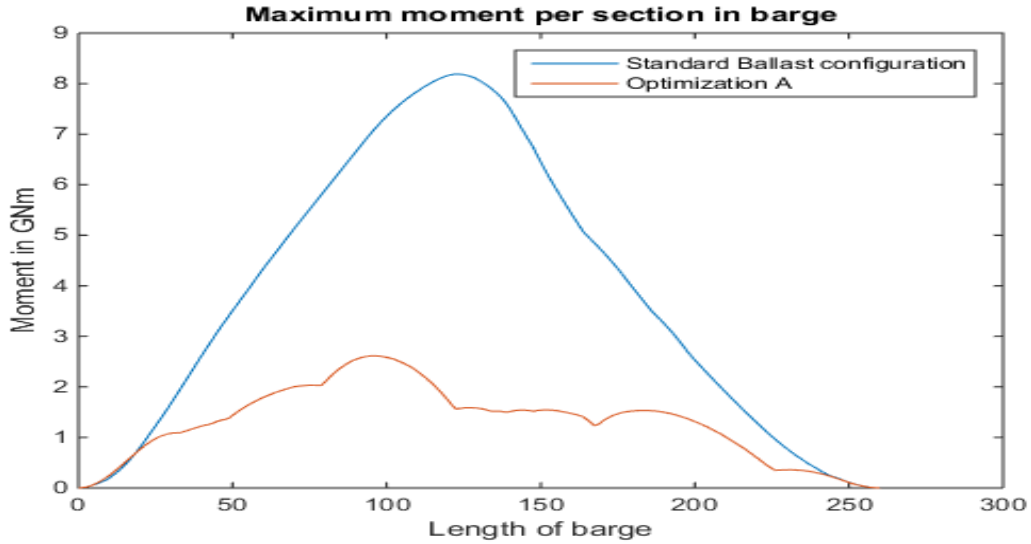

Figure 5-7 Maximum moment per section of barge

In Figure 5-7 it could be seen that the maximum moment per section of barge is significantly reduced. This is mostly due to the sagging which the barge does in the standard ballast configuration but doesn't do in the optimized version. These results were expected with this type of optimization. The resulting reduction in peak moment is from 8.1 GNm to 2.5 GNm which is a reduction of 70%. The maximum shear force is also reduced as can be seen in Figure 5-8.

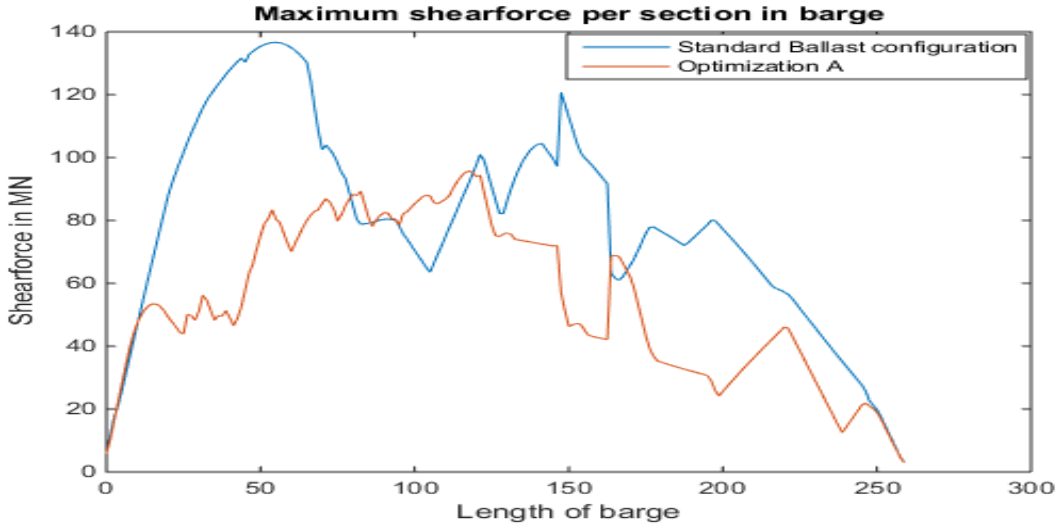

Figure 5-8 Maximum shear force per section barge

The results for the maximum moment per section of the skidbox aren't as clear-cut as it is for the barge as can be seen in Figure 5-9. The effects of the optimization clearly benefit the last section of the skidbox the most with a reduction from 66 MNm to 21 MNm in the last peak. In the 0m to 40m range however the optimization negatively influences the max moment. The highest peak moment for optimization equals 78 MNm whilst for the standard ballast configuration the highest peak moment was 66 MNm albeit in a different location on the skidbox.

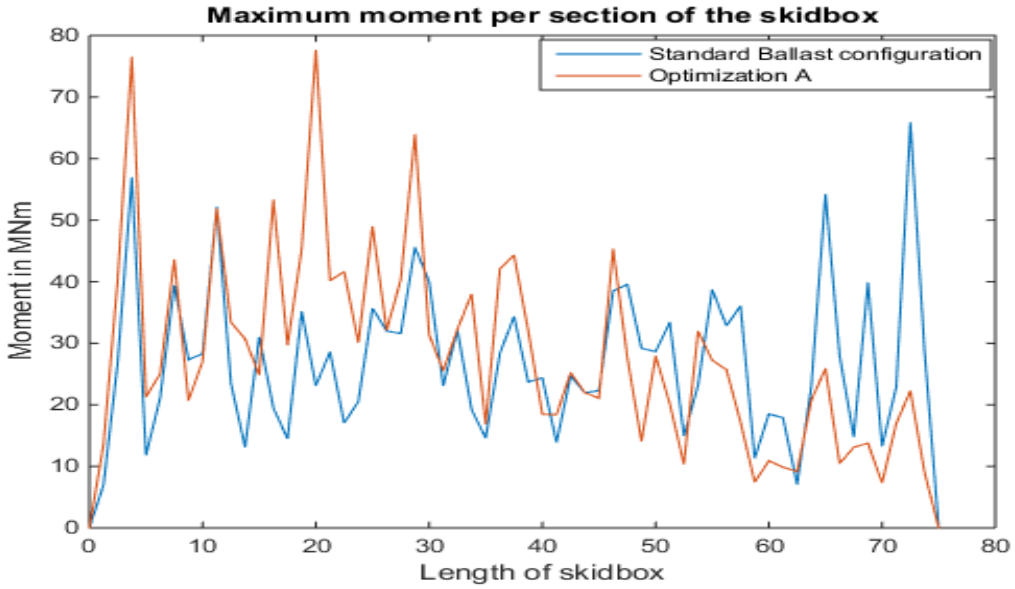

Figure 5-9 Maximum moment per section skidbox

Almost the same can be said for the maximum shear force seen in Figure 5-10. In order to understand these results better it is also interesting in which step the maximum moment occurs for the barge and the skidbox, this can be seen in Figure 5-11.

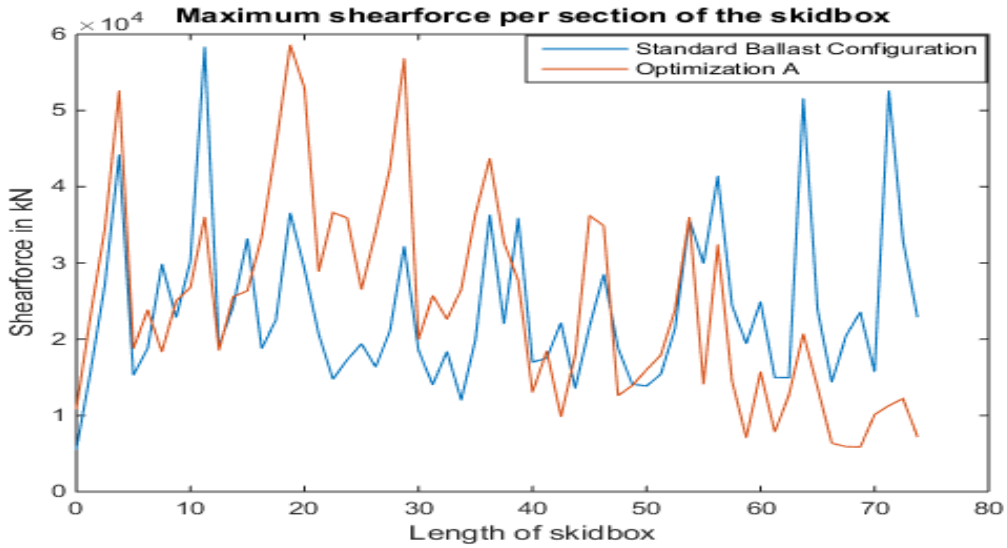

Figure 5-10 Maximum shear force per section skidbox

Looking at Figure 5-11 it is evident that for the optimized ballast configuration the highest maximum moment occurs in the steps in which the skidbox is still partially on the quay. After step 61, which is the step where the skidbox leaves the quay and is placed on the barge, the maximum moment in the optimized situation becomes very small due to the fact that the barge forms a level platform. In the standard situation one can identify the increasing sagging of the barge as the skidbox travels along the barge in both figures. The skidbox will "form" after the deformation of the barge and will also have a sagging shape. For the barge the optimization performs very well for all the steps, the increasing sagging for steps 61+ which occur in the standard ballast configuration don't occur at all in the optimization.

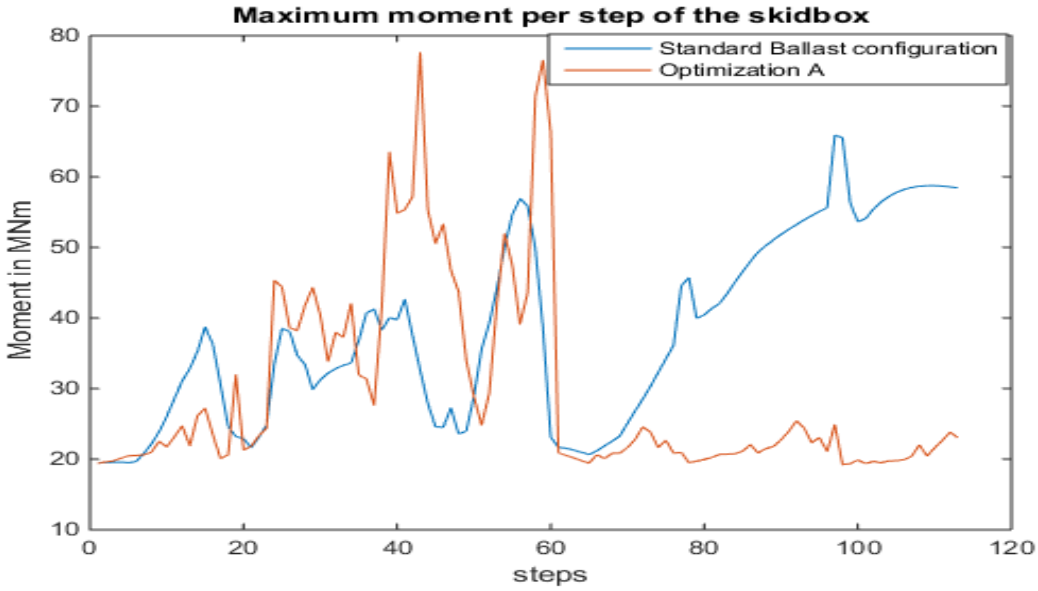

Figure 5-11 Maximum moment per step for skidbox

This increasing sagging of the barge can also clearly be seen in Figure 5-12. Especially after step 66 the maximum moment over the barge keeps increasing.

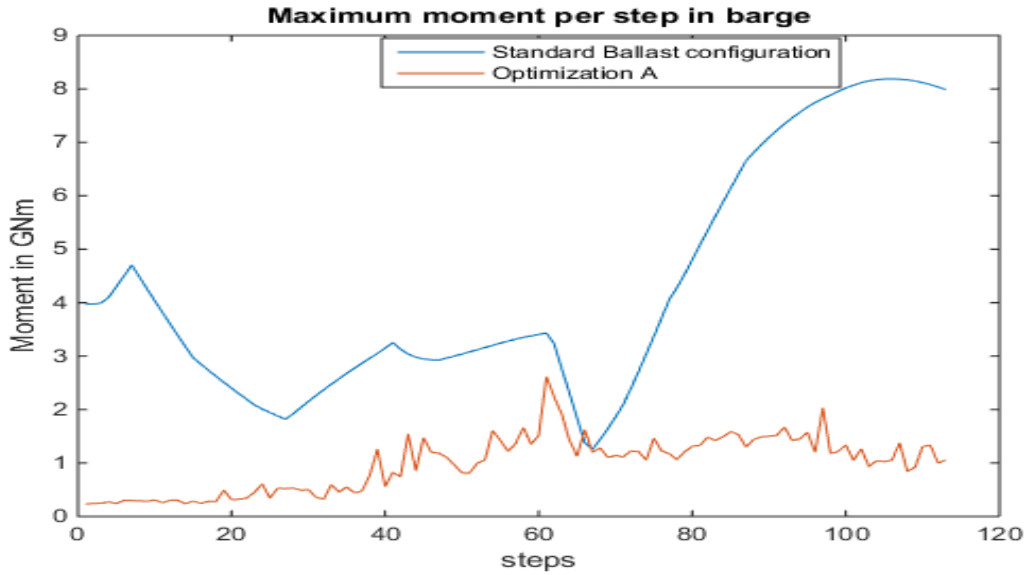

Figure 5-12 Maximum moment per step for barge

So concluding it can be said that considering all the load-out steps the optimization in which the barge is kept as level as possible is very beneficial for the barge with a reduction in maximum moment of almost 6 GNm. However for the skidbox there is an increase in the peak moment using this optimization. As could be seen in the graphs about the maximum moment per step in the skidbox, the steps in which the skidbox is still partially on the quay causes high moments in the skidbox using optimization A. It is believed that an optimization which puts more emphasis on keeping the alignment between quay and barge as perfect as possible whilst maintaining a level barge is a more suitable optimization for the ballast arrangement during the load-out. This is the topic of the next paragraph.

5.3 Optimization of Barge to Quay connection alignment

A crucial point in the load-out process of a topside as well as a jacket is the alignment of the barge with the quay. Misalignment at this point can lead to very high stresses in the barge as well as the topside. For example if the deck of the barge extends beyond the level of the quay causing the edge of the barge to "carry" very high loads because at the quayside the topside will be unsupported.

The optimization in the previous paragraph was based on keeping the barge as level as possible, meaning the average deflection of the barge was overall as close to 0 as possible. Another optimization can however be made, which makes sure that the alignment between the barge and the quay is perfect. It is to be expected however that this condition creates a worse performance in keeping the barge level meaning the results from the least squares method will be worse thus the deflections overall of the barge will increase. To achieve this a look back is taken at Equation 5-1. In the previous optimization the only boundaries that were imposed on the linear least squared method used in MATLAB were the lower and upper bound which could be achieved by the ballast forces. In this section an addition is made to these bounds.

Looking back at Equation 5-1, the linear equality constraints $Aeq*x=beq$ which were previously ignored are now used to force perfect alignment between barge and quay. This will be achieved by isolating the displacement at the stern of the barge in Equation 5-6. In the matrix Equation 5-7 below U_{y1} should be equal to the opposite of the displacement caused by the forces excluding the ballast force added with the displacement of the last node of the quayside. Therefore U_{y1} is isolated from the other displacements as shown below by taking the first row of $(K_{\text{Barge, Ballast tank forces}})^{-1}$ and multiplying it with the ballast vector so U_{y1} is received.

Equation 5-7

Row 1		Ballast 1		U_{y1}
		Ballast 2		U_{y2}
		Ballast 3		U_{y3}
		⋮		⋮
$(K_{\text{Barge, Ballast tank forces}})^{-1}$	•	⋮	=	⋮
		⋮		⋮
		Ballast 9		U_{y207}
		Ballast 10		U_{y208}
		Ballast 11		U_{y209}

The linear equality constraints Aeq will now represent the first row of the matrix K_{Barge}, and beq which represents U_{y1} will be equal to the opposite of the displacement of the first node of the barge when the ballast force is excluded added with the displacement of the quayside.

5.3.1 Results

With this optimization the results are expected to improve significantly for the skidbox. First a look will be taken what the effects will be on step 40 as this makes it easy to compare with the previous optimization. The results on both the barge and the skidbox with the new optimization, which is called optimization B, will be compared to the results of optimization A and the standard ballast configuration.

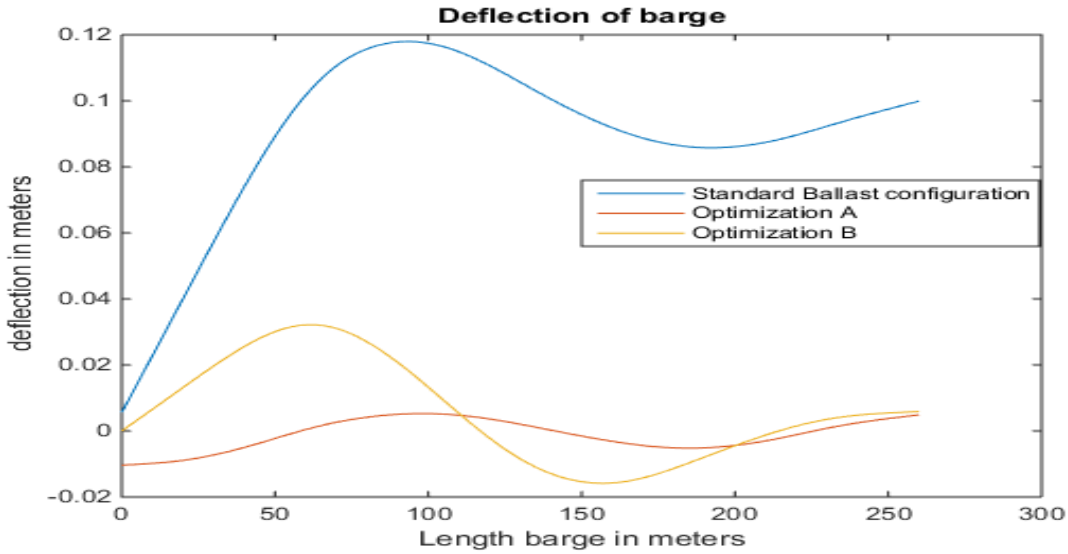

Figure 5-13 Deflection of barge for step 40, optimization A&B

It can be seen that in the case of step 40 the supposed sacrifice which is made in barge deflection due to the optimization now having to take into account another boundary condition doesn't happen as severe as was expected. The average deflection in Optimization B is larger than for optimization A but it still performs better than the standard ballast configuration. The effects on the moment distribution for the barge can be seen in Figure 5-14. Here it can be seen that for optimization B the maximum moment in the barge is higher than for optimization A, so here a significant sacrifice is made, although it still outperforms the standard ballast configuration in terms of absolute maximum moment. Compared to optimization A the highest moment increases from 0.45GNm to 2.6 GNm which is an increase of 577%.

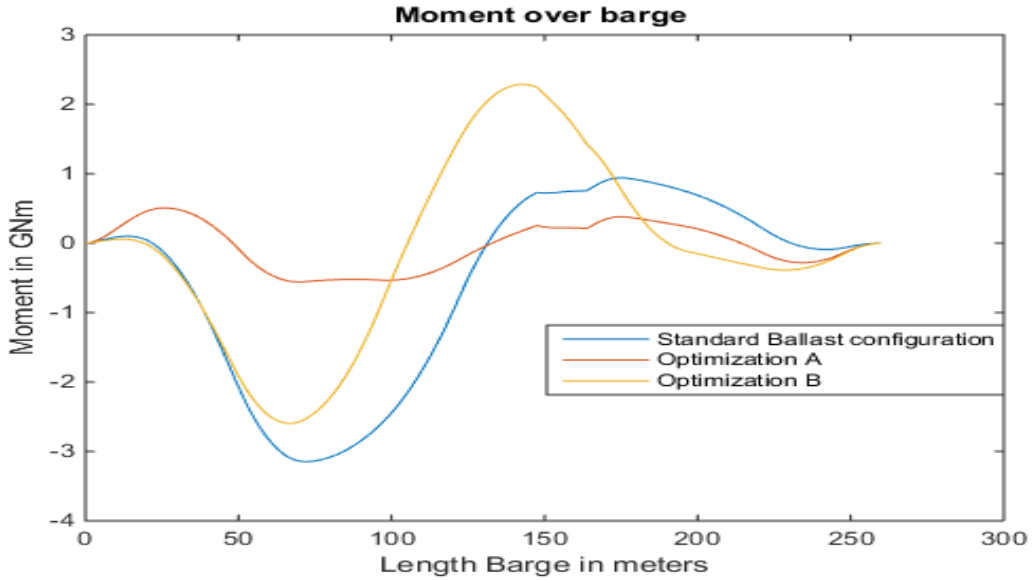

Figure 5-14 Moment over barge for step40, Optimization A&B

The results of the effects on the shear force over the barge are similar to the effects on the moment. The shear force increases compared to optimization A and is more similar to the standard ballast configuration as can be seen in Figure 5-15.

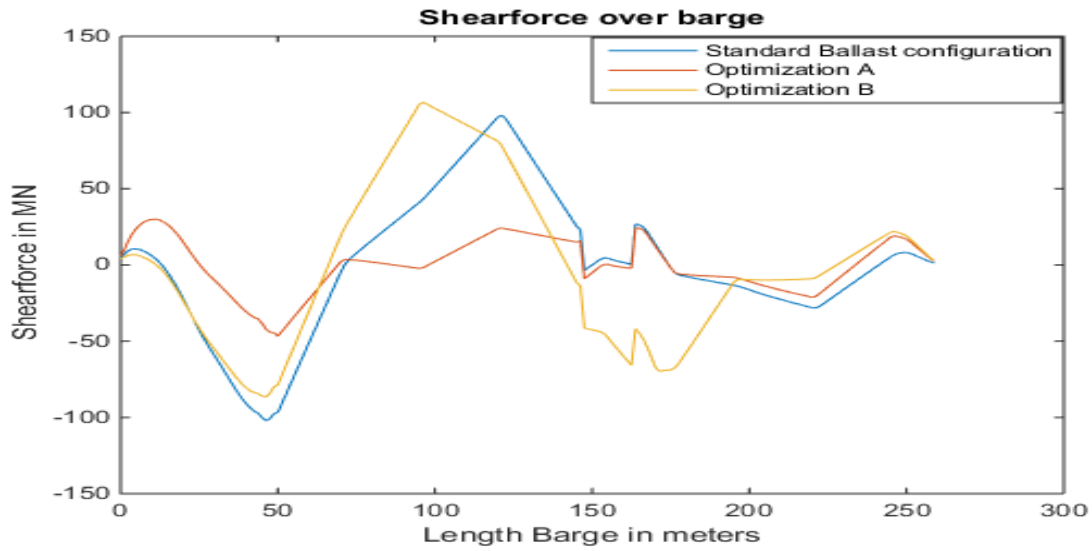

Figure 5-15 Shear force over barge for step40, Optimization A&B

For Optimization A step 40 gave a high moment in the skidbox due to incorrect alignment of barge and quay. Optimization B is aimed specifically to reduce this misalignment. It can be seen in Figure 5-16 that the deflection of the skidbox is definitely less than in the standard configuration and it doesn't have the drop off which occurs at the quay-barge connection (which for step 40 is at 28.75m) with optimization A.

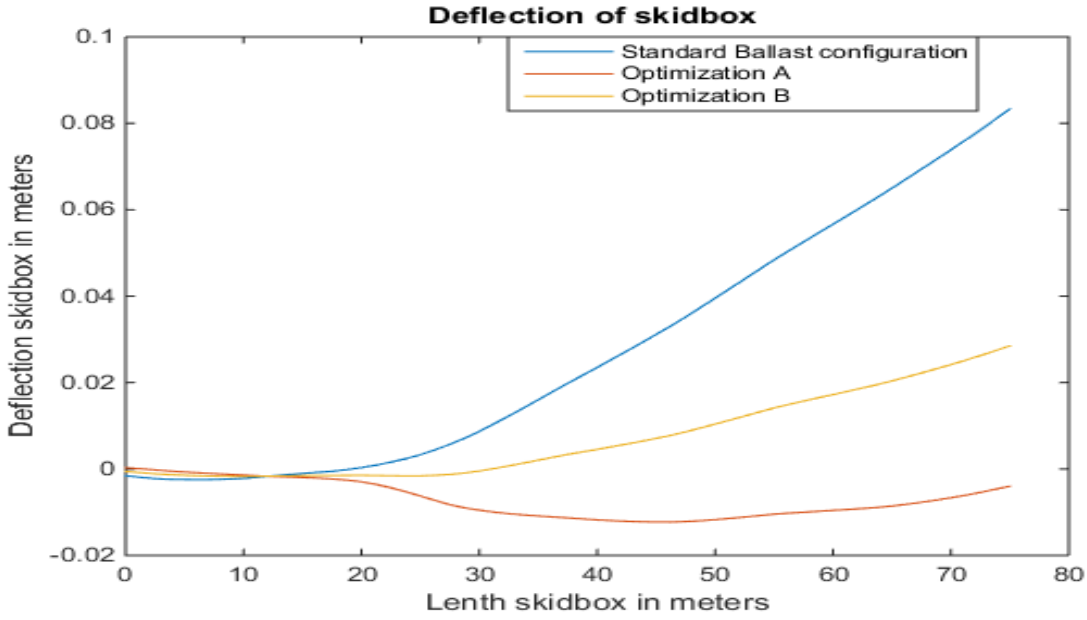

Figure 5-16 Deflection of skidbox for step 40, Optimization A&B

The effects on the moment distribution over the skidbox will thus also be significant. As can be seen in Figure 5-17 the reduction in moment compared to both optimization A and the standard situation is very large. A reduction of 61% compared to A (from 55 MNm to 21 MNm) and a reduction of 44% (from 38 MNm to 21 MNm) compared to the standard configuration. It also performs better for the shear force as can be seen in Figure 5-18. Especially around the barge-quay connection the shear force over the skidbox is significantly reduced.

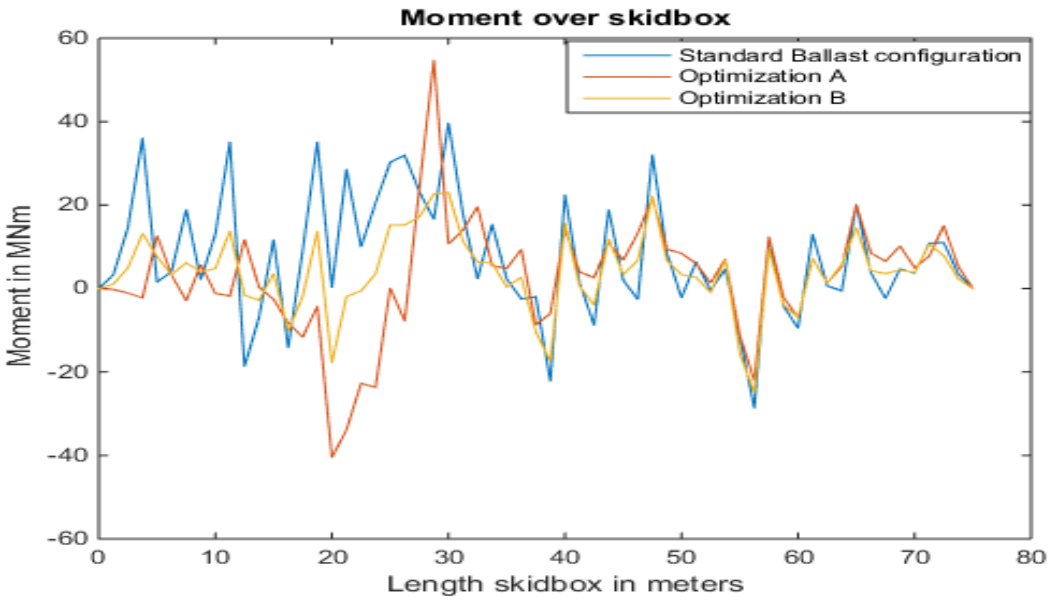

Figure 5-17 Moment over skidbox for step 40, Optimization A&B

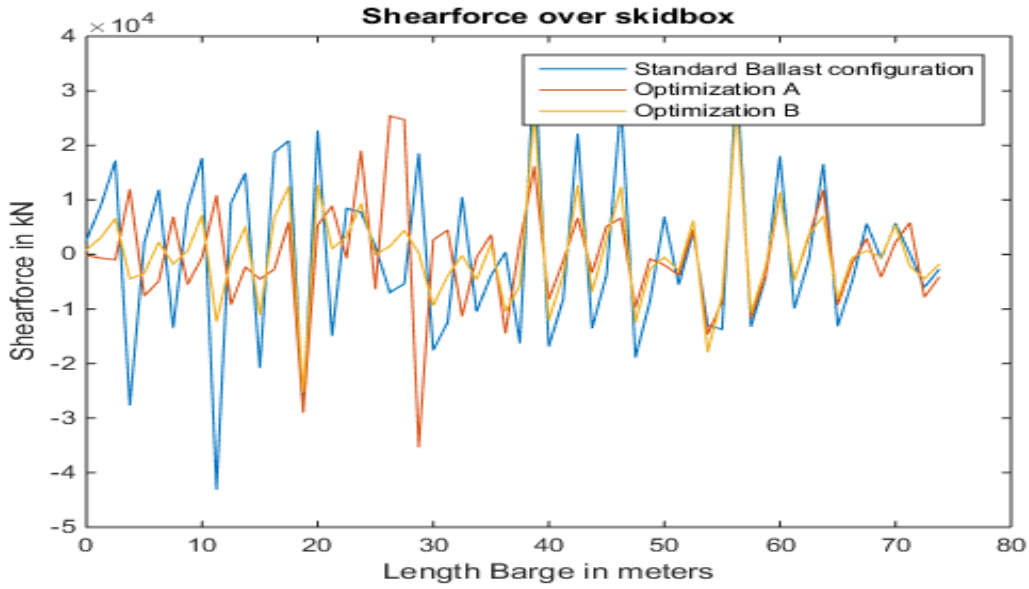

Figure 5-18 Shear force over skidbox for step 40, Optimization A&B

So for step 40, optimization B performs much better with a lower peak moment for the skidbox. However it does make sacrifices in terms of maximum moment in the barge.

Next the performance over the whole load-out needs to be compared. Just like with the previous optimization the maximum moment per section for both the skidbox and the barge will be the indicator to which the optimizations will be compared, the same will be done for the shear force. First a look is taken at the performance for the barge, seen in Figure 5-19. The expected sacrifice optimization B would make compared to optimization A for the maximum moment in the barge for all the steps isn't as significant as was expected. Apparently the extra boundary condition doesn't affect the optimization as much as was expected, as the increase compared to optimization A only equals 0.4 GNm.

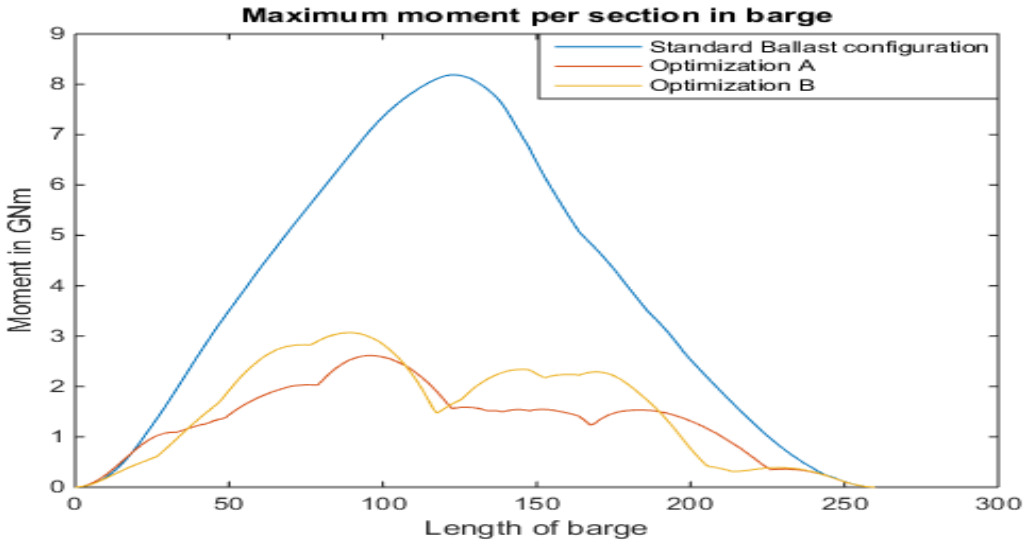

Figure 5-19 Maximum moment in barge per section, Optimization A&B

For the maximum shear force in the barge the sacrifice which optimization B makes compared to optimization A is more significant, as can be seen in Figure 5-20. Especially in the 100-150 meter range the difference is significant. The highest shear force for optimization B is 148 MN whilst for optimization A this was only 93 MN.

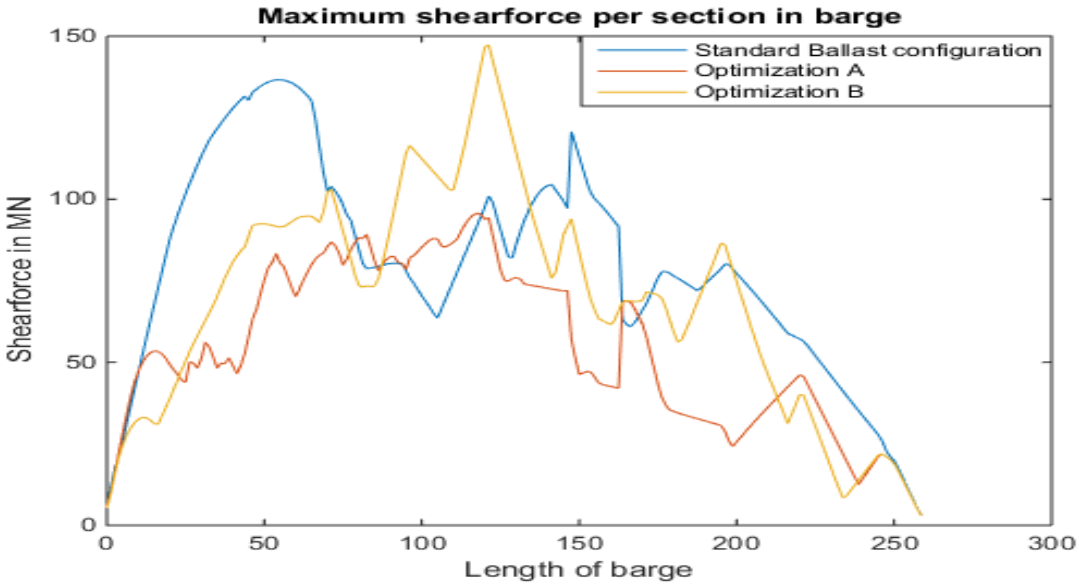

Figure 5-20 Maximum shear force in barge per section, Optimization A&B

For the skidbox optimization B was expected to perform much better compared to both optimization A and the standard configuration. It can be seen in Figure 5-21 that this reduction in maximum moment for optimization B is very significant. A reduction of 67% is achieved for the peak moment compared to optimization A (from 78 MNm to 25 MNm) and a reduction of 62% (from 65 MNm to 25 MNm) compared to the standard optimization.

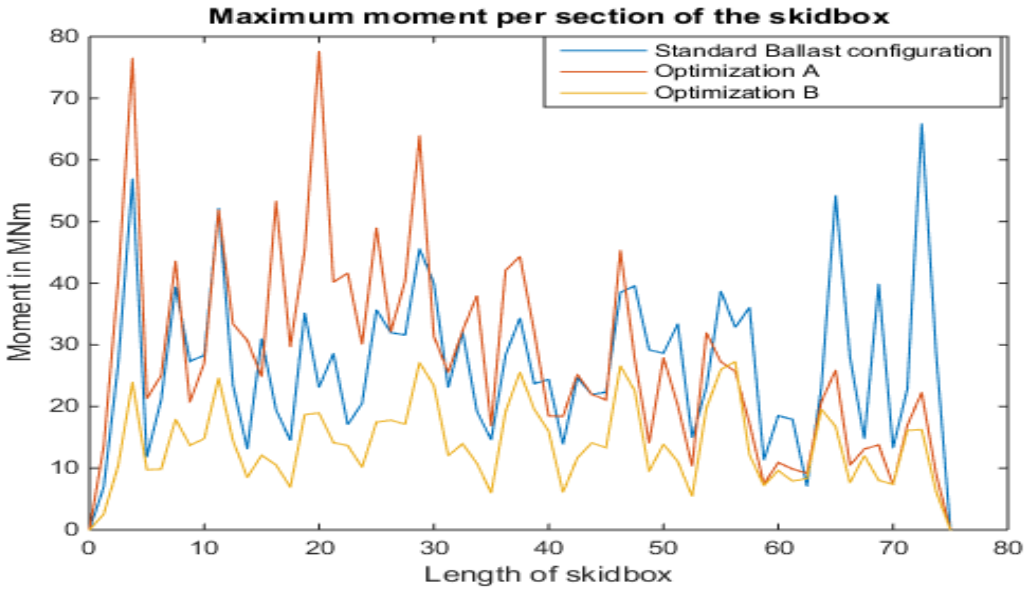

Figure 5-21 Maximum moment in skidbox per section, Optimization A&B

As can be seen in Figure 5-22 the maximum shear force per section is also reduced over all the sections using optimization B. The highest shear force is reduced from 5.8 *10^4 kN using optimization A to 2.8*10^4 kN using optimization B.

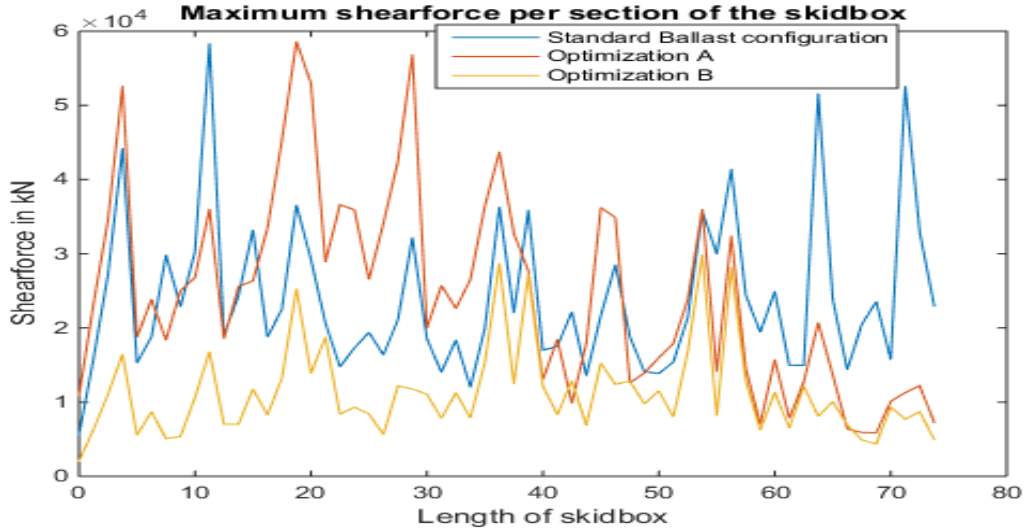

Figure 5-22 Maximum shear force in skidbox per section, Optimization A&B

It is also interesting to look at the maximum moment per step for the barge and the skidbox. Here the shear force is omitted because the “per step” comparison gives a similar picture for the maximum moment per step and the maximum shear force per step. The maximum moment per step can be seen in Figure 5-23 for the barge and in Figure 5-24 for the skidbox. It can clearly be seen that especially

for the skidbox the most critical steps in the standard configuration and in optimization A are completely reduced with optimization B. Where optimization A still showed a high moment as long as the skidbox was still partially on the quay, using optimization B these high moments are completely gone. For the barge it can be seen that as long as the skidbox is still partially on the quay the maximum moment it experiences is slightly higher than compared to optimization A, however this difference is marginal compared to the difference with the standard ballast configuration for steps 61+.

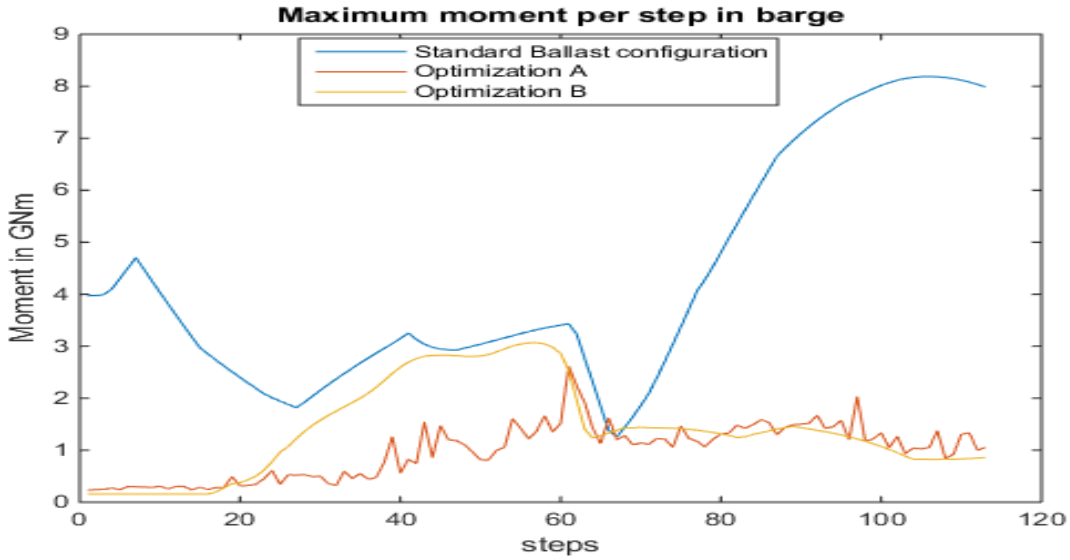

Figure 5-23 Maximum moment in barge per step

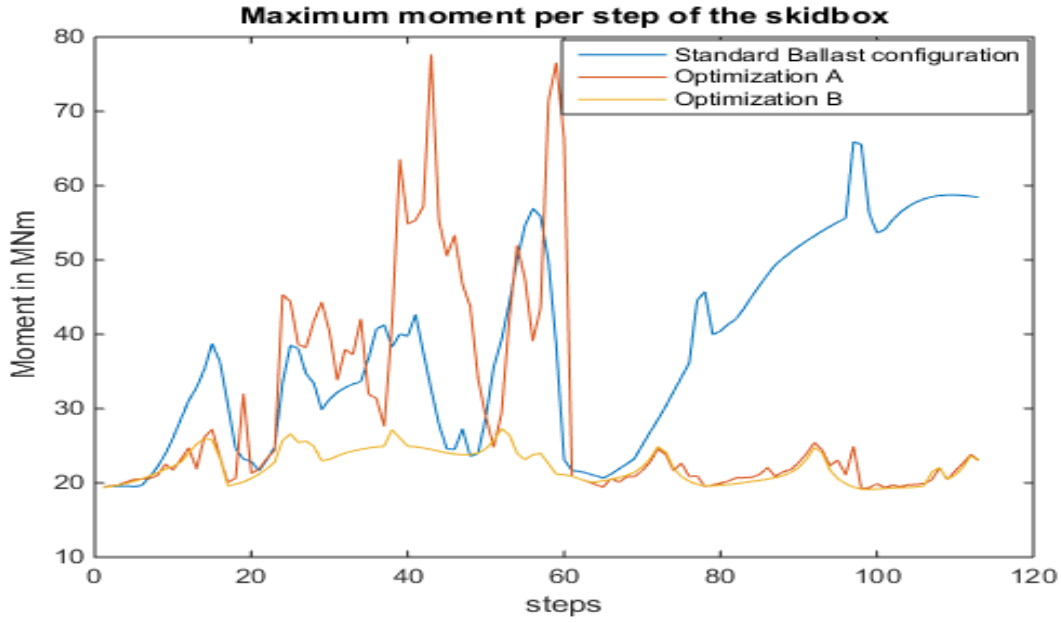

Figure 5-24 Maximum moment in skidbox per step

5.4 Optimization of Topside rotations

In the previous two paragraphs the norm to which the ballast was optimized was the barge aligning with the quay and being as level as possible. However other optimizations can be made. The optimization where the barge is as level as possible doesn't necessarily have to be the optimum situation for the forces in the topside or jacket which is being loaded-out. In this model the forces in the topside are also taken into account and thus can also be optimized.

The norm which will be used for the optimization will be the rotations at 4 specific points in the topside-DSF connection, see Figure 5-25. It is assumed that keeping the rotation at these points as low as possible will result in reducing the forces over the entire topside.

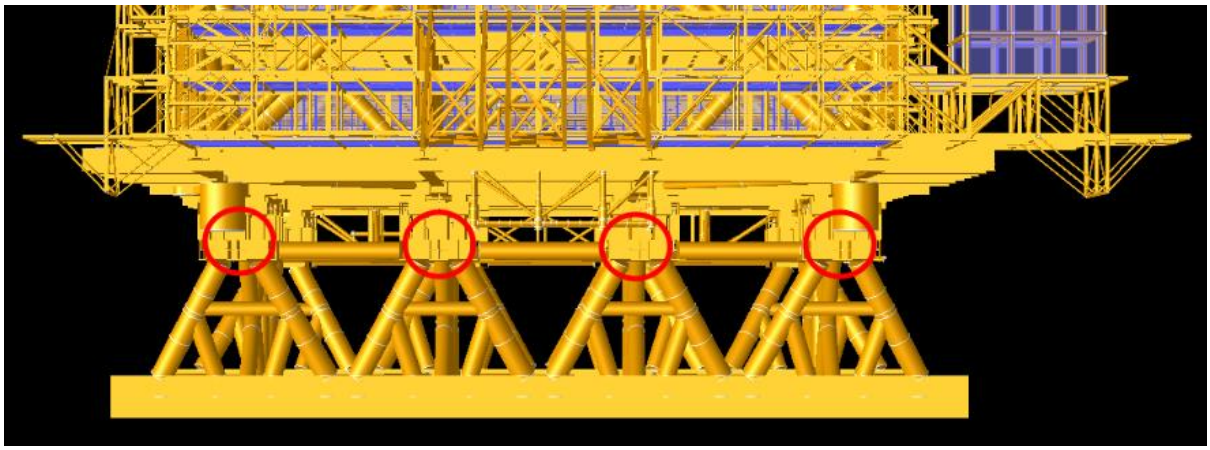

Figure 5-25 4 locations which form the standard for optimization

The optimization will strive to keep these rotations to a bare minimum. The method to achieve this is similar to the method which was used in paragraph 5.2. The linear least squares method is used once again. The goal of the optimization is:

$$min\left\|\Phi_{Topside}\right\|^2$$

Which is divided into the rotations caused by the ballast forces and the rotations due to all other factors:

$$min\left\|\Phi_{due\ to\ ballast} - \Phi_{Topside\ due\ to\ Topside+Barge\ weight}\right\|^2$$

Which is rewritten into:

$$min\left\|K * F_{Ballast} - \Phi_{Topside\ due\ to\ Topside+Barge\ weight}\right\|^2$$

Just like with optimization A, the matrix K still needs to be determined. How to get to this matrix equation is explained below. The starting point is once again the matrix Equation 5-3.

This time the relationship which is sought after is the one between the ballast forces, $F_{Ballast}$, and $U_{Topside}$. This is a difference from previous relation. In the matrix equation the section from the stiffness matrix which represents this relation is denoted by $(K_{T\text{-}B})^{-1}$ which is cell (2,3). (Remember that this matrix is the inverse so this section isn't only the connecting springs). So the matrix equation which is received is:

Equation 5-8

$$(K_{t\text{-}b})^{-1} \bullet \begin{bmatrix} F_{x1} \\ F_{y1} \\ F_{M1} \\ \vdots \\ F_{x209} \\ F_{y209} \\ F_{M209} \end{bmatrix} = \begin{bmatrix} U_{Quay} \\ U_{Topside} \\ U_{Barge} \end{bmatrix}$$

From this matrix equation the relevant forces and displacements need to be derived. The relationship which is sought after is once again between the vertical forces on the barge and differing from the previous case the rotational displacement of specific points on the topside. Therefore only the relevant columns and rows are selected. For columns these are 2:3:209 and for rows 3:3:209.

Equation 5-9

$$(K_{t\text{-}b,\text{Vertical forces}})^{-1} \bullet \begin{bmatrix} F_{v1} \\ F_{v2} \\ F_{v3} \\ \vdots \\ F_{y207} \\ F_{y208} \\ F_{y209} \end{bmatrix} = \begin{bmatrix} U_{\Phi 1} \\ U_{\Phi 2} \\ U_{\Phi 3} \\ \vdots \\ U_{\Phi 207} \\ U_{\Phi 208} \\ U_{\Phi 209} \end{bmatrix}$$

Similar as was done in the previous paragraph this needs to be rewritten into a matrix equation where only the 11 ballast tanks are in the force vector:

Equation 5-10

$$(K_{t\text{-}b,\ \text{Ballast forces}})^{-1} \bullet \begin{bmatrix} \text{Ballast 1} \\ \text{Ballast 2} \\ \text{Ballast 3} \\ \vdots \\ \text{Ballast 9} \\ \text{Ballast 10} \\ \text{Ballast 11} \end{bmatrix} = \begin{bmatrix} U_{\Phi 1} \\ U_{\Phi 2} \\ U_{\Phi 3} \\ \vdots \\ U_{\Phi 207} \\ U_{\Phi 208} \\ U_{\Phi 209} \end{bmatrix}$$

5.4.1 Results for optimization "DSU con"

This optimization is different compared to the previous 2 optimizations in that this optimization has no direct relation with the deflections of the barge. Just like with previous optimizations first a look will be taken at step 40 before looking at the load-out as a whole.

An important question which will be answered in this paragraph is how does optimizing for these 4 points of the topside construction influence the barge. Since optimization C is for other factors than keeping the barge as level as possible it is expected that their might be negative effects on the barge peak moment. However just like with the previous optimizations all strive for the same principle but put the emphasis on other variables. All optimizations namely strive to keep the alignment between

barge and quay as good as possible. This in turn will probably minimalize the rotation in the 4 points of the upper bar.

Again a first run is done for step 40 in the MATLAB model. Since optimization B proved more successful than optimization A, optimization "DSU con" will only be compared to the standard and optimization B. It is to be expected that optimization "DSU con" will outperform both optimization B and the standard for step 40 for rotation of the 4 nodes since that is the focus of this optimization. Looking at Figure 5-26 this is confirmed. The optimization is very effective and there hardly is any rotation at all in the 4 DSU connection nodes.

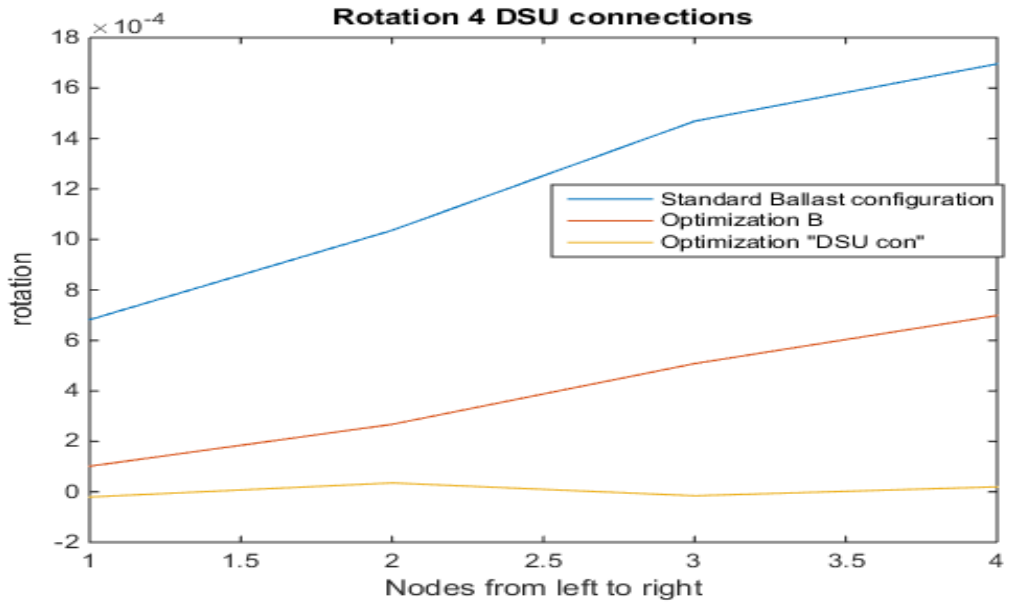

Figure 5-26 Rotation of 4 DSU connections, Standard, Opt. B and DSU con

The moment over the barge will suffer with this optimization compared to the other optimization since the variables to which the current optimization is performed are not directly linked to the barge. This can be seen in Figure 5-27. For step 40 the performance for the barge is much worse than it was using optimization B or the standard ballast configuration. The increase in peak moment in the barge for this step is 230% (from 3 GNm to 9.9 GNm in absolute values)

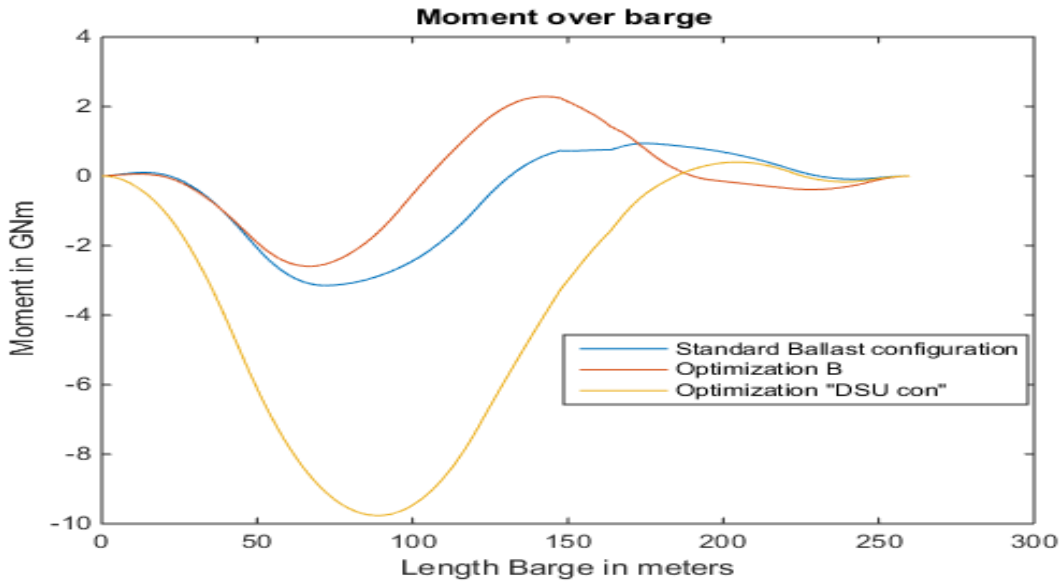

Figure 5-27 Moment over barge for step 40, Standard, opt. B and opt. DSU con

Also for the shear force in the barge the results using optimization "DSU con" are much worse compared to optimization B and the standard ballast configuration as can be seen in Figure 5-28. The increase in peak shear force is almost 95% (from 105 MN to 205 MN).

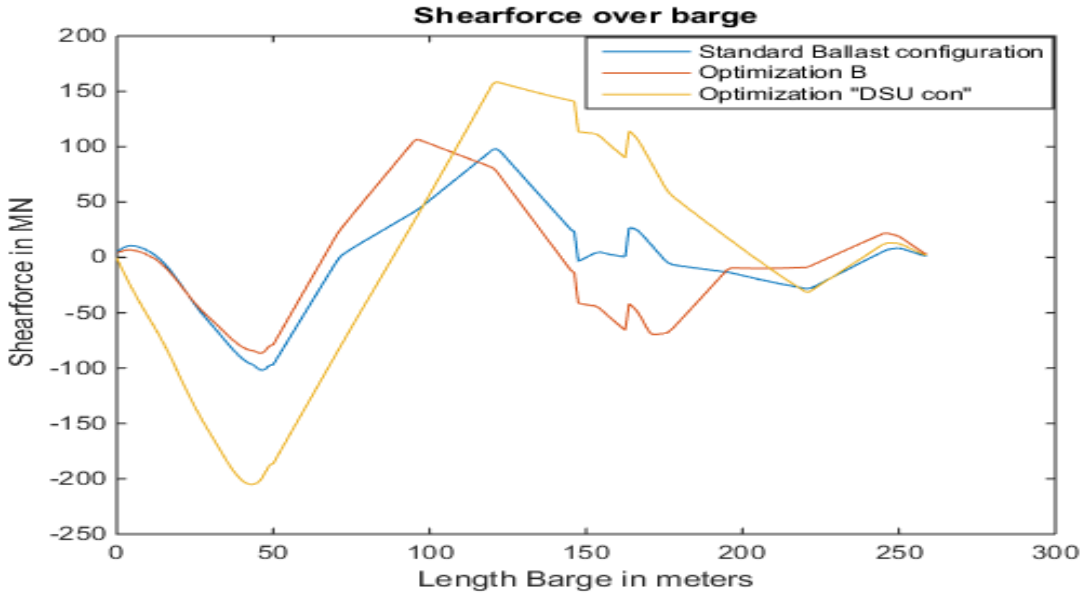

Figure 5-28 Shear force over barge for step 40, Standard, opt. B and opt. DSU con

Since the skidbox and the DSU connection are directly linked via the DSF it is expected that reducing the rotations in the 4 DSU nodes will also be effective in reducing the rotation and thus the moment in the skidbox. As can be seen in Figure 5-29 the moment in the skidbox is especially reduced with optimization "DSU con" from 0 meters up unto the quay-barge connection. For step 40 this is at 26.25 meters of the skidbox. The peak moment in this step however is almost the same for optimization B and "DSU con". It is also in the same location, at around 57 meters. The peak moment for optimization "DSU con" is -28 MNm compared to -25 MNm for optimization B.

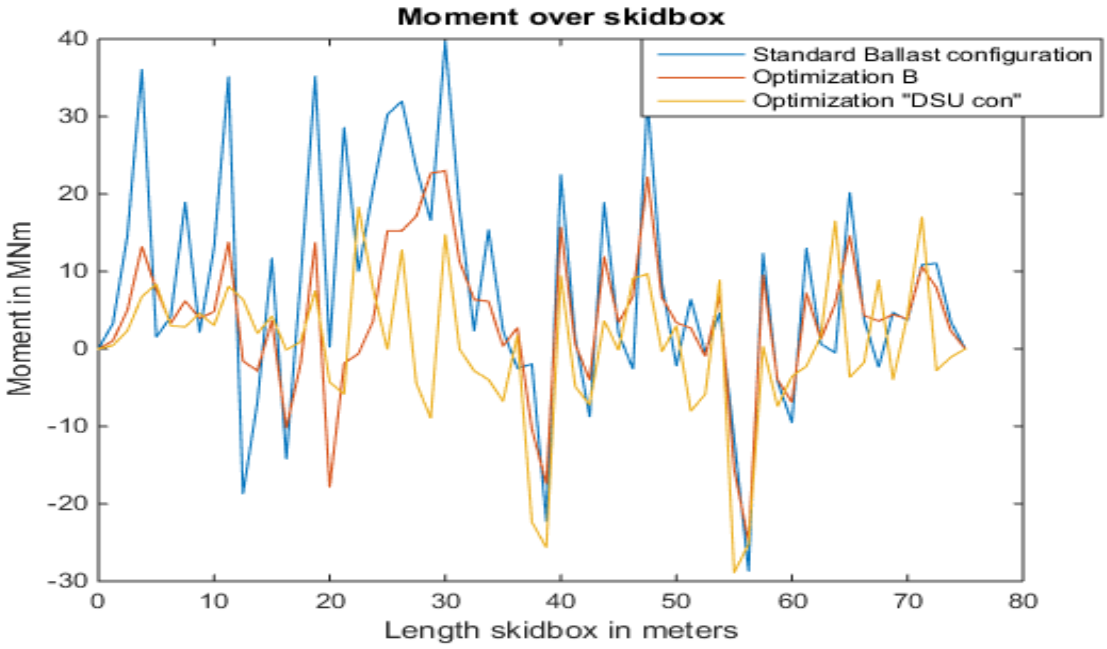

Figure 5-29 Moment over skidbox for step 40, Standard, opt. B and opt. DSU con

The shear force results are , as expected, similar to the results for the moment in the skidbox in that up until the barge-quay connection the optimization "DSU con" performs better than the other optimization and the standard ballast configuration. However for the latter part of the skidbox the results for the optimization are similar or worse than optimization B and the standard ballast configuration.

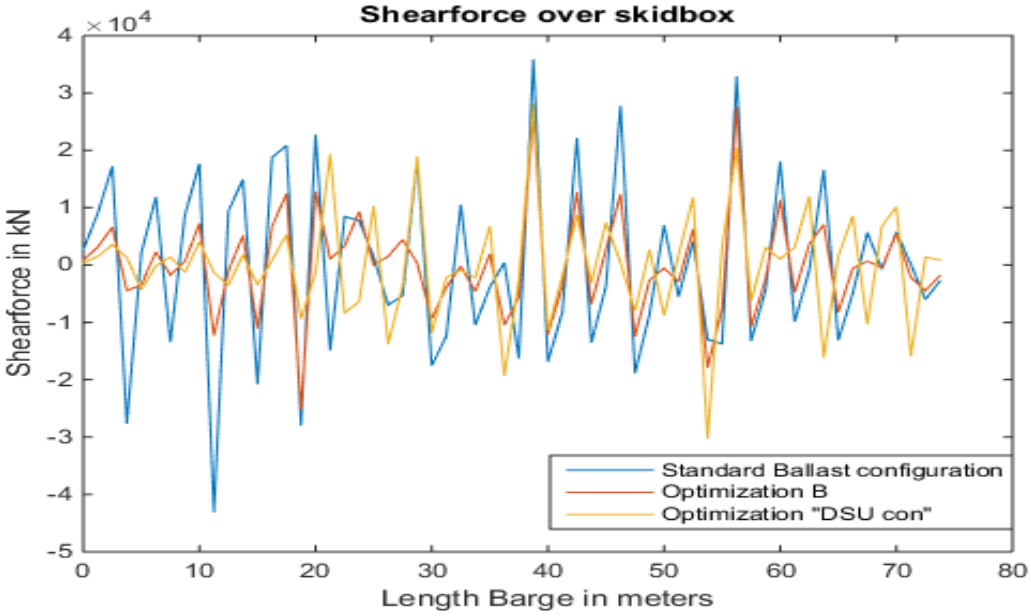

Figure 5-30 Shear force over skidbox for step 40, Standard, opt. B and opt. DSU con

Just like with the previous optimizations the effects will be looked at for the overall load-out as well. These are expected to be similar to the results which were found for only step 40. In Figure 5-31 it can be seen that optimizing for the rotation in the DSU connection works very effective in reducing these rotations until the point where they almost don't happen at all during the entire load-out.

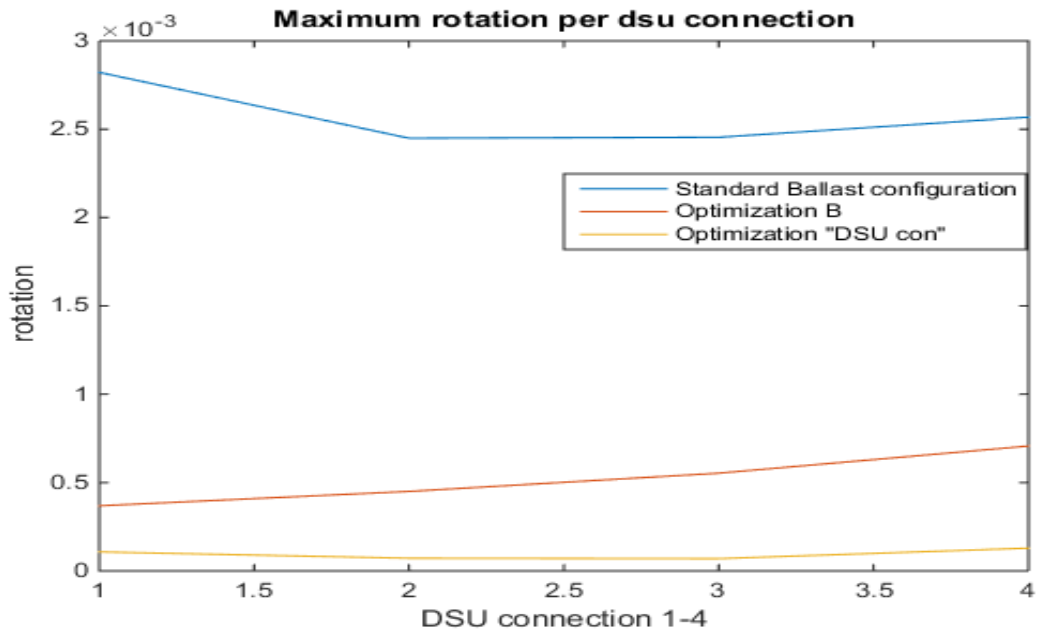

Figure 5-31 Maximum rotation per DSU connection, Standard, opt. B and DSU con

However as can be seen in Figure 5-32 the optimization performs worse for the skidbox than the standard and optimization B when looking at the highest peak moment. Considering the construction used this is an unexpected result as limiting the rotation at the DSU connection would also limit the rotation in the skidbox and thus cause a lower moment there. This needs further inquiry.

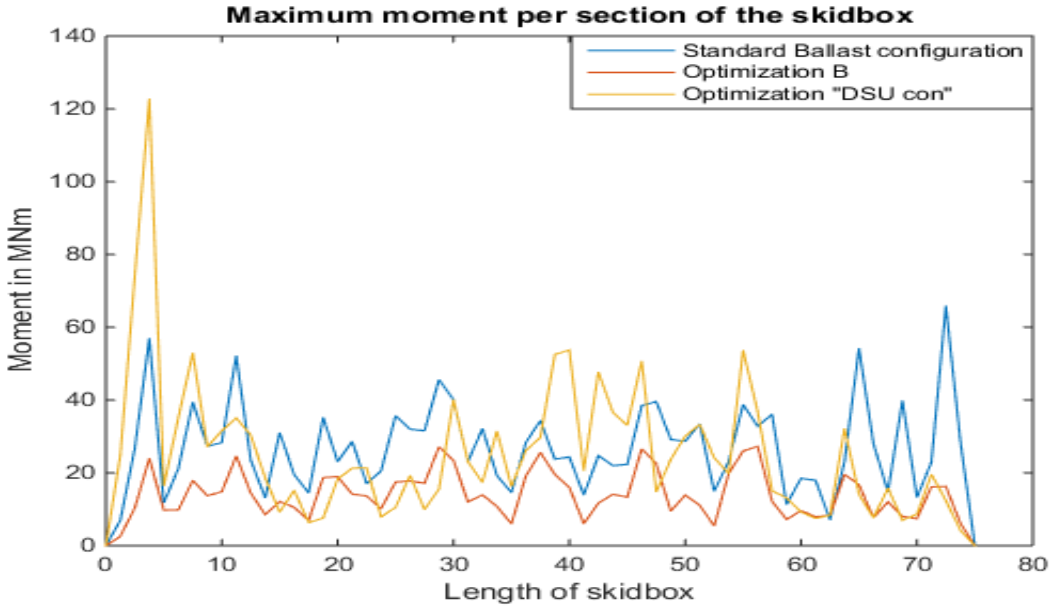

Figure 5-32 Maximum moment per section of the skidbox, Standard, opt. B and DSU con

The same can be said for the maximum shear force per section of the skidbox. The performance of optimization “DSU con” is worse than optimization B in terms of the highest peak moment. This was to be expected from the results for the maximum moment per section of the skidbox. However what is of interest is that the maximum allowable shear force, 8.1*10^4 kN, is exceeded by the first peak by 0.4*10^4 kN. The cause of this will be investigated later on.

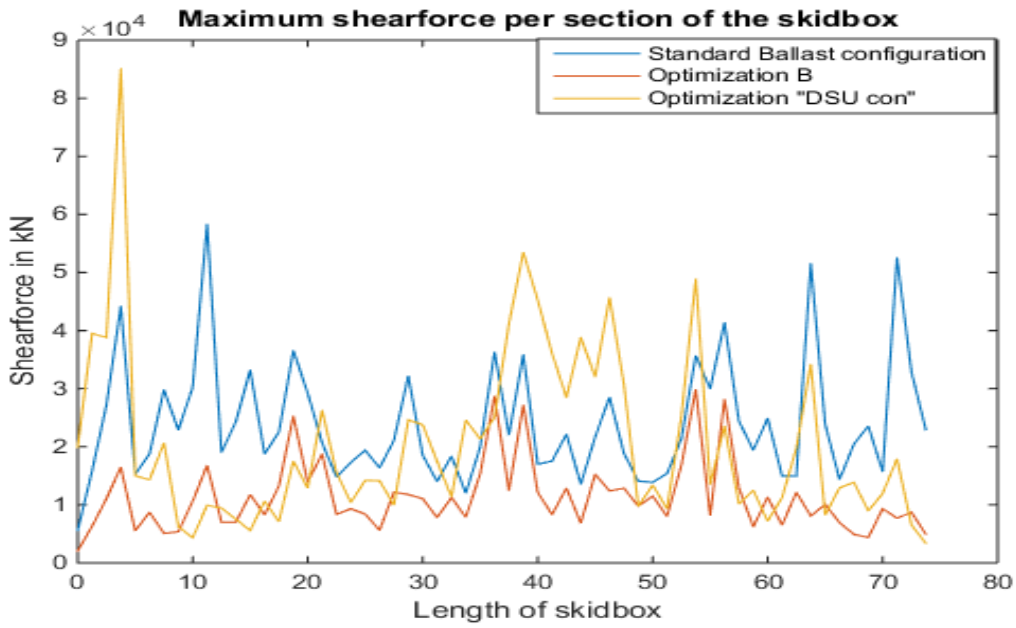

For the peak moment in the barge this optimization performs much worse compared to optimization B as can be seen in Figure 5-33. This was to be expected due the criteria for the optimization having no direct relationship with the deflection of the barge. This optimization will keep the barge level on the section where the skidbox is but neglects the level of deflection for the rest of the barge. The peak moment is even worse to that for the standard ballast configuration. This is mostly due to the steps where the skidbox is still on the quay. It was seen with further analysis that the front of the barge is deflected downwards significantly for these steps causing a high moment in the barge. For the later steps the moment in the barge is comparable with optimization B since a high moment there would mean a lot of sagging and this would translate to rotation at the DSU connections

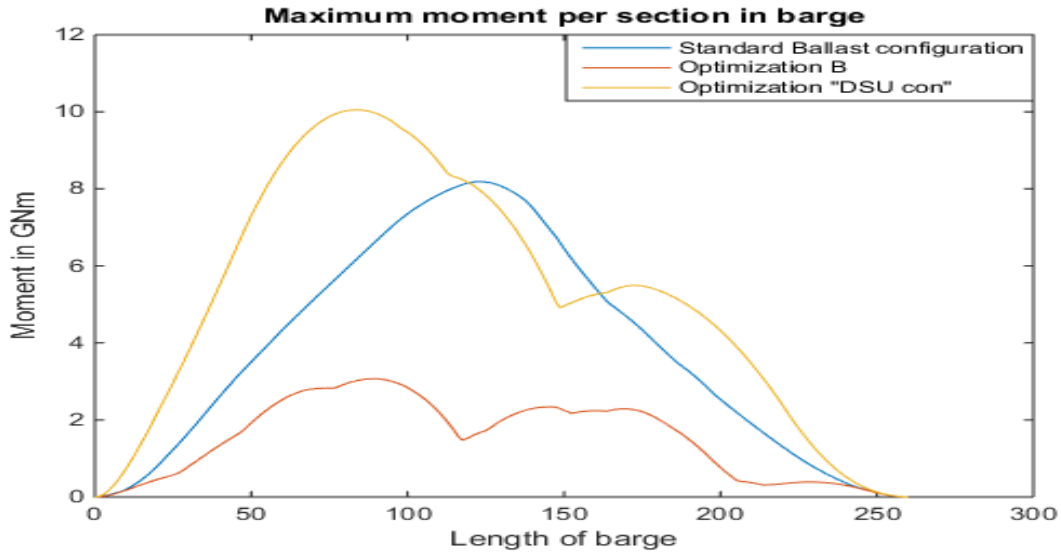

Figure 5-33 Maximum moment per section in barge

As is to be expected from Figure 5-33 the results for the maximum shear force per section in the barge will also be worse than compared to optimization B. As can be seen in Figure 5-34, the maximum shear force is higher for almost every section of the barge with the peak shear force reaching 203 MN compared to a max of 144 MN for optimization B.

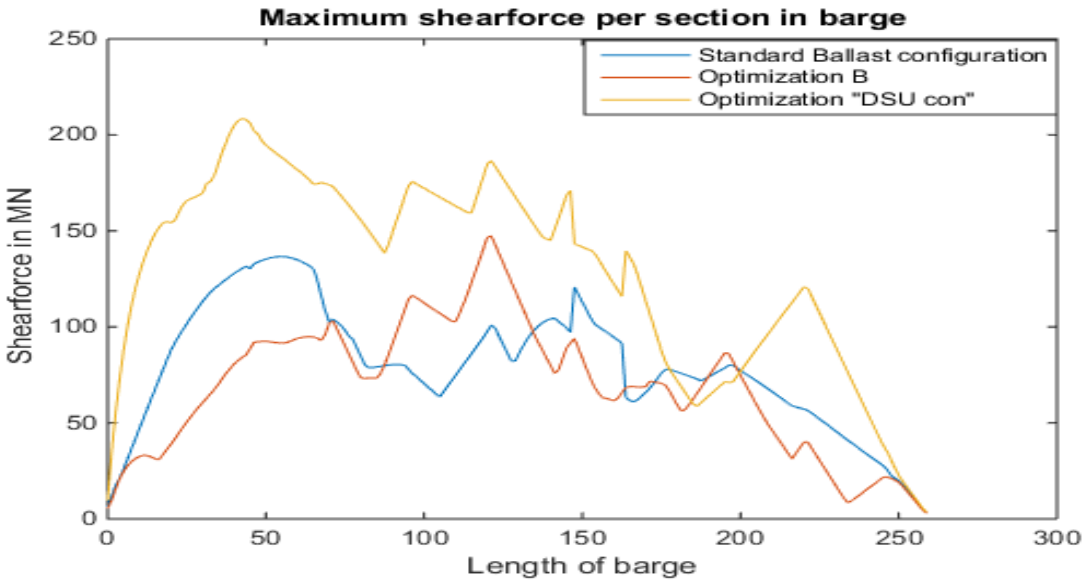

Figure 5-34 Maximum shear force per section in barge

Coming back to the higher than expected moment in the skidbox, a view is taken at the highest moment per step in Figure 5-35. It can be seen that the worse performance is mostly down to a couple of steps, step 60 in particular. Since this result is unexpected a closer look is taken to step 60.

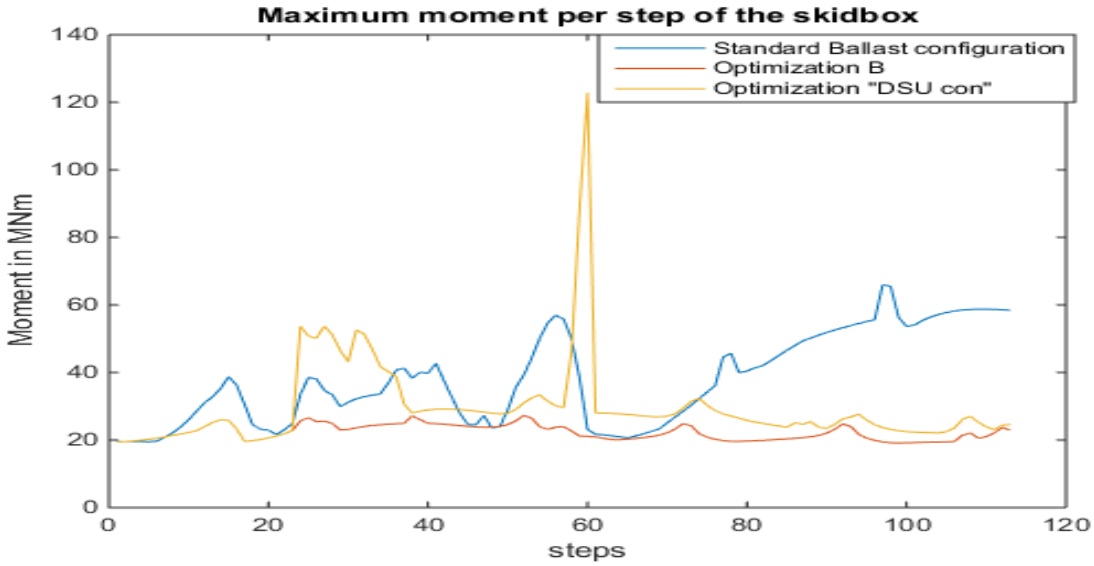

Figure 5-35 Maximum moment per section of the barge, Standard, opti B and DSU con

For step 60 the skidbox deflection can be seen below. At step 60 only 1 node is still attached to the quayside, this is the utmost left point in the graph of Figure 5-36. The nodes just to the right of the 1 node attached to the quay are unsupported because the barge is ballasted lower with this algorithm. At this unsupported section the first member of the DSF is connected. This causes a large deflection at this point causing a very large moment in the first part of the skidbox as can be seen in Figure 5-37.

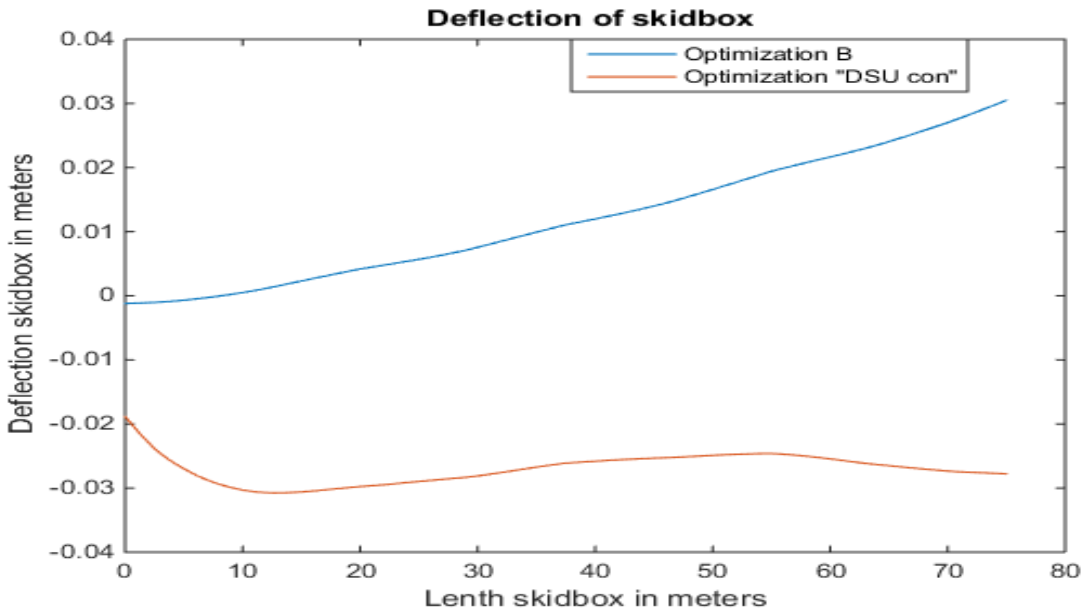

Figure 5-36 Deflection of skidbox for step 60

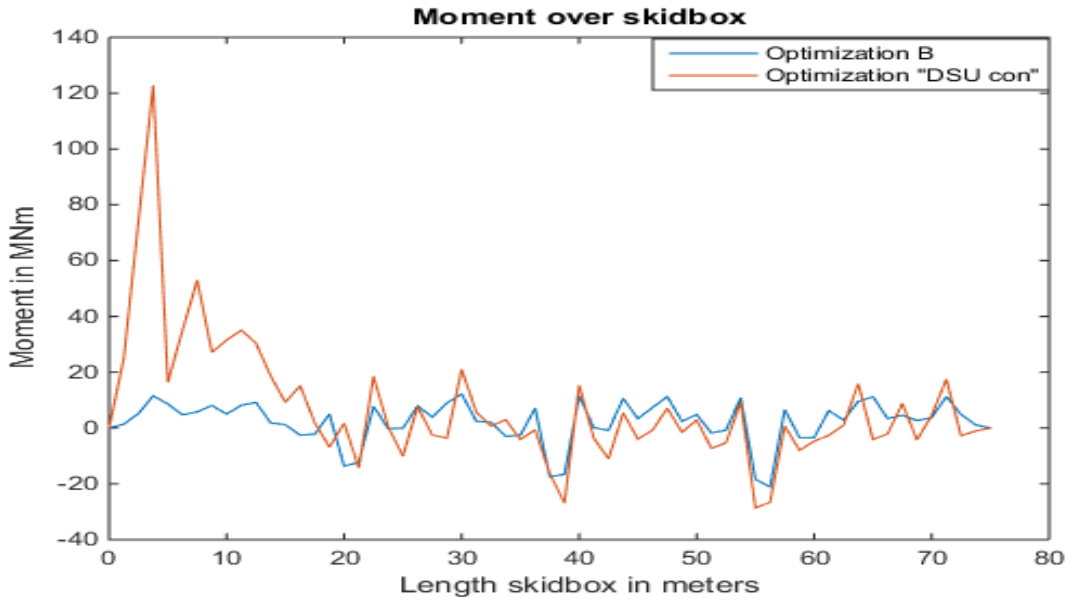

Figure 5-37 Moment over skidbox, step 60

As can be seen in Figure 5-38 the rotation for the 4 DSU connections is the lowest using the current optimization method. The maximum moment peak at step 60 thus isn't an error or glitch in the algorithm. The algorithm does what it is supposed to do in this step, unfortunately due to the unsupported section of the skidbox aligning with the location where a member of the DSF is connected a high peak moment is created. The shear force peak resulting from this is 8.5*10^4 kN which surpasses the maximum allowable shear force for the skidbox. This optimization therefore is not suited in its current form for the base case scenario. A solution could be to manually adjust it for step 60. Despite this flaw it is believed that this optimization can definitely have its benefits since the goal, which was to reduce the rotations, was achieved.

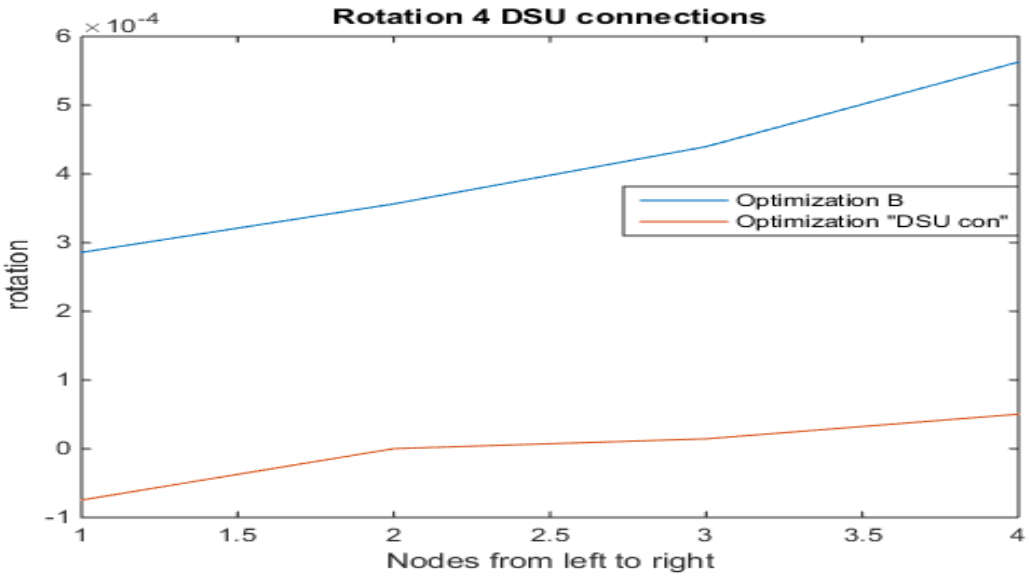

Figure 5-38 Rotation DSU connections

5.4.2 Conclusion from the optimizations

The results for the optimizations are summarized in Table 5-3. It contains all the maximum forces in the barge and the skidbox for each optimization.

Table 5-3 Summarization of maximum force per optimization

	Opt A	Opt B	Opt "DSU con"	Standard
Max M in barge	2.6 GNm	3 GNm	10.1 GNm	8.2 GNm
Max V in barge	93 MN	144 MN	203 MN	135 MN
Max M in skidbox	78 MNm	25 MNm	121 MNm	65 MNm
Max V in skidbox	5.8*10^4 kN	2.8*10^4 kN	8.5*10^4 kN	5.8*10^4 kN

The same table is repeated using unity check, dividing the maximum value with the allowable value. Since the location of each peak is different for each optimization and the allowable forces aren't constant over the barge either, the allowable forces by which is divided is also different for each optimization. For the skidbox the allowable forces are considered constant over the length as was calculated in paragraph 4.2.2.

Table 5-4 Summarization of maximum force per optimization, unity check

	Opt A	Opt B	Opt "DSU con"	Standard
Max M in barge	0.15	0.18	0.59	0.4861
Max V in barge	0.31	0.41	0.30	0.20
Max M in skidbox	0.49	0.16	0.76	0.41
Max V in skidbox	0.72	0.34	1.05	0.72

Concluding this paragraph it can be said that Optimization B is the superior method overall. It performs well in reducing the peak moments in the barge as well as in the skidbox. Optimization "DSU con" can be useful as well. The method used for achieving optimization "DSU con" can also be applied to other elements in the entire system making it an interesting alternative. If for example a certain element is known to be critical the optimization "DSU con" can be applied to that element. However it needs to be kept in mind that the other structures are still to be within their allowable forces.

5.5 Effects of the optimization on the ballast procedure

In the MATLAB model each step in the process is independent of the previous step. For the optimizations this means that for each step a new optimization is calculated. Therefor it is of interest to investigate the percentage of how much the ballast tank is filled in each step. It is possible due to the nature of the optimizations that in one step the ballast tank is almost completely filled whilst in the next it is almost completely empty. This is an unwanted situation and is one of the flaws of calculating the ballast optimizations using this method.

The process of checking the effects of the optimizations on the filling of the ballast tanks is checked for each optimization.

5.5.1 Optimization A

The results for optimization A can be seen in Figure 5-39 and Figure 5-40. The graphs are separated between tanks 1-6 and 7-11 with the only reason being to improve graph visibility. In the graphs it can be seen that for each step small adjustments are made. However for each tank a general trend can be seen which shows no major jumps, so from filled at 97% to 3%. The lack of major jumps in the tank percentages is positive because this would require a very large pump capacity. The solution for the small corrections can be to filter out these results and use the general trend for each tank. These small corrections would still be there if the optimizations were constructed in such a way that there is a dependency between the steps for the percentage in which the ballast is filled. For example if for each step the percentage for which the ballast tank is filled can only vary with 10 percent from the previous step, it is expected that minor adjustments will still happen.

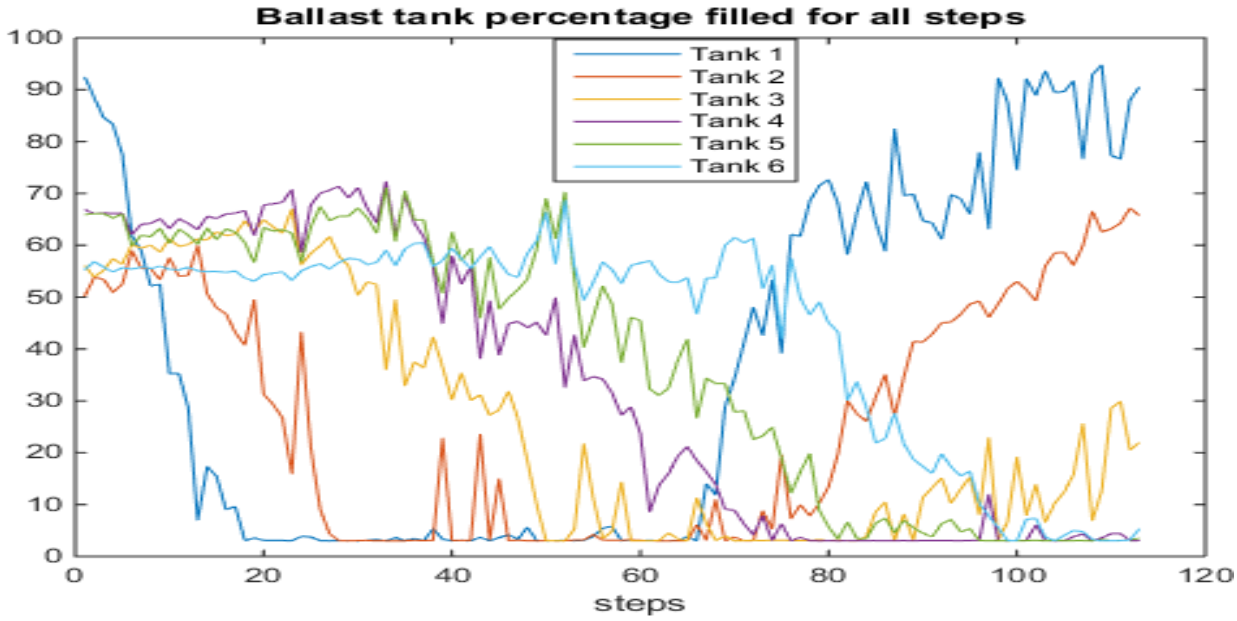

Figure 5-39 Ballast tank (1-6) percentage for all steps of optimization A

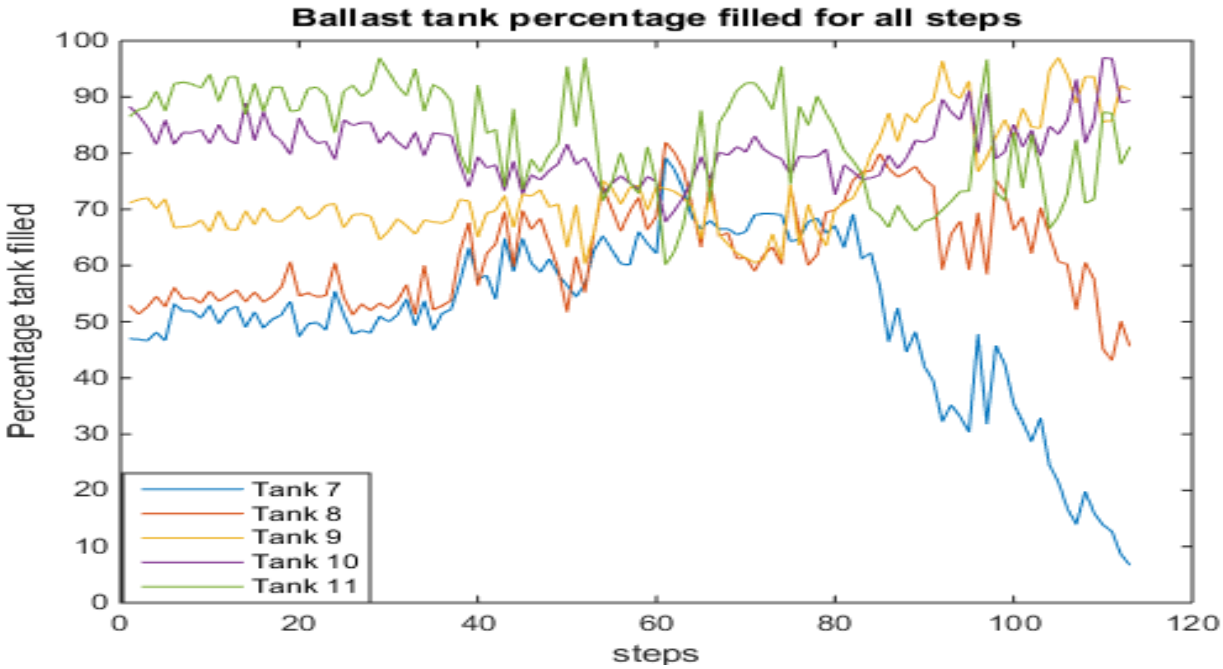

Figure 5-40 Ballast tank (7-11) percentage for all steps of optimization A

5.5.2 Optimization B

The results for optimization B can be seen in Figure 5-38Figure 5-41 and Figure 5-42. It can be seen that the results are remarkably different when compared to optimization A. Optimization B doesn't have the small differences seen in Optimization A. However whereas Optimization A didn't show any major jumps in the general trend of the graphs, these jumps can be seen in Optimization B. Almost all tanks are both almost empty and full during a single load-out. This requires a so much pump capacity which is almost unattainable.

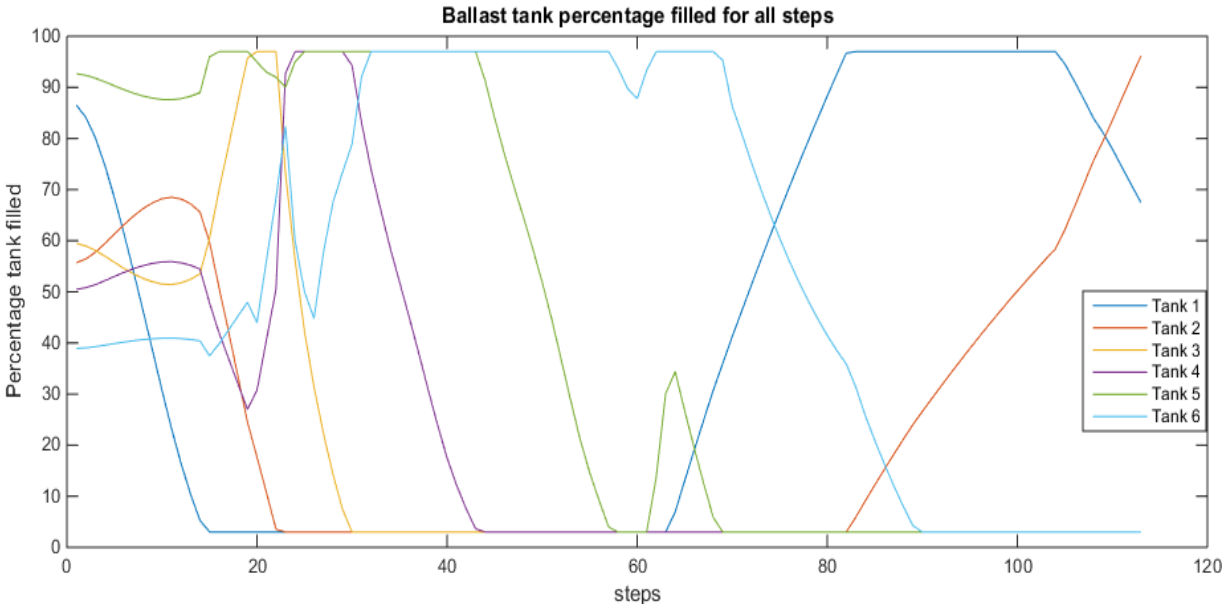

Figure 5-41 Ballast tank (1-6) percentage for all steps of optimization B

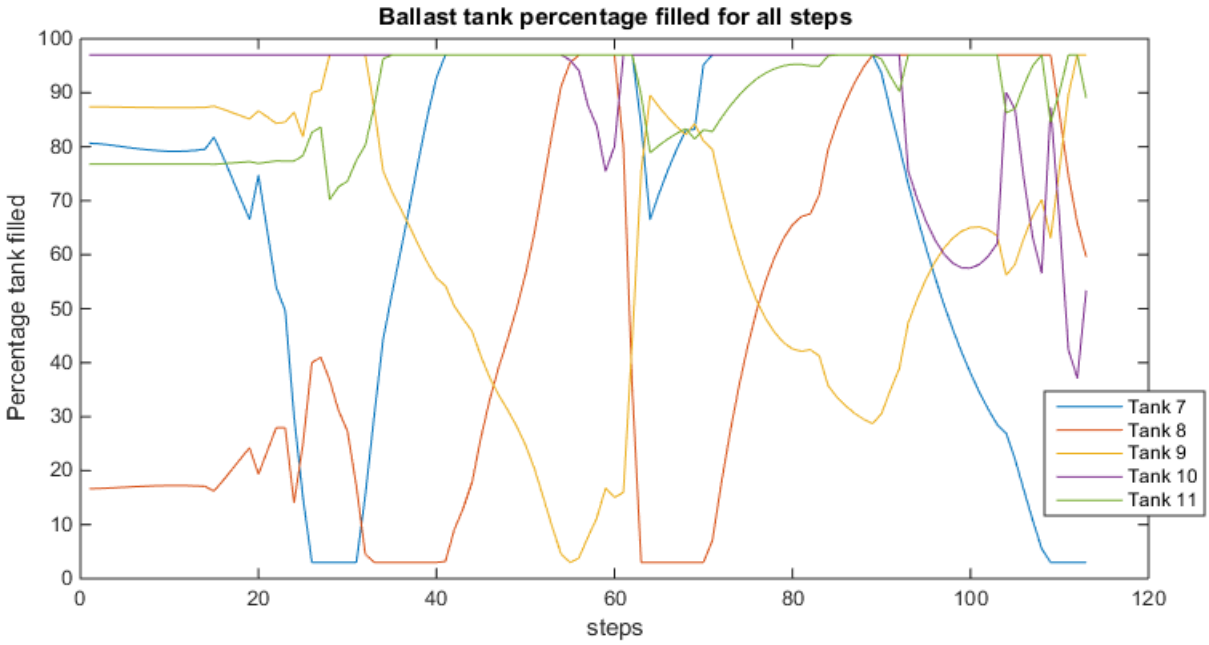

Figure 5-42 Ballast tank (7-11) percentage for all steps of optimization B

5.5.3 Optimization "DSU con"

The results for optimization "DSU con" can be seen in Figure 5-43 and Figure 5-44. It can be seen that with this optimization big jumps in percentages occur quite often. Especially around steps 20 to 40 the steps are very radical. In this optimization some tanks are also going from completely full to completely empty in one step, for example step 38 for tank 5. This optimization however doesn't have the small corrections which could be seen for optimization A.

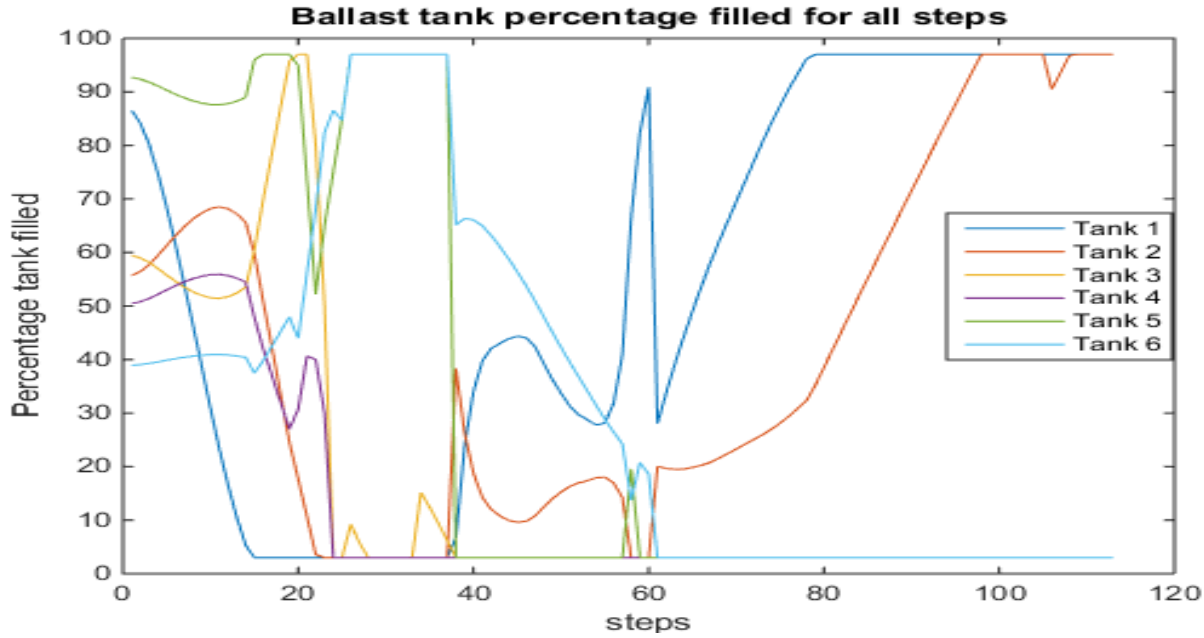

Figure 5-43 Ballast tank (1-6) percentage for all steps of optimization "DSU con"

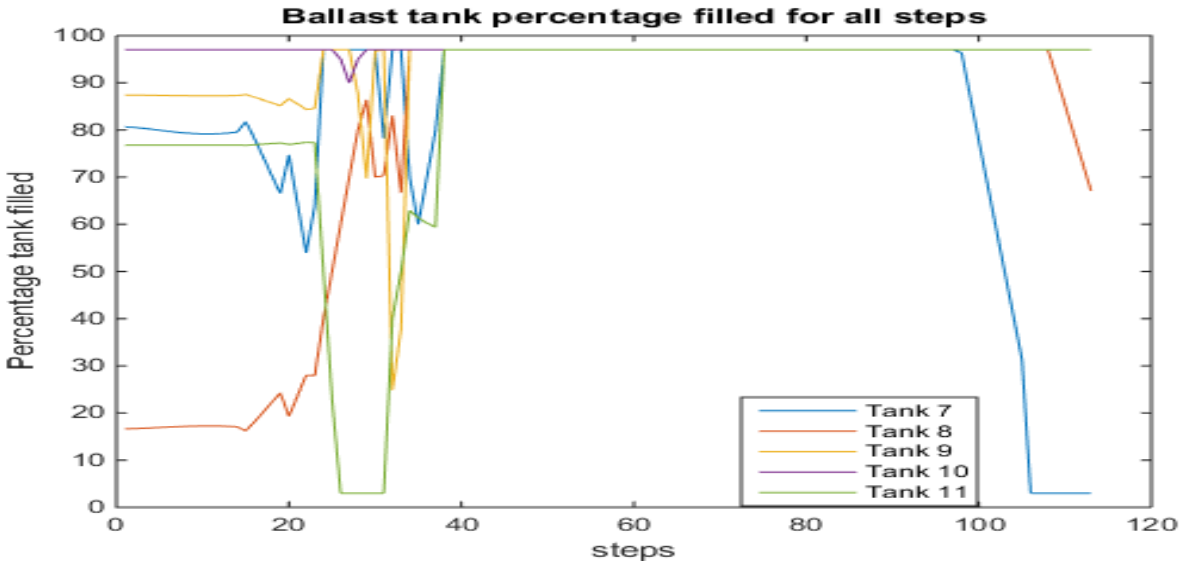

Figure 5-44 Ballast tank (7-11) percentage for all steps of optimization "DSU con"

Concluding it can be said that the model in its current form doesn't give an ideal ballasting situation. Although the optimizations are theoretically possible when there is infinite available time, in the real world some optimizations would simply result in too much ballasting time which is unwanted for a host of practical reasons (employees time, weather window, keeping up with the current becomes a factor). Therefore the model would have to be adjusted by making the boundaries of the optimization depend on the ballast situation of the previous step.

5.6 Other optimization possibilities

As stated earlier each optimization for each step is à mathematical solution. There may be many other possibilities which are able to achieve the same requirements. For example looking at step 40 for optimization A. Optimization A's goal was to keep the barge as level as possible. However the results for the deflection of the barge seen in Figure 5-45 satisfy this least squares problem equally as much. This is a pure hypothetical case and isn't checked if this is possible considering the boundaries set by the size of the ballast tanks.

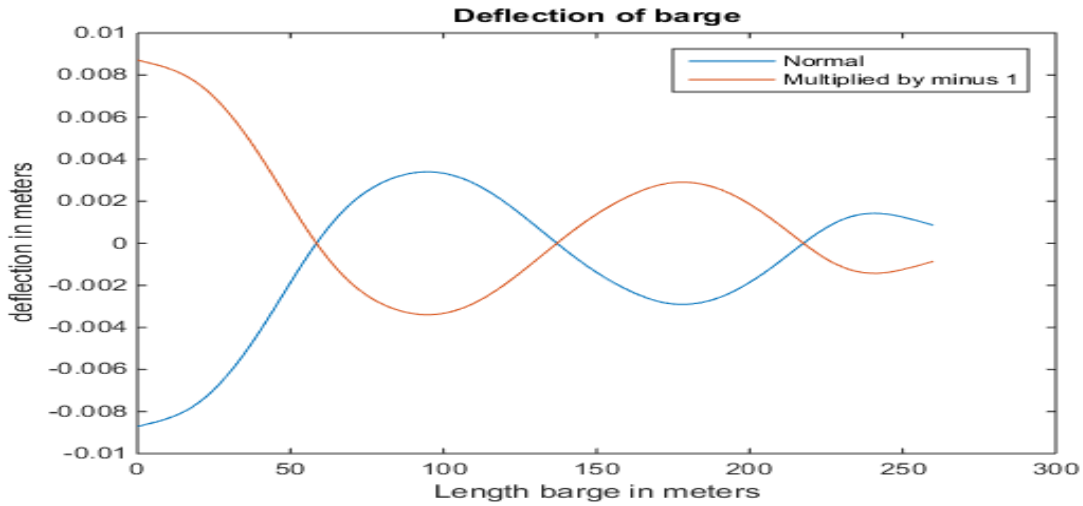

Figure 5-45 Hypothetical other optimization result

Each optimization is dependent on the starting point, from there it iterates to a solution. To check if there is more than one optimization result possible, the starting point is changed. For the optimizations used earlier the starting point was a situation in which the ballast tanks were completely empty. If the starting value is changed the boundaries have to change with them. If for example the starting point is changed to the ballast tanks being 50 % full, the boundaries for each ballast tank change to +47% and -47% of the full ballast tank.

It was tested that when using a starting point different than zero ballast present in the ballast tank, if the resulting optimization would be different. The result was that varying the starting point has absolutely no effect on the resulting optimization. Apparently, despite the different starting position, the optimization converges to the same best solution for the given boundaries.

6 Barge Deck Stiffness

In this chapter a look is taken at the stiffness of the deck of the barge. This is an essential part of the model because this forms the connection between the topside and the barge. It transfers the loads exerted by the topside into the construction of the barge. The stiffness of the deck isn't homogenous over the whole surface off the barge due to the presence of the transverse and longitudinal bulkheads. The software SACS is used to calculate the deck stiffness at various points. This knowledge is than applied to see what the effects are of relocating the skidbeams to an area of lower deck stiffness.

6.1 Transverse deck stiffness

For calculating the transverse deck stiffness use is made of a software program called SACS. SACS is a software program for the offshore industry. It's a standard FEM program using beam and plate elements. It was specifically designed for the offshore industry by Bentley and can apply offshore specific loading. It also contains up to date international design code coverage.

The cross section of the barge is different varying from stern to bow. Therefor multiple SACS models of cross sections of the barge exist. HMC uses 3 models for the cross section of the barge. One is a typical mid-ship section representing frames 31-56. The second section represents frames 65-88, which is a representation of the section after the narrowing of the barge. The last section represents the front of the barge (frames 89-99). Due to the final position of the topside on the barge not exceeding frame 65, only the mid-ship section (frames 31-56) will be used.

In Figure 6-1 one can see a wireframe representation of this section. The deck, side shells, bottom plate and longitudinal bulkheads are clearly distinguishable

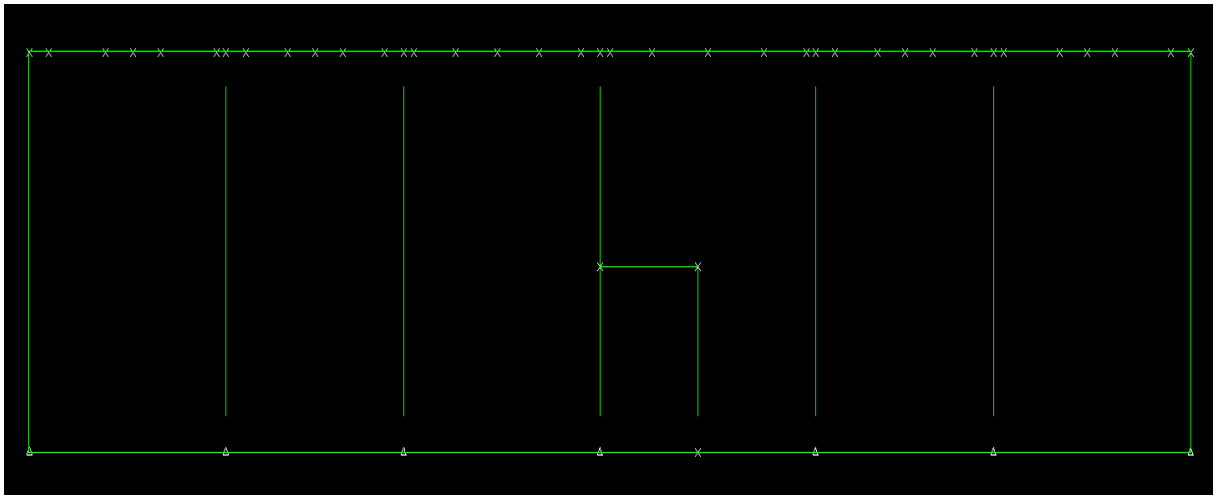

Figure 6-1 Web frame model frames (31-56)

This cross section of the barge is supported on 7 fixed rigid connections, each underneath a side shell or longitudinal bulkhead. This way if a force is applied on to the deck there isn't any movement of the

barge itself like in the MATLAB model, thus the nodal displacement of the deck node is pure deflection of the deck.

The method to calculate the deck stiffness from the SACS software is quite simple. From the figure can be seen that there are several nodes along the deck. To know the stiffness along the deck a force is exerted at a node, SACS then calculates the displacement of the node. Using equation below the stiffness K_{Deck} can be calculated.

$$\frac{Force\ at\ node}{Displacement\ of\ node} = K_{Deck}$$

This is repeated for every single node, see Figure 6-2 for an example of a force exerted on a node in SACS. In this situation node 2 of the deck is loaded with a force, in this case a force of 1 kN is used to measure the displacement.

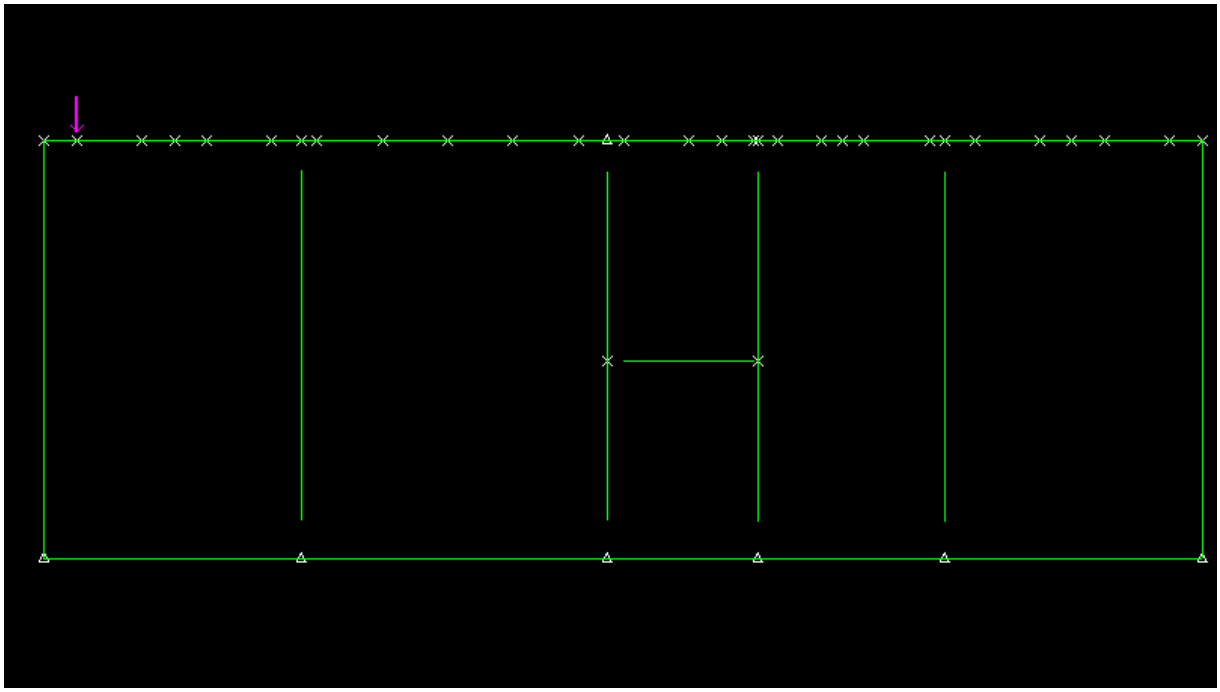

Figure 6-2 Applying a force, testing deck stiffness

This is repeated for every node in the deck. The found stiffness at these nodes can be found in Table 6-1.

Table 6-1Deck stiffness results

Nodes	Frames 31-56
1	1.45E+09
2	1.40E+09
3	6.21E+08
4	5.34E+08
5	7.03E+08
6	1.71E+09
7	1.84E+09
8	1.88E+09
9	8.23E+08
10	6.58E+08
11	8.16E+08
12	1.58E+09
13	1.85E+09
14	1.70E+09
15	8.20E+08
16	5.39E+08
17	7.50E+08
18	1.58E+09
19	1.87E+09
20	1.72E+09
21	7.71E+08
22	4.47E+08
23	7.66E+08
24	1.66E+09
25	1.82E+09
26	1.58E+09
27	8.16E+08
28	6.57E+08
29	8.21E+08
30	1.58E+09
31	1.84E+09
32	1.71E+09
33	7.04E+08
34	5.34E+08
35	6.20E+08
36	1.40E+09
37	1.45E+09

This can also be put into a graph corresponding with the width of the deck, on an overlay of the wireframe. This is done for all cross sections and from Figure 6-3 it can clearly be seen that the deck stiffness is highest above the longitudinal bulkheads and lowest at the halfway points between the bulkheads. That is why normally high loads on the deck are preferred to be situated along the longitudinal bulkheads. This is also the case for the skidbeams during the load-out of a topside. The effect of placing the skidbeam on another location will be the topic of the next paragraph.

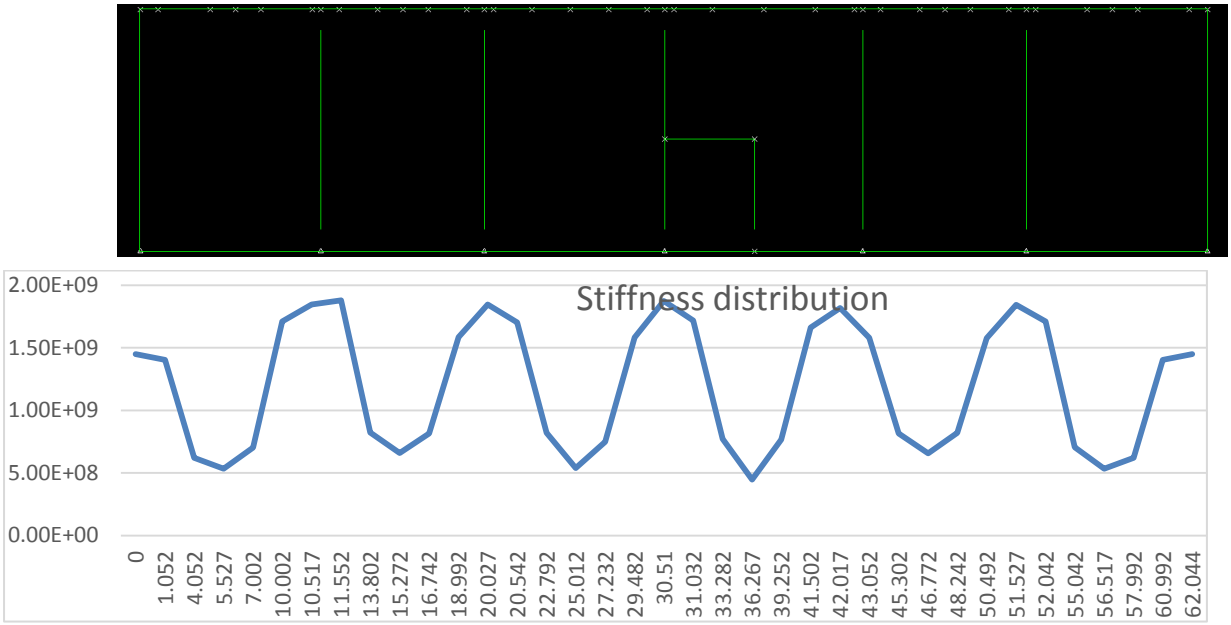

Figure 6-3 Stiffness distribution transeverse

The above section was primarily focused on the transverse distribution of the deck stiffness but there is also a longitudinal distribution of the deck stiffness. This shouldn't be confused with what was mentioned earlier about the various sections. The longitudinal distribution for each section is constant only to be interrupted by the transverse bulkheads. The bulkheads form the separation between the ballast tanks.

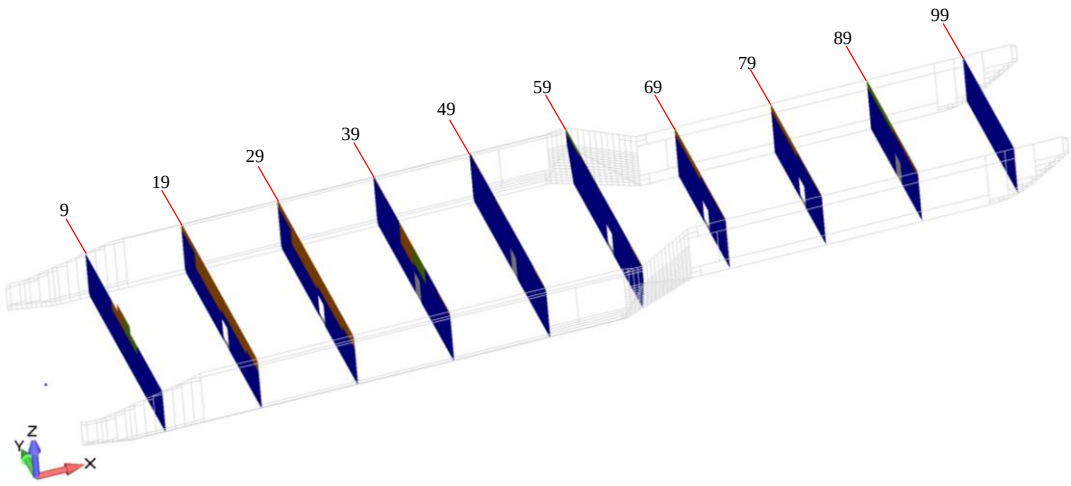

Figure 6-4 Transverse Bulkheads

The bulkheads can be seen as a wall covering the whole cross section of the barge. This is quite different from the sections of barge where the cross section is a web frame as seen in Figure 6-4. The deck stiffness at the bulkheads therefore behaves quite different compared to the stiffness at the other web frames. To calculate the stiffness at the transverse bulkheads using SACS software isn't an option or necessary. The method used by HMC is simply the stiffness of compression of the material, so just calculate it as a normal force on the bulkhead. The resulting stiffness at the bulkhead is 3354

kN/mm or 3.354*10^9 N/cm. Just like with the other calculated stiffness, for the MATLAB model the stiffness of the wood layer still needs to be incorporated.

$$\left(\frac{1}{k_{wood}} + \frac{1}{k_{transverse\ bulkhead}}\right)^{-1} = k_{con\ at\ TBHD} = 2.8508 * 10\text{^}9$$

6.2 Effects of changing skidbeam location

The normal situation during the load-out is that the forces caused by the topside on the barge are transferred via the skidbeams to the longitudinal bulkheads as most as possible. This causes the stiffest connection. The reason for this is that applying the loads at the deck strongpoints allows for the loads to travel safely into the barge structure. Applying very high loads at for example the half-way point in between the longitudinal bulkheads puts unnecessary stresses in the deck. However if during the load-out the forces would be led to the areas of the barge in between the LBHD it can be shown that the resulting stresses in the deck are within the range that is acceptable.

It is expected that changing the skidbeam location transversely over the barge will have an effect on the load-out. The deck as mentioned earlier forms the connection between the barge and the skidbox. In the MATLAB model this connection is formed by springs. If the forces of skidbeams are no longer transferred to the hardpoints on the deck but to the less stiff points this will change the way the barge and the skidbox interact. Lowering the stiffness of the connection between barge and skidbox might be beneficial to the forces on the skidbox and thus the topside. This due to the fact that the forced displacements caused by the barge onto the skidbox are reduced. This is visualized in Figure 6-5.

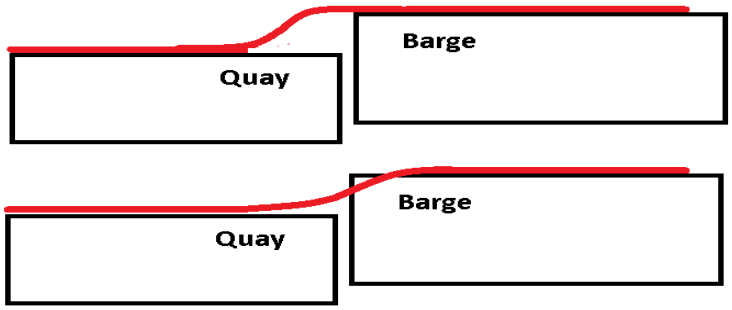

Figure 6-5 Deck stiffness comparison

In Figure 6-5 the upper sketch is a representation of a load-out situation with rigid deck, so very stiff deck, and the bottom sketch shows the situation with a lower stiffness of the deck. In this example in which the quay is lower than the barge having a lower stiffness of the deck results in a smoother "smoother" transition of the skidbox over the barge and the quay.

In order to quantify these assumptions use is made of the MATLAB model. The possible stiffness's of the deck and the corresponding locations are known from previous paragraph. Several locations and stiffness's are chosen for evaluation. The point in the load-out which is chosen for evaluation will be step 4, also the effects on the total load-out is watched.

In the original situation the stiffness of the deck is formed by the average of the stiffness at the 4 LBHD which is 1.84E+9. If the skidbeams are to be placed at the least stiff deck location and the forces transferred there, an average stiffness of the deck of 6E+9 is received which is approximately 1/3 of the stiffness of the standard situation. Keep in mind that these values in the MATLAB model are incorporated with the wood layer. The effects are of changing the deck stiffness to the displacement of the skidbox is first viewed.

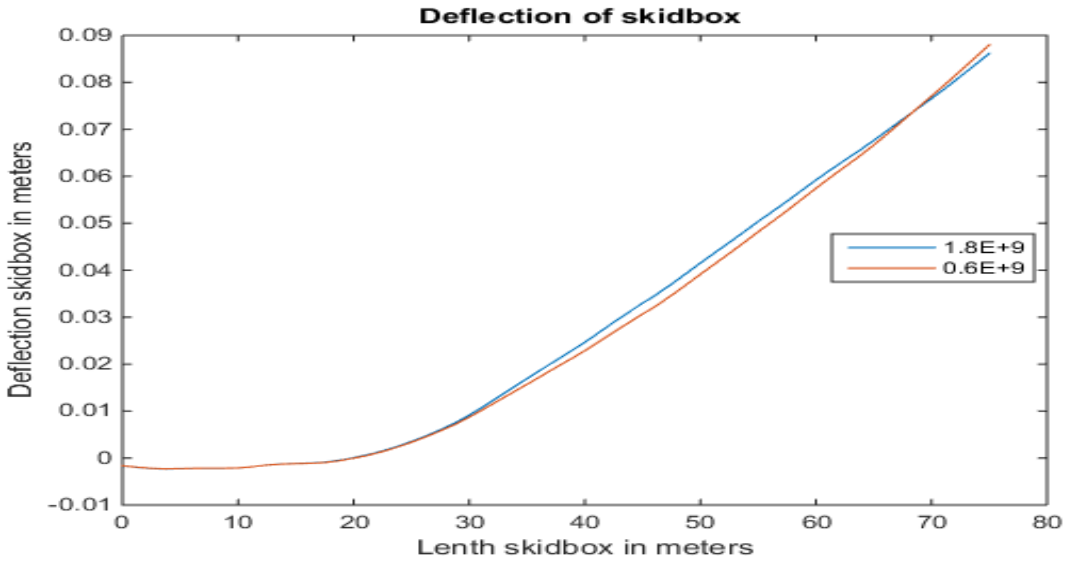

Figure 6-6 Skidbox displacement with varying deck stiffness

In Figure 6-6 the displacement of the skidbox during step 40 with various deck stiffness' is shown. At step 4 the first 26.25 meter of the skidbox are still on the quay, the rest is on the barge. This transition can clearly be seen in the figure. It can also be seen in Figure 6-6 that decreasing the deck stiffness by 1/3 by relocating the skidbox has little effect on the displacement of the skidbox. The displacement caused by the barge is quite large in this example, causing the effect of decreasing the deck stiffness to be neglectable since this is in order size much smaller. Since the effects on the displacement are minimal, the effect on the moment over the skidbox is also expected to be minimal. This can be seen in Figure 6-7.

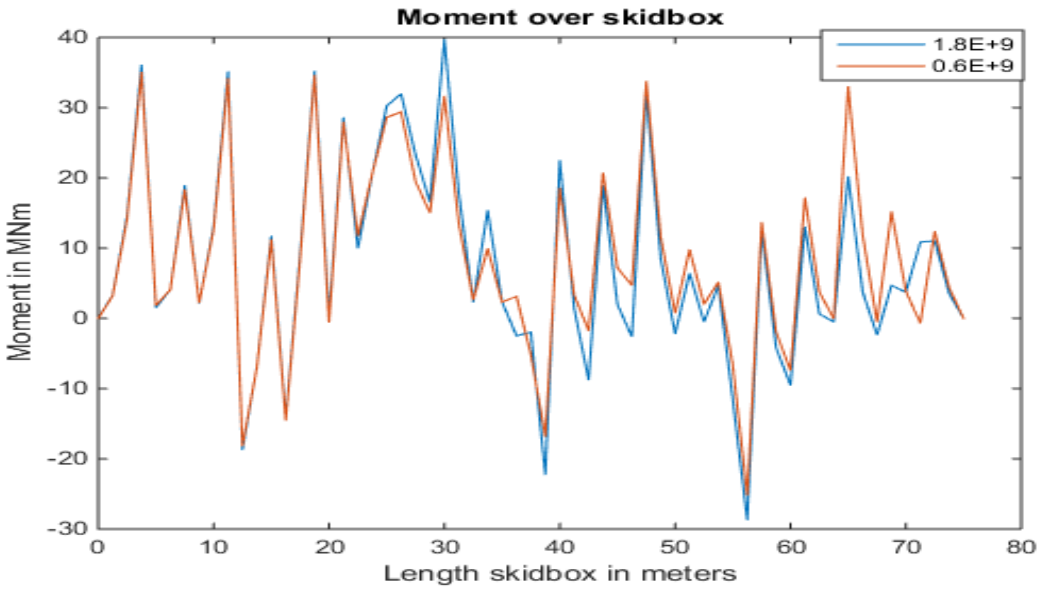

Figure 6-7 Moment over Skidbox, varying deck stiffness

So reducing the deck stiffness by almost (1/3) causes the peak moment in the area surrounding the barge-quay transition (20 m to 50 m) to decrease with 10 MNm, and for overall peak moment to decrease from 40 MNm to 36 MNm which equals a reduction of 10%. For the shear force over the skidbox the effects aren't very significant either as can be seen in Figure 6-8. The largest peak force which was around 12 meters shows a very minimal change.

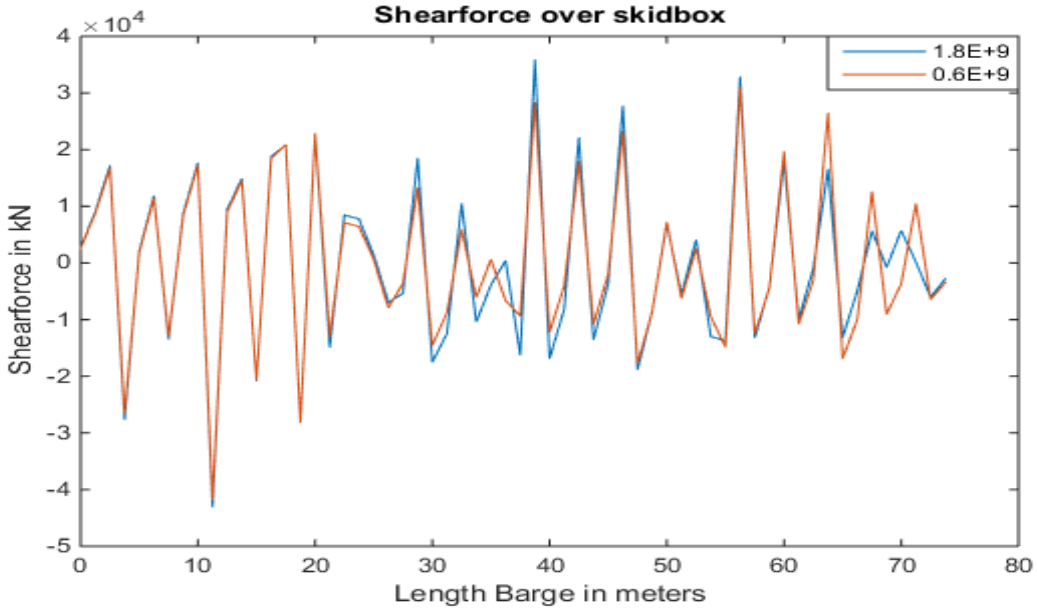

Figure 6-8 Shear force over Skidbox, varying deck stiffness

The effects to the moment on the barge are very minimal to non-existent as can be seen in Figure 6-9. The results of the shear force are therefore omitted because no significant effect is recorded.

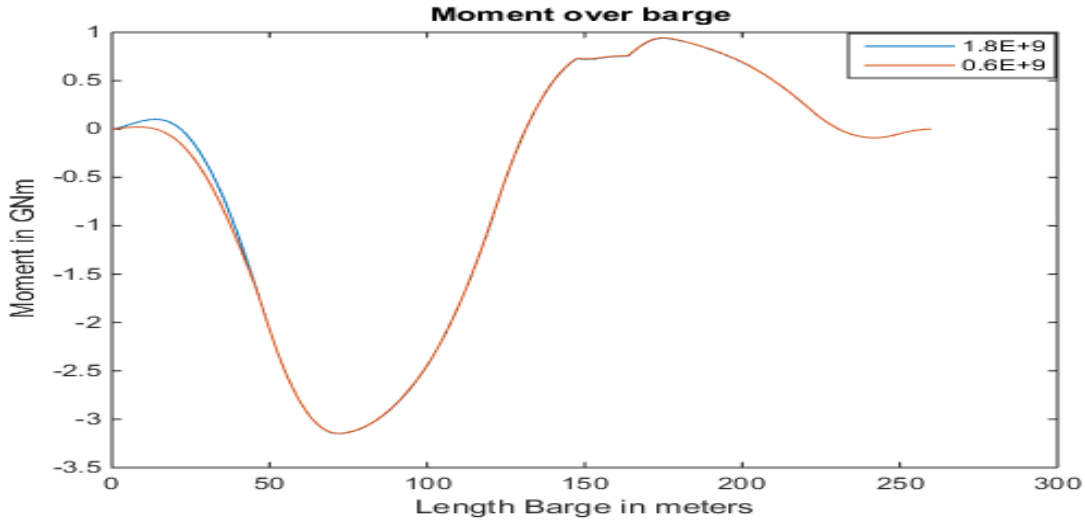

Figure 6-9 Moment over barge for step 40, skidbeam movement

The reduction of the peak moment for step 40 was 10 percent. For this step relocating the skidbeams proved effective in reducing the peak moment in the skidbox in a certain area. This doesn't necessarily have to be the case for all the steps. The problem is that relocating the skidbeams only changes the deck stiffness between the transverse bulkheads. To gain a proper insight into the effects overall the 2 deck stiffness are plotted but also included is a plot in which the skidbeams are relocated and the transverse bulkheads are given the same stiffness as the rest of the deck. This is a hypothetical situation but is sketched in order to clarify certain effects.

For all the steps combined the peak moment per section of skidbox are shown in Figure 6-10.

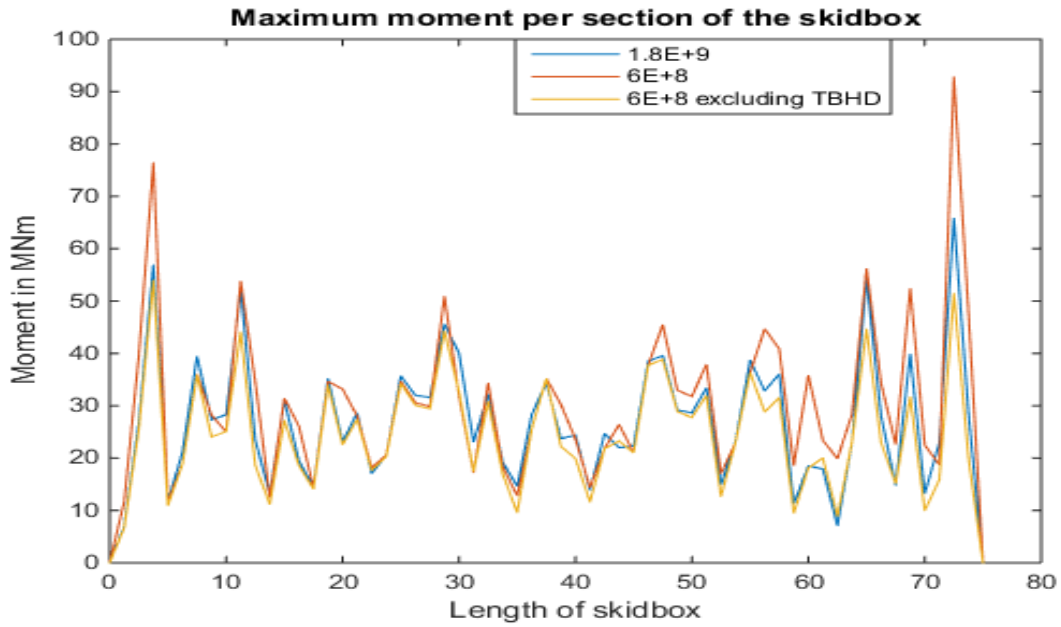

Figure 6-10 Maximum moment per section, various deck stiffness

It can be seen that reducing the deck stiffness is ineffective in reducing the peak moments in the skidbox, even significantly increasing the peak moment especially at the first connection and last connection to the DSF. These same results can be seen in Figure 6-11 for the maximum shear force per section. Reducing the deck stiffness is also ineffective in reducing the peak shear force in the skidbox.

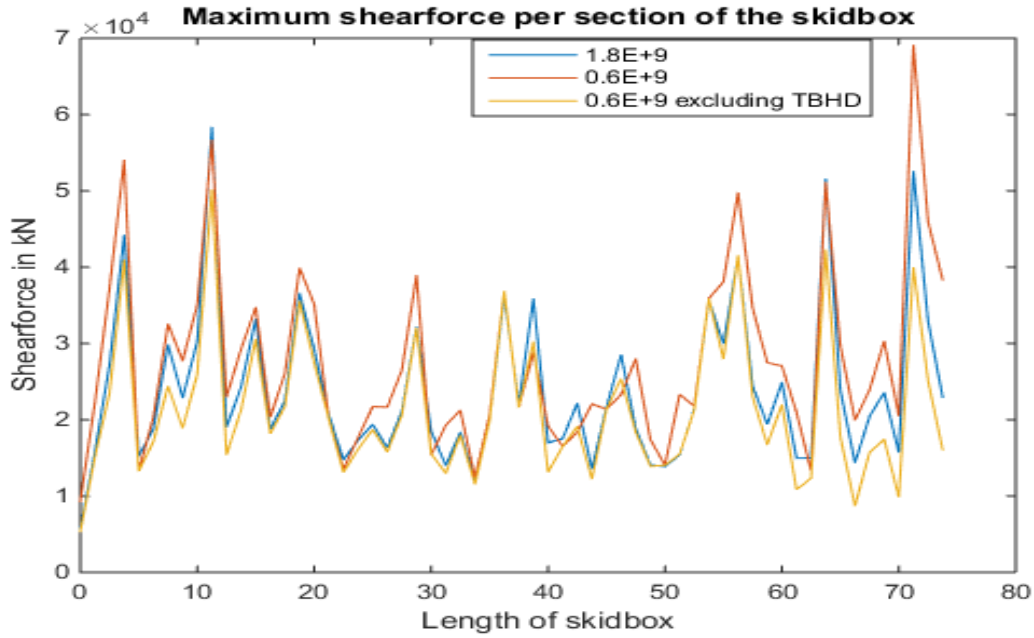

Figure 6-11 Maximum shear force per section, various deck stiffness

In order to gain more insight in this effect a look is taken to the peak moment in the skidbox per step, seen in Figure 6-12

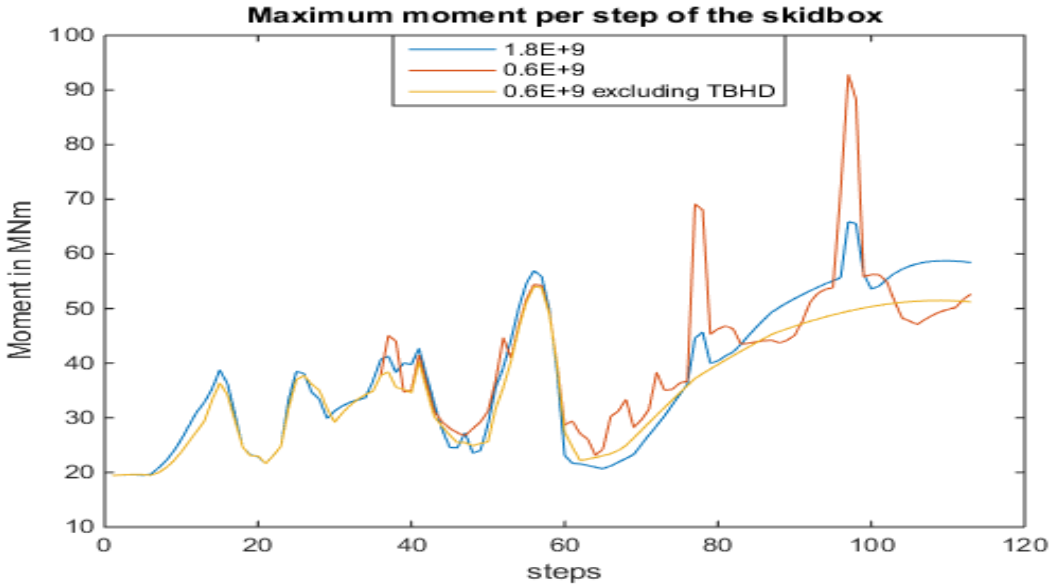

Figure 6-12 Maximum moment per step, various deck stiffness

In Figure 6-12 it can be seen that as long as the skidbox is still partially on the quay the effects of decreasing the barge deck stiffness by relocating the skidbeams is minimal. When the skidbox is fully

on the barge however an effect can be seen. The explanation for this is as follows. After step 61 the barge will increasingly start to sag. The skidbox will have to "follow" this shape. The softening effect which was explained earlier can't not come to full effect because of the TBHDs. It can be seen that the effects of the TBHD is significant. When these TBHDs are given the same stiffness as the rest of the deck, the maximum moment will decrease. If the barge deck is less stiff the skidbox will not have to follow this forced displacement as much causing a lower peak moment for steps 61 and above.

Concluding it can be said that relocating the skidbeam to the area of the deck with the lowest stiffness has no positive effect on the peak moment in the skidbox. The transverse bulkheads neglect the effect that reducing the deck stiffness has on the peak moment in the skidbox.

7 Quayside Stiffness

Initially the topside+DSF is located fully on the quay before it is transferred to the barge during the load-out. The properties of the quay have an influence on the load distribution during the load-out. Up until now the model used the quayside stiffness used by HMC. In this chapter the effects of the quayside properties on the force during the load-out will be investigated using the MATLAB model.

The quay used in the base case is the quay from the base case topside load-out, at the Daewoo Shipbuilding and Marine Engineering yard at Okpo, South Korea. Unfortunately not a lot of data was available about the quayside at the DSME yard.

7.1 HMC model with varying stiffness

HMC uses the most simple model for the quay. Hereby the quay is modeled as a set of uniform independent springs with an assumed stiffness of 26579mT/m/m. This model neglects the fact that a load on a certain area of quay also effects the displacement of the surrounding area right next to it. This model will first be used to test the effects of different quayside stiffness on the load-out. The quayside stiffness used by HMC will be set to 100%, the range of stiffness's will be set as a percentage of the original stiffness. A look is taken at a broad range from fully rigid, to 10%, and 5% and 1 % of the HMC value. The deflection of quay, barge and skidbox and also the moment distribution over the barge and skidbox will be discussed.

First the effects of the quayside stiffness on the forces distribution during the load-out are checked for the standard ballast configuration in step 40 to get an understanding of what is happening during changing quayside stiffness.

As can be seen in Figure 7-1 the quay will deflect more when the stiffness drops. The difference between fully rigid and the value used by HMC don't differ that much. What can clearly be seen in this example is that the springs of the quay are independent in this model causing a steep difference between the area affected by the skidbox and the area just to the left of it. In reality however this isn't the case.

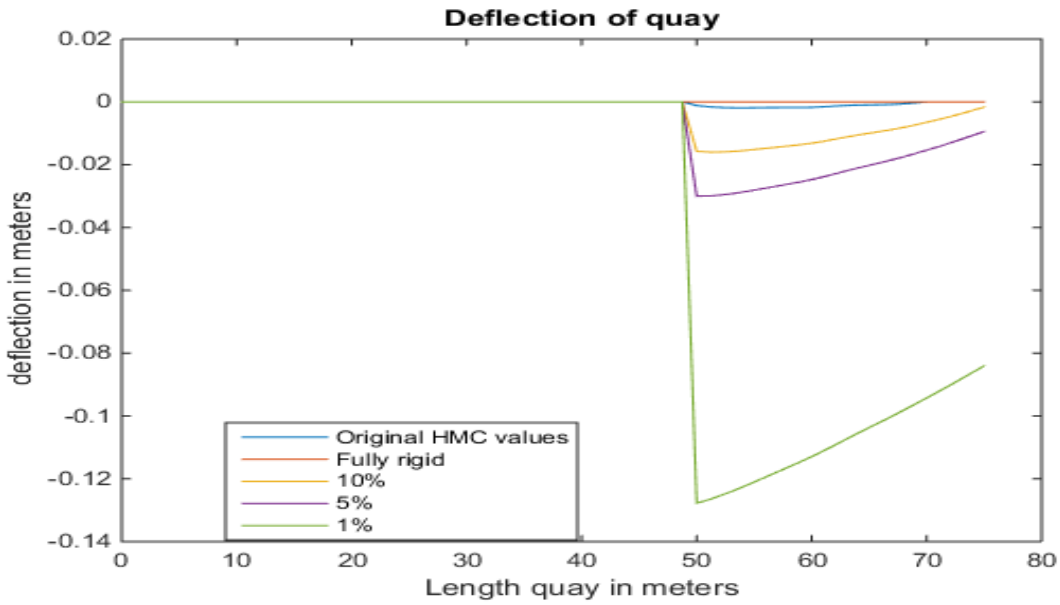

Figure 7-1 Quayside deflection vs quayside stiffness

The deflection of the skidbox also changes significantly with a significant reduction of quayside stiffness as can be seen in Figure 7-2. Using also Figure 7-3 it is interesting to note that a decrease in quayside stiffness also causes the barge to deflect down in this example. The barge will be pushed down more by the weight of the topside as the quayside stiffness reduces. So what doesn't happen in this case is that the skidbox on the quay will deflect downwards and the part on the barge will remain the same causing a steeper inclination in skidbox deflection, as one might have expected. Contrary to this the effect of reducing quayside stiffness leads to a more smooth transition between quay and barge.

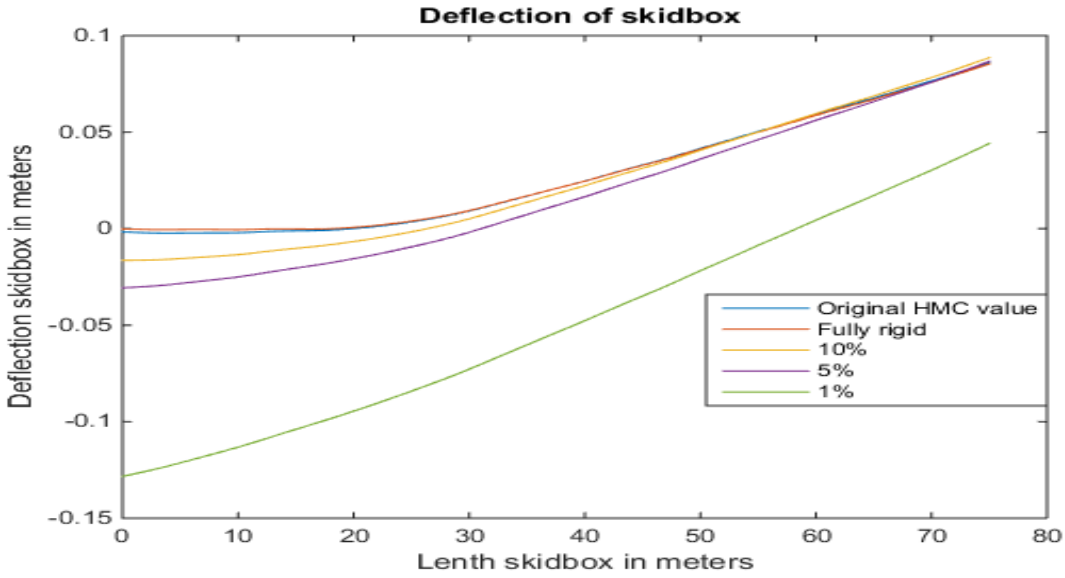

Figure 7-2 Skidbox deflection vs quayside stiffness

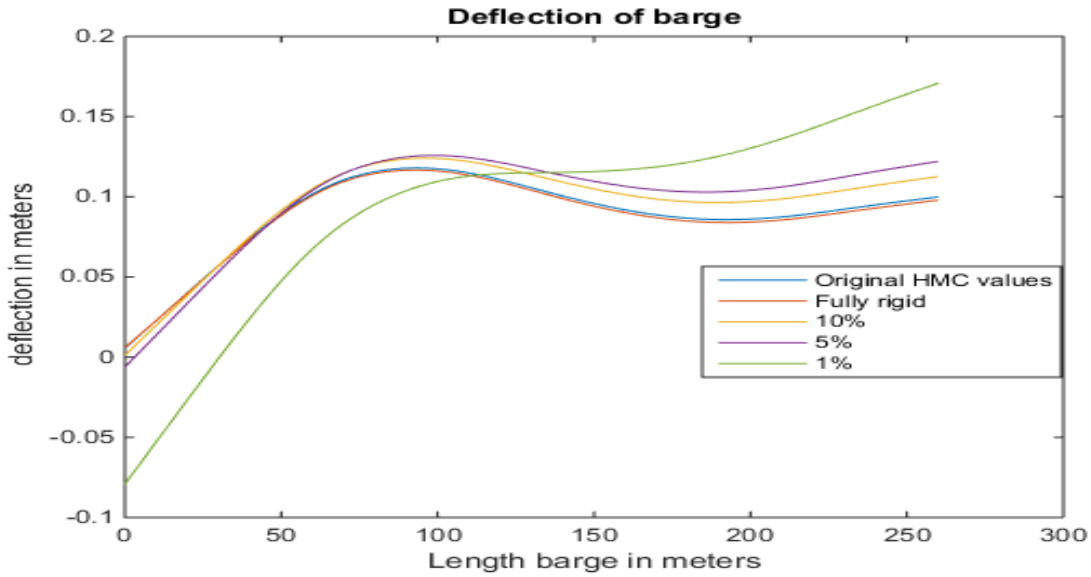

Figure 7-3 Barge deflection, vs quayside stiffness

This more smooth transition translates into a lower peak moment around the barge-quay connection (at 26.25m for step 40) as can be seen in Figure 7-4, however this effect isn't very significant. For the highest peak moment at the first DSF connection the contrary is the case since here a fully rigid quay has the lowest moment.

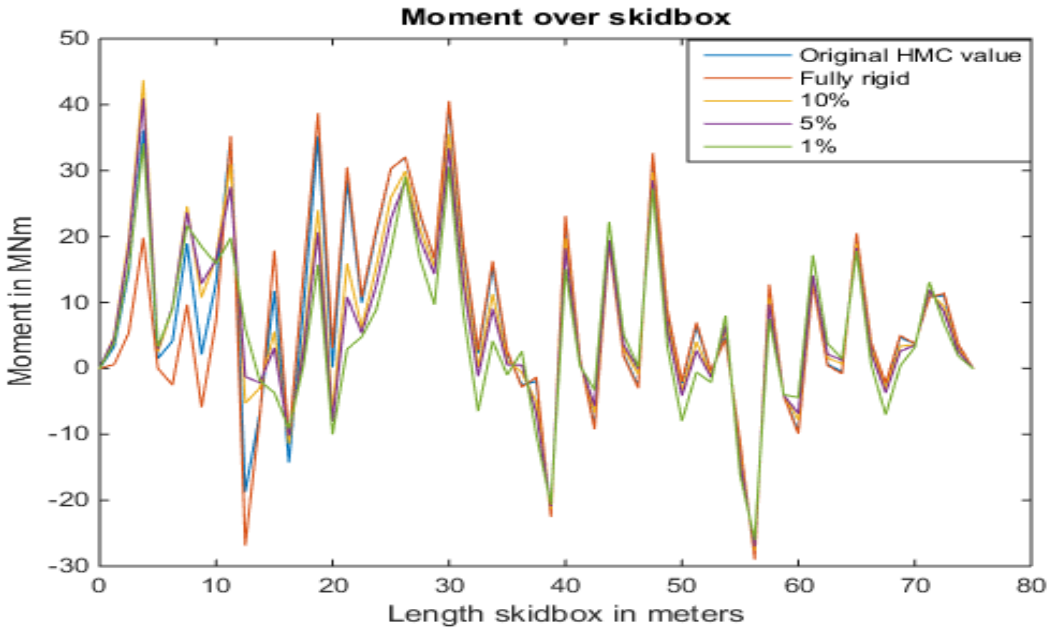

Figure 7-4 Moment over skidbox vs quayside stiffness

The effects on the forces on the barge were also tested but despite the changes of the barge deflection there was no significant effect on the moment distribution. The effect on the peak moments over the entire load-out until the barge leaves the quay will be investigated next. For the entire load-out until step 61 the peak moment results vs the quay stiffness are seen below:

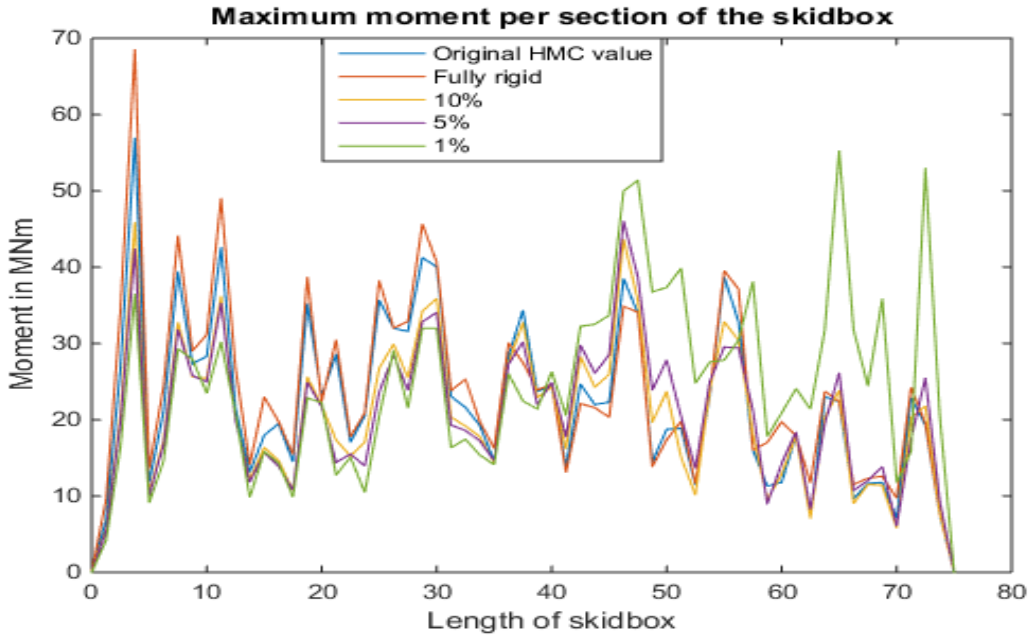

Figure 7-5 Maximum moment per section, vs Quayside stiffness

It can be seen from Figure 7-5 that the effect of reducing the quay stiffness differs from the back of the skidbox towards the front of the skidbox. For the first 37.5 meters the effect is that a reduction of the quay stiffness leads to a lower peak moment in the skidbox. For the latter 37.5 it's the other way around as a reduction of the quay stiffness here leads to a higher peak moment, most noticeably at 1% of the original value. The effects on the shear force is omitted since these results proved to be in line with the results for the maximum moment. In order to gain more insight into the peak moment over the skidbox, the peak moment over the skidbox per step is also shown.

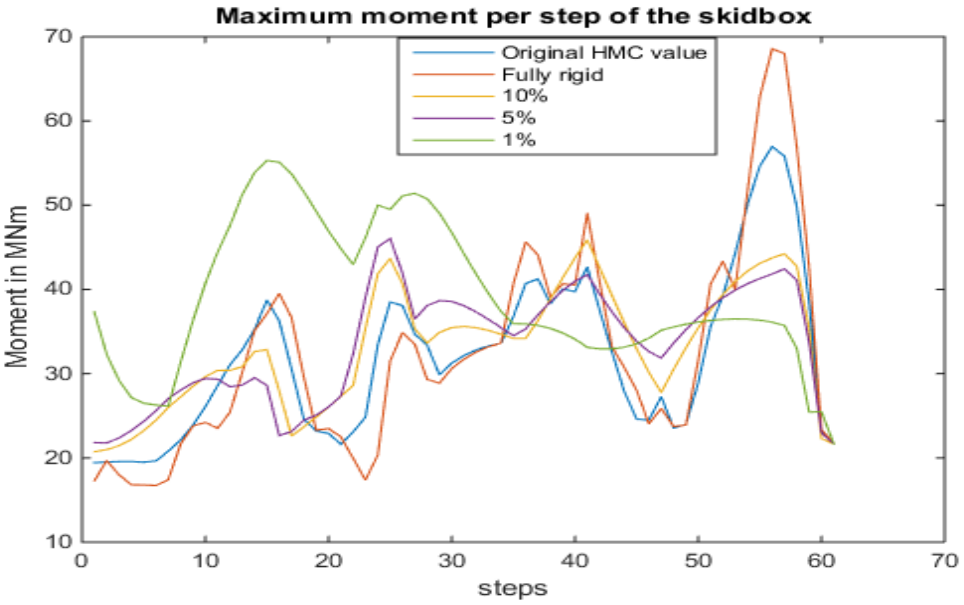

Figure 7-6Maximum moment skidbox per step, vs quay stiffness

Here it can be seen that the high peak moment for 1% quay stiffness seen in Figure 7-5 was mostly down to step 10 to 35. This was investigated further to see what is happening at that location. Only the deflection of the skidbox is shown, see Figure 7-7. The explanation for the high moment in these

steps is that due to the low quay stiffness the skidbox deflection becomes a steep curve downwards until the part that is in contact with the barge can't continue this trajectory and has to flick upwards, this in turn causes a high moment in this location. This could also be seen in Figure 7-5 because the high moment at 1% quay stiffness was mostly focused at the last 35 meters of the skidbox.

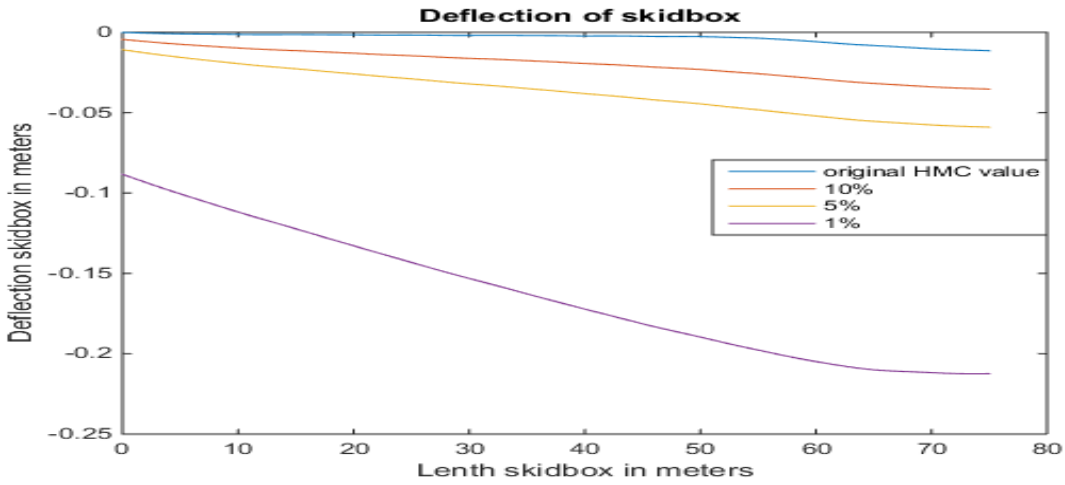

Figure 7-7 Deflection of skidbox for step 15, vs quay stiffness

7.2 Adjusted Winkler model

In the previous paragraph the springs in the quay had no connection to each other meaning that the stiffness of a single piece of soil has no relationship to what's happening to the soil around it. In this paragraph we will investigate what the effect is of using a different model, one in which the springs are coupled by the foundation layer. This difference is seen in Figure 7-8.

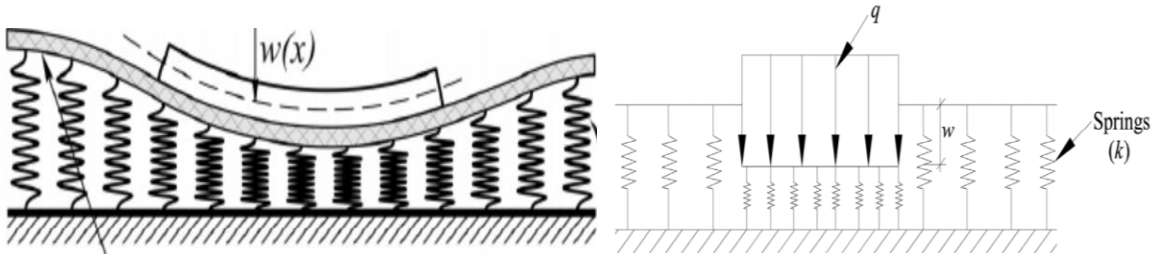

Figure 7-8 Winkler model (left) vs HMC model (right)

The effects of the quayside foundation stiffness, so of the beam representing the foundation layer and not the springs below, have been checked and the effects are minimal using the original HMC quayside stiffness. The displacements of the foundation beam are too small for the stiffness of this beam to have a significant effect on the load-out.

In order to see the full effects the 5% quay stiffness is selected for step 40. An initial estimate is calculated for a reinforced concrete foundation, this calculation can be seen in appendix C. The other stiffness's for the foundation are expressed as a percentage of the estimation from appendix C**.** A fully rigid foundation is also included. The calculated stiffness from the example has an *EI* for the foundation of $2.57*10^{11}$ Nm^2.

The deflection of the quay is looked at first in Figure 7-9. It can be seen that there is a distinct difference in quayside displacement between the HMC method and the calculated method set at 100%. The deflection is less the more rigid the foundation because with a rigid foundation, areas of the soil which aren't directly under the skidbox are carrying the load as well. However in at the end of the quay it is the other way around. This also affects the deflection of the skidbox as can be seen in Figure 7-10. The smooth transition between barge and quay is damped by a more rigid foundation. This is due to the deflection being less but also the angle between barge and quay is negatively affected. The effect is different from reducing the quay stiffness, there the skidbox just had a larger deflection overall.

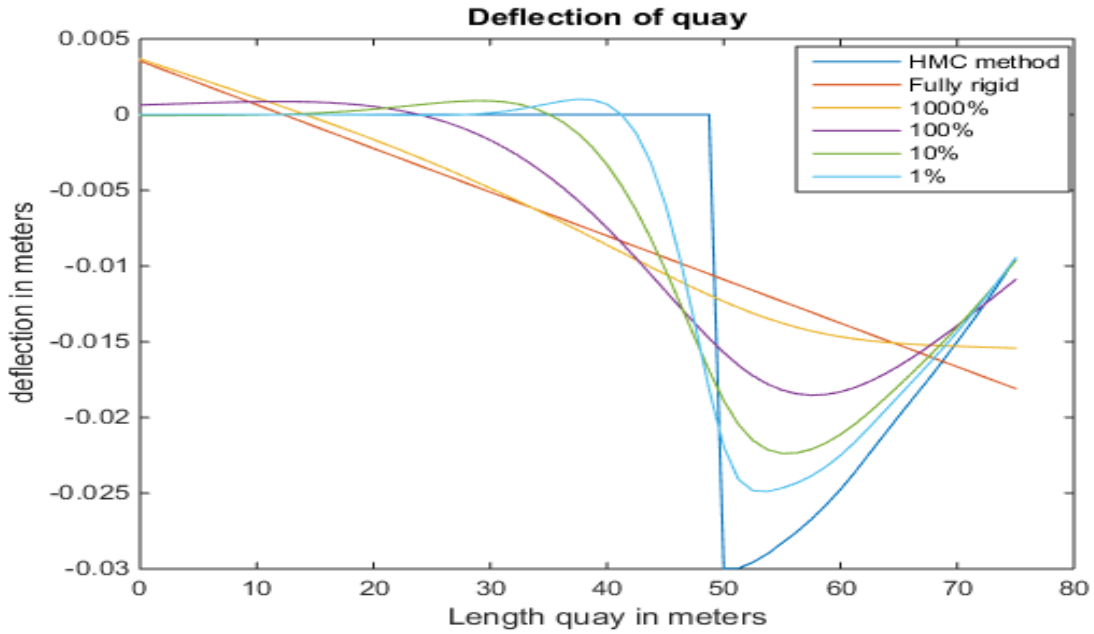

Figure 7-9 Deflection of quay, step 40, various foundation stiffness

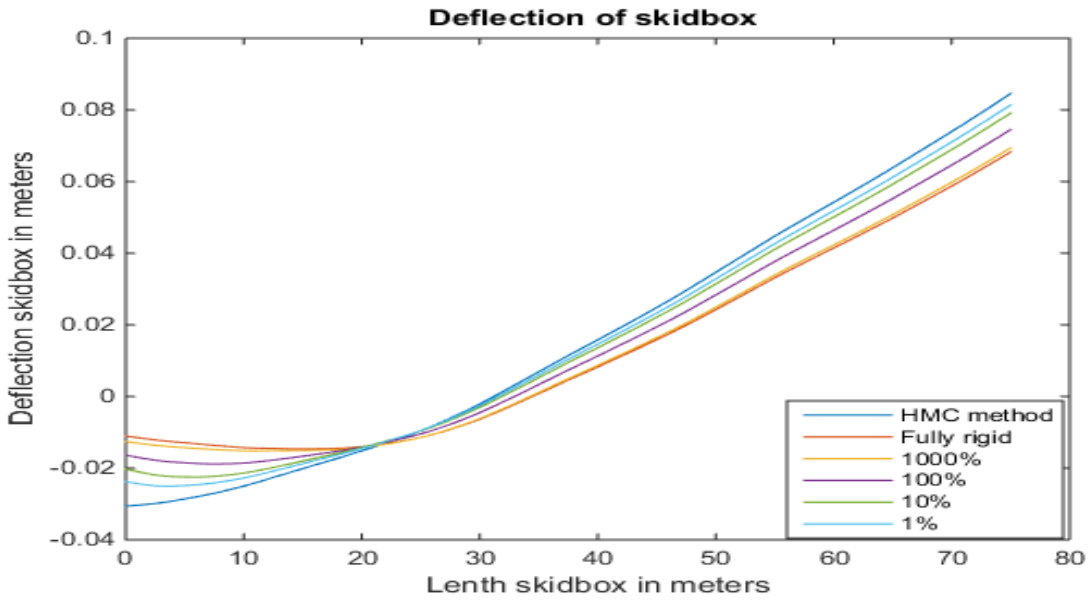

Figure 7-10 Deflection of skidbox, step 40, various foundation stiffness

The effects this shift in foundation stiffness has on the moment over the skidbox isn't uniform over the skidbox as can be seen in Figure 7-11. For the skidbox section on the barge there is hardly any difference although here the effect is the more rigid the foundation the higher the moment over the skidbox but these effects are marginal. For the section on the quay a significant effect can be seen however. Especially for the first few meters the effects on the moment distribution are very large. A difference of 62 MNm between the 1% stiffness and the fully rigid occurs. The reason for this can be seen in the quay deflection. The deflection of the quay has a very steep curve for the first 5m of skidbox in the 100%,10% and 1% stiffness results. It can be seen that the skidbox wants to follow that curve. This in turn creates a high peak moment at this section of skidbox for these stiffness values.

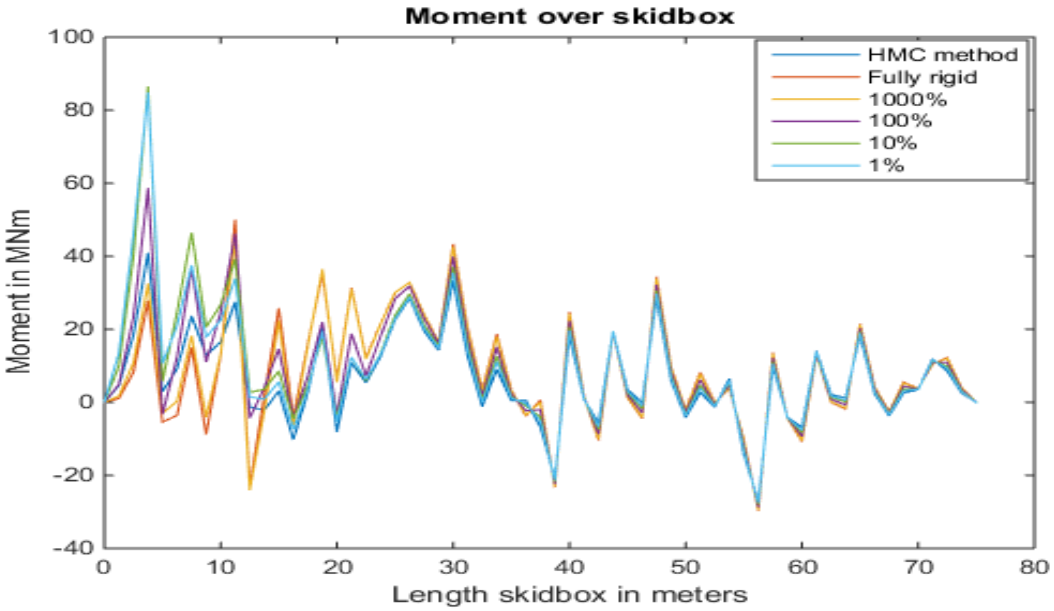

Figure 7-11 Moment over skidbox, step 40, various foundation stiffness

In Figure 7-12 it can be seen that the results for the shear force over the skidbox are in conjunction with the results for the moment over the skidbox in that here too the impact of varying the foundation stiffness has significant effects for the part of the skidbox still located on the quayside.

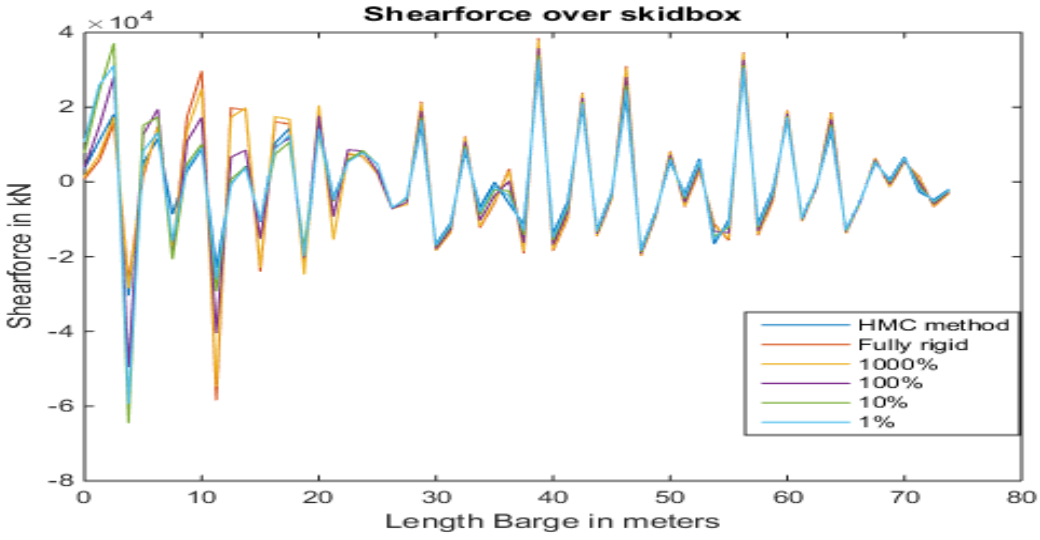

Figure 7-12 Shear force over skidbox, step 40, various foundation stiffness

The overall results for the skidbox for the entire load-out are discussed next. In Figure 7-13 it can be seen that the results are in line with the results for step 40 alone, in that the effects of the foundation stiffness mostly affect the first half of the skidbox. Looking at the first peak, which is around the first connection with the DSF, the HMC method shows by far the lowest maximum moment, with a value of 93 MNm for the 100% stiffness and a value of 41 MNm for the HMC value. The HMC method thus results in a very significant underestimation of the forces for the gives quay stiffness. The reason for this already became apparent for step 40.

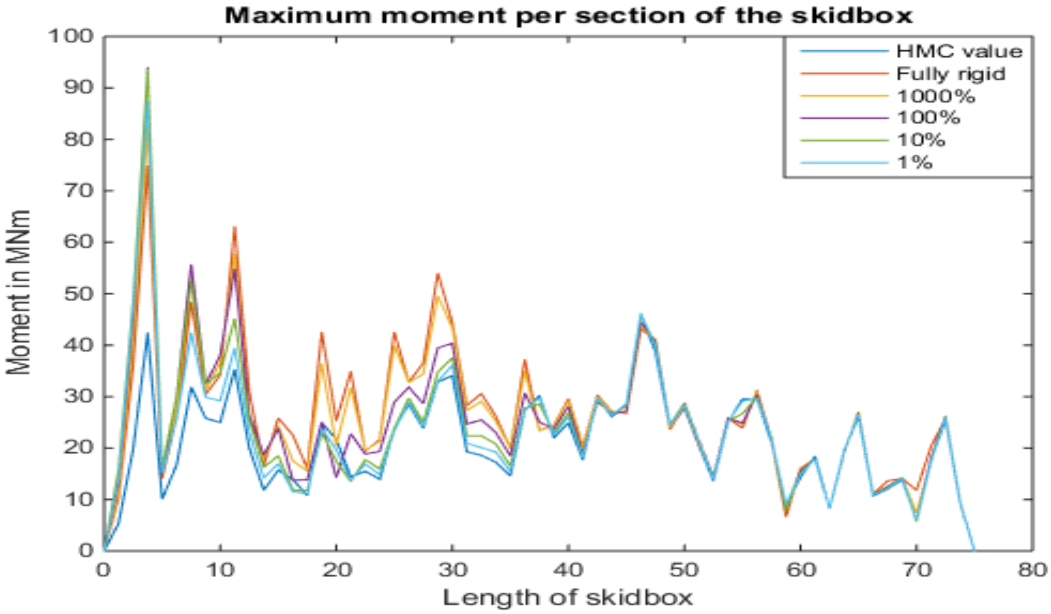

Figure 7-13 Maximum moment per section of the skidbox, various foundation stiffness

The results for the shear force, as seen in Figure 7-14 show comparable results. Here too, a very significant difference between the 100% stiffness value and the HMC value can be seen. The maximum shear force at 100% for the first peak is 6.9*10^4 kN whilst for the HMC value this is far less with 3.3*10^4 kN.

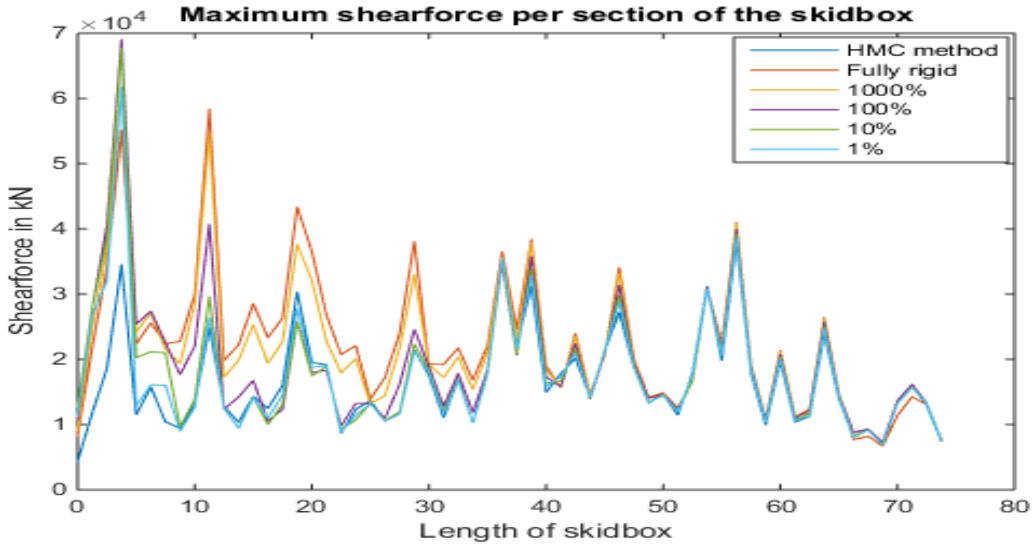

Figure 7-14 Shear force over skidbox, step 40, various foundation stiffness

The effects per step are only looked at for the maximum moment as this will give a sufficient enough picture of the distribution of the forces over the steps. From Figure 7-15 it can be seen that the major differences occur after step 27. From there the maximum moment per step starts to diverge for each different stiffness with the HMC method showing the lowest maximum moment. The reason for this is that before step 27 the part of the quay on which the skidbox is positioned shows the same deformation for varying stiffness as can be seen in Figure 7-16

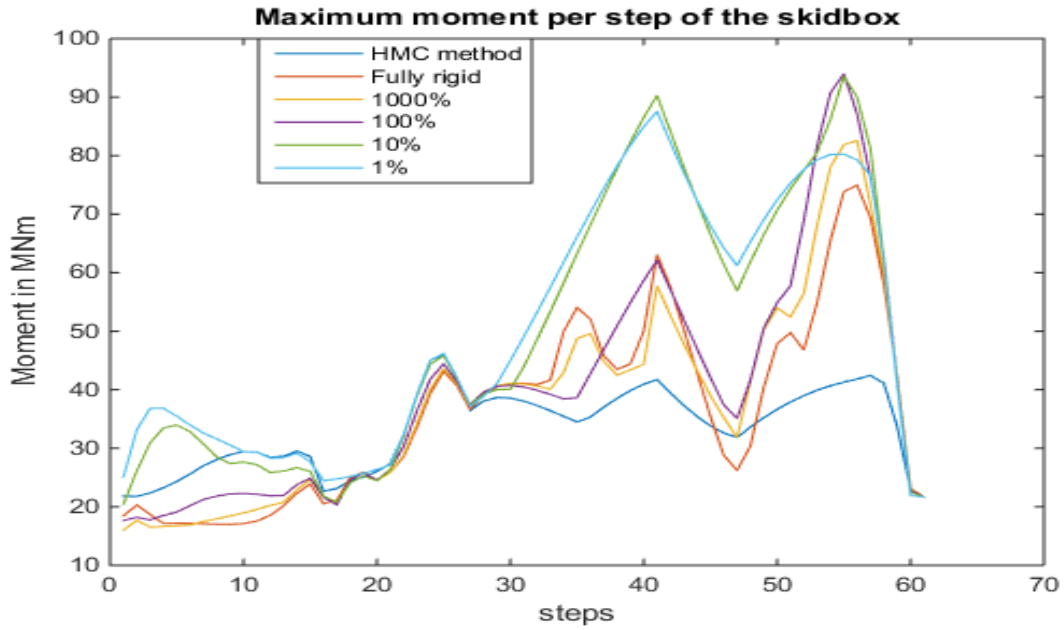

Figure 7-15 Maximum moment per step of the skidbox, various foundation stiffness

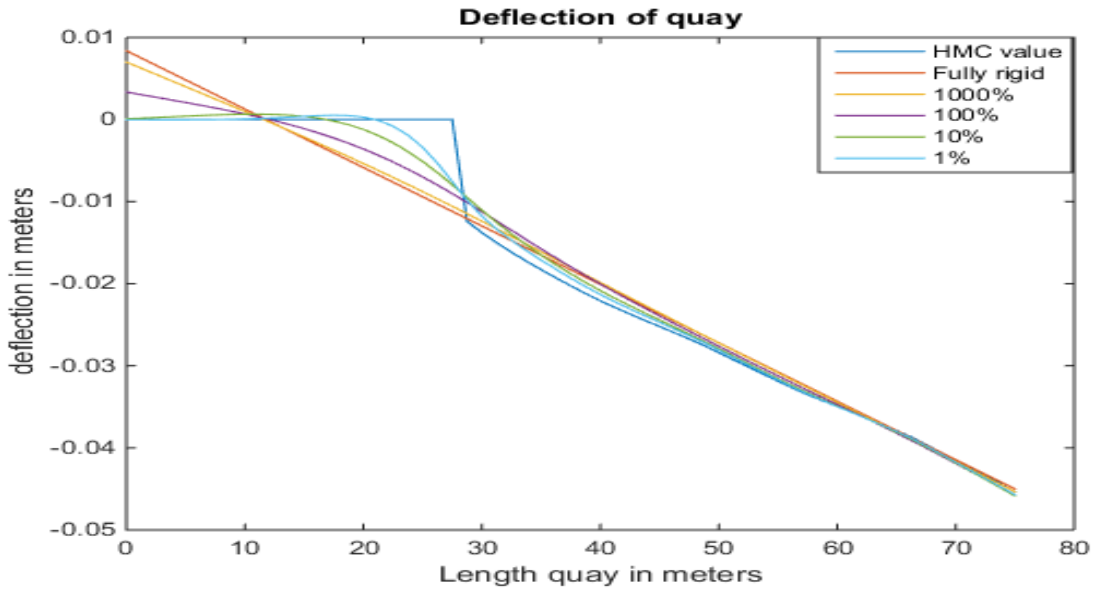

Figure 7-16 Deflection of quay, various foundation stiffness, step 23

The most important conclusion which should be drawn from this research into varying foundation stiffness is that not taking into account the stiffness of the foundation layer can lead to a severe underestimation of the forces involved, especially in combination with a quayside which has a low soil stiffness.

8 Conclusions

This thesis research has dealt with many aspects which are involved in the load-out. The ballast configuration, the quayside and the deck of the barge; the effects of these aspects all have been included in the model and were extensively analyzed. In this section conclusion will be drawn from the previous thesis research.

The first topic which will be looked at is the ballast configuration optimizations. Three different optimizations were performed each with its own criteria. The first optimization was optimization A which performed the best of all the optimizations in terms of keeping the forces in the barge as low as possible. However this came with the downside that it didn't perform very well in keeping the forces in the skidbox as low as possible, even performing worse than the standard ballast configuration. The second optimization, optimization B, put more emphasis on the barge-quay alignment hereby sacrificing performance in keeping the forces in the barge as low as possible. This optimization still performed better than the standard ballast configuration in keeping the forces in the barge as low as possible although it didn't perform as well in this area as optimization A. However optimization B also performed a lot better than the standard ballast configuration in keeping the forces in the skidbox as low as possible. Optimization B thus combined the best of both worlds in performing well for the two different criteria. The final optimization which was performed differed significantly from the previous two optimizations. This optimization focused entirely on keeping the rotations as low as possible on 4 strategic chosen positions in the topside. Keeping the rotations low at those locations will result in low forces in the topside deck. This optimization did succeed in keeping these rotations very low until the point where they don't happen at all. However it, surprisingly, didn't succeed in reducing the forces in the skidbox although it has to be pointed out that this was mostly due to one step in the load-out process. Unsurprisingly, the results for the barge were the worst using this optimization. It had the highest peak forces of all the optimizations and the standard ballast configuration. Which optimization is superior to the other is project dependent. In the base case optimization B was chosen to be superior because it performed well in all criteria. However load-outs in which the barge is the limiting factor due to a very heavy topside might be better suited for the use of optimization A and load-outs where critical elements in the topside can be identified might be better suited for optimization "DSU con"

A structural solution which could help in reducing the forces during the load-out was also investigated with relocating the skidbeams to a position on the barge with lower stiffness. This investigation showed that this has no beneficial effects on the forces, contrary the forces became even higher when using the lower stiffness. This was due to the fact that the transverse bulkheads, which are hard points on the deck, remain in place. Lowering the stiffness in between these hard points causes the peak forces at these hard points to become even higher.

The effects of the quayside stiffness were also investigated for the base case scenario. Although the effects on the forces in the barge were minimal the effects on the forces in the skidbox were significant. Although no unambiguous result can be given as the effects of the lower stiffness depends on each situation individually, it can be said that changing the stiffness of the quay has significant

effects and that a precise figure needs to be known for quayside stiffness when carrying out a load-out in order to properly model the expected forces. It could also be seen that when adding the stiffness of the quayside foundation to the model the results changed significantly for lower stiffness quaysides and that neglecting this effect could lead to an underestimation of the forces involved.

9 Recommendations

The model made in this thesis research has the potential to be improved even further. The current models strength lies in its simplicity to make fast load-out optimizations for a 2-D situation. These results can then be used as an indication for the real world 3-D situation. The current MATLAB model however can also be modified into a 3-D MATLAB model. The method for this which is recommended is to use 2 beams for the barge which are similar to the one beam used in this model for the barge. These beams are then interconnected with other beams. The same needs to be done with the DSF, topside and skidboxes. In the 3-D model one would have 2 skidboxes sliding over 2 barge beams. This new model would also take into account torsion forces and roll of the barge. It would also provide a better indication of the transverse distribution of the ballast, something which the current model ignores.

In the model each step of the load-out is independent and the factor of time doesn't play any role. This is a proper method because the load-out can be seen as a quasi-static process because the speeds involved are so low. However for the ballast optimizations this approach has a downside. For each step in the load-out, the ballast optimization is performed independently of the previous step. This can cause a ballast tank to be empty in one step, be filled in the next and be empty again in the following step. This is an unwanted situation because this causes the whole process to take even more time due to the max pump capacity. It is therefore recommended that for future research in each step a dependency on the previous step's ballast situation is incorporated into the model.

Recommendations for future load-outs:

Looking at the results for the ballast optimizations, it can be stated that significant improvements can be achieved by using a different ballasting configuration. It could also be seen that the forces experienced during the load-out are well within the limits of the designated structures for every optimization except "DSU con".

Therefore it is recommended that for future load-out procedures critical elements are identified within the barge, topside and DSF which is already the procedure now. The ballast configuration can then be adjusted accordingly to reduce the stress on this critical element. The method used for this is similar as was performed in Optimization "DSU con". However it is project dependent on which ballast optimizations, B or C, is the best choice.

It is also recommended that in the future the method of modelling the quay is changed. As was shown in chapter 7 modelling the quay as independent springs is incorrect. Modelling the quay as a foundation beam supported by springs led to significant changes in the case of low quay stiffness. Although for a topside load-out a low stiffness quay is unlikely, it should be taken into account in other load-outs which might take place from a low stiffness quay.

Bibliography

[1] Robert D. Cook, Concepts and Applications of Finite Element Analysis, Wiley

[2] C. Hartsuijker, J.W.Welleman, Engineering Mechanics volume 2 Stresses, strains, Displacements, Springer

[3] L.A.G. Wagemans, Quick Reference Guide civil engineering, TU Delft

Appendices

Appendix A: MATLAB model

Below the MATLAB code is given for the entire model. Excluded from this code is all the code which returns the plots, also the code which builds the topside and DSF is excluded.

```
clc
clear all

%number of topside nodes
d=25;

%number of quaynodes
q=60+1;
%number of nodes next to dsf and barge
l=d+q;
%number of elements barge
j=208 ;
%number of elements skidbox
k=60;
%each spring(kcon,khydro,kquay) is the continuos value,
%% INPUTS
Ball=zeros(11,4);
eib=xlsread('importantbargeattributes0.xlsx','H1:H105')';
EIb=repmat(eib,2,1);EIb=EIb(:);
EIb(1)=[];EIb(209)=[];

%Force along the barge;ballast and own weight
w=xlsread('importantbargeattributes9.xlsx','Y1:Y105')';
W=repmat(w,2,1);W=W(:);
W(1)=[];W(209)=[];
%ballast%%%%%%%%%%%%%%%%%%%%%%%%%%%%%%%%%%%%%%%%%%%%%%%%%%%%%%%%%%%%%%%%%%%%%%%
%%%%%%%%%%
bal=xlsread('ballastarrangement1.xlsx','AT1:BC208');
Bal=transpose(bal);
Ballast=interp1([0 6 14 26 40 46 61 76 86 113],Bal,0:113);
Ballast=transpose(Ballast);
%%%%%%%%%%%%%%%%%%%%%%%%%%%%%%%%%%%%%%%%%%%%%%%%%%%%%%%%%%%%%%%%%%%%%%%%%%%%%%%
%%%%%%
%correction for buoyant force
cor=ones(j,1);
cor(1:124)=0.97*1025*9.81*63*11.2;
cor(124:200)=0.97*1025*9.81*42*11.2;
cor(201:208)=0.7*1025*9.81*42*11.2;

%Lengths
%DSF values
```

```
AEs=0.3*(10^12)*ones(k,1);
EIs=1*1.31754*200*10^9*ones(k,1);
EIq=2.54*10^11*ones(q,1);
%EIq=1*ones(q,1);
Ls=1.25*ones(k,1);


%values topside
AE12=[4.57073E+11 4.24733E+11 4.24733E+11 4.57073E+11];
AE2=[2.04431E+11 1.11951E+11 59933733849];
 AE4=[29966866924 1.96436E+11];
AE2=1*ones(4,1);
AE4=1*ones(4,1);
AE6=[4.57073E+11 4.24733E+11 4.24733E+11 4.57073E+11];
 AE8=[1.86791E+11 1.11951E+11 59933733849];
 AE10=[29966866924 1.99609E+11];
AE8=1*ones(4,1);
AE10=1*ones(4,1);
EI12=[2.57743E+12 2.13999E+12 2.13999E+12 2.57743E+12];
 EI2=[1.08491E+12 5.01655E+11 2.58268E+11];
 EI4=[2.58268E+11 1.16352E+12];
%EI12=1*ones(4,1);
EI2=1*ones(4,1);
EI4=1*ones(4,1);
EI6=[2.57743E+12 2.13999E+12 2.13999E+12 2.57743E+12];
 EI8=[1.11807E+12 5.01655E+11 2.58268E+11];
 EI10=[2.58268E+11 1.06218E+12];
EI6=ones(4,1);
EI8=1*ones(4,1);
EI10=1*ones(4,1);
L12=7.5*ones(4,1); L2=11.52*ones(4,1);
L4=12.2*ones(4,1);L6=8.5*ones(4,1); L8=12.2*ones(4,1);
L10=11.52*ones(4,1);
AEU=4.25102E+11*ones(6,1);
AEL=4.0104E+11*ones(6,1);
AEC=2.5088E+11*ones(6,1);
AEDSU=4.2468E+11;
EIc=59064800000*ones(6,1);
EIu=1.99187E+11*ones(6,1);
EIl=1.81079E+11*ones(6,1);
EIdsu=1.19777E+13;
LsU=8.75*ones(6,1);
LsL=8.75*ones(6,1);
LsC=8.75*ones(6,1);
LsDSU=0.5;
AED=[1.13551E+11 1.13551E+11 1.13551E+11 75987272309
75987272309];
EId=[8.67365E+11 8.67365E+11 8.67365E+11 3.95371E+11
3.95371E+11];
LsD=[14.23 12.1 14.23 13 13];
AE0=75987272309;
```

```
Ls0=17.5;
EI0=3.95371E+11;


Lq=1.25*ones(q,1);


kquay=0.05*1.3*10^9*ones(q,1);
AE=1*(10^12)*ones(j,1);
kcon=zeros(k+1,1);
%horizontalspring
kx=zeros(j);
kx(1)=10;
%% STORE FUNCTIONS
w_bargeindex=zeros(209,61);
w_skidboxindex=zeros(61,61);
M_skidboxindex=zeros(61,61);
M_bargeindex=zeros(209,61);
V_bargeindex=zeros(208,61);
V_skidboxindex=zeros(60,61);
theta_upperbarindex=zeros(4,61);

%% Video
% vidObj =
VideoWriter('\\ALECTO\users$\nickyve\desktop\1to6skid.avi');
% vidObj.FrameRate=1;
% open(vidObj);
%% start run
%x is number of connections between skid and barge
for x=40;
    %% MODEL connectionsprings
    %Input
    z=ones(k+1,6);
%spring test

    for spring=1:6
%Define connection between skidbox and barge+quay
    kcon_barge=1.644*10^9*ones(j+1);
   kcon_quay=1.9*10^10;
   kcon_infill=1.644*10^9;
   kcon_barge(1:25)=kcon_infill;
   kcon_barge(37:20:197)=2.8508*10^9;



 if x<=61
   kcon(1:k+1-x)=kcon_quay;
   kcon(k+1-(x-1):k+1)=kcon_barge(1:x);
   else
       kcon(1:k+1)=kcon_barge(x-60:x);
 end
```

```
    kcon_list=zeros(1,3+3*k);
    kcon=z(1:k+1,spring).*kcon;
%forming kcon_list
    for i=1:k+1
        P=[0 kcon(i)*1.25 0];
        kcon_list(-2+3*i:3*i)=P;
    end

    kcon_list(2)=kcon_list(2)*0.5;
    kcon_list(3*k+2)=kcon_list(3*k+2)*0.5;



%number of nodes besides the skidbox see figure drawing !
%% Deck
Kdeck=zeros(3*21);


%Forming 3 decks

%Center
for i=1:6

Kselement_deckC=[AEC(i)/LsC(i) 0 0 -AEC(i)/LsC(i) 0 0;
    0 (12*EIc(i)/(LsC(i)^3)) 6*EIc(i)/LsC(i)^2 0 -
12*EIc(i)/LsC(i)^3 6*EIc(i)/LsC(i)^2;
    0 6*EIc(i)/LsC(i)^2 4*EIc(i)/LsC(i) 0 -6*EIc(i)/LsC(i)^2
2*EIc(i)/LsC(i);
    -AEC(i)/LsC(i) 0 0 AEC(i)/LsC(i) 0 0;
    0 -12*EIc(i)/LsC(i)^3 -6*EIc(i)/LsC(i)^2 0
(12*EIc(i)/(LsC(i)^3)) -6*EIc(i)/LsC(i)^2;
    0 6*EIc(i)/LsC(i)^2 2*EIc(i)/LsC(i) 0 -6*EIc(i)/LsC(i)^2
4*EIc(i)/LsC(i)];

Kdeck(-2+3*i:3*i+3,-2+3*i:3*i+3)=Kdeck(-2+3*i:3*i+3,-
2+3*i:3*i+3)+Kselement_deckC;
end

%Upper
for i=1:6

Kselement_deckU=[AEU(i)/LsU(i) 0 0 -AEU(i)/LsU(i) 0 0;
    0 (12*EIu(i)/(LsU(i)^3)) 6*EIu(i)/LsU(i)^2 0 -
12*EIu(i)/LsU(i)^3 6*EIu(i)/LsU(i)^2;
    0 6*EIu(i)/LsU(i)^2 4*EIu(i)/LsU(i) 0 -6*EIu(i)/LsU(i)^2
2*EIu(i)/LsU(i);
    -AEU(i)/LsU(i) 0 0 AEU(i)/LsU(i) 0 0;
    0 -12*EIu(i)/LsU(i)^3 -6*EIu(i)/LsU(i)^2 0
(12*EIu(i)/(LsU(i)^3)) -6*EIu(i)/LsU(i)^2;
```

```
    0 6*EIu(i)/LsU(i)^2 2*EIu(i)/LsU(i) 0 -6*EIu(i)/LsU(i)^2
4*EIu(i)/LsU(i)];

Kdeck(19+3*i:3*i+24,19+3*i:3*i+24)=Kdeck(19+3*i:3*i+24,19+3*i:
3*i+24)+Kselement_deckU;
end
%Lower

for i=1:6

Kselement_deckL=[AEL(i)/LsL(i) 0 0 -AEL(i)/LsL(i) 0 0;
    0 (12*EIl(i)/(LsL(i)^3)) 6*EIl(i)/LsL(i)^2 0 -
12*EIl(i)/LsL(i)^3 6*EIl(i)/LsL(i)^2;
    0 6*EIl(i)/LsL(i)^2 4*EIl(i)/LsL(i) 0 -6*EIl(i)/LsL(i)^2
2*EIl(i)/LsL(i);
    -AEL(i)/LsL(i) 0 0 AEL(i)/LsL(i) 0 0;
    0 -12*EIl(i)/LsL(i)^3 -6*EIl(i)/LsL(i)^2 0
(12*EIl(i)/(LsL(i)^3)) -6*EIl(i)/LsL(i)^2;
    0 6*EIl(i)/LsL(i)^2 2*EIl(i)/LsL(i) 0 -6*EIl(i)/LsL(i)^2
4*EIl(i)/LsL(i)];


Kdeck(40+3*i:3*i+45,40+3*i:3*i+45)=Kdeck(40+3*i:3*i+45,40+3*i:
3*i+45)+Kselement_deckL;
end


%Force Matrix

%% DSF

%Matrix forming
    Kskid1=zeros(3+3*k);

%Skidbox is modeled with springsupport,
    for i=1:k
    %Constructing stiffness matrix and fill in elements
    Kselement=[AEs(i)/Ls(i)+kx(i) 0 0 -AEs(i)/Ls(i) 0 0;
    0 (12*EIs(i)/(Ls(i)^3)) 6*EIs(i)/Ls(i)^2 0 -
12*EIs(i)/Ls(i)^3 6*EIs(i)/Ls(i)^2;
    0 6*EIs(i)/Ls(i)^2 4*EIs(i)/Ls(i) 0 -6*EIs(i)/Ls(i)^2
2*EIs(i)/Ls(i);
    -AEs(i)/Ls(i) 0 0 AEs(i)/Ls(i) 0 0;
    0 -12*EIs(i)/Ls(i)^3 -6*EIs(i)/Ls(i)^2 0
(12*EIs(i)/(Ls(i)^3)) -6*EIs(i)/Ls(i)^2;
    0 6*EIs(i)/Ls(i)^2 2*EIs(i)/Ls(i) 0 -6*EIs(i)/Ls(i)^2
4*EIs(i)/Ls(i)];
    Kskid1(-2+3*i:3*i+3,-2+3*i:3*i+3)=Kskid1(-2+3*i:3*i+3,-
2+3*i:3*i+3)+Kselement;
    end
```

```
Kdsf=zeros(3+3*k+3*4);
Kdsf(3*4+1:3+3*k+3*4,3*4+1:3+3*k+3*4)=Kdsf(3*4+1:3+3*k+3*4,3*4
+1:3+3*k+3*4)+Kskid1;

%bovenste bar connection
for i=1:3
   Kselement_dsfu=[AE0/Ls0 0 0 -AE0/Ls0 0 0;
    0 (12*EI0/(Ls0^3)) 6*EI0/Ls0^2 0 -12*EI0/Ls0^3
6*EI0/Ls0^2;
    0 6*EI0/Ls0^2 4*EI0/Ls0 0 -6*EI0/Ls0^2 2*EI0/Ls0;
    -AE0/Ls0 0 0 AE0/Ls0 0 0;
    0 -12*EI0/Ls0^3 -6*EI0/Ls0^2 0 (12*EI0/(Ls0^3)) -
6*EI0/Ls0^2;
    0 6*EI0/Ls0^2 2*EI0/Ls0 0 -6*EI0/Ls0^2 4*EI0/Ls0];


Kdsf(-2+3*i:3*i+3,-2+3*i:3*i+3)=Kdsf(-2+3*i:3*i+3,-
2+3*i:3*i+3)+Kselement_dsfu;
end

%insert dsf
beta=[-121.8 -90 -58.2 -111.43 -68.57];


%Constructing force vector and fill in elements
weight_dsf=4218*1000*9.81;
Tdsf=weight_dsf/75;

qs=Tdsf*ones(k,1);
% qs(1:30)=qs(1:30)*0.8*T;
% qs(31:60)=qs(31:60)*1.2*T;

    Fskid=zeros(3+3*k,1);
for i=1:k
    %Felement=[-q(i)*L(i)/2; -q(i)*L(i)^2/12; -q(i)*L(i)/2;
q(i)*L(i)^2/12];
    Fselement=[0; -qs(i)*Ls(i)/2; 0;0; -qs(i)*Ls(i)/2; 0];
    Fskid(-2+3*i:3*i+3)=Fskid(-2+3*i:3*i+3)+Fselement;
end
    Fdsf=zeros(3*4+3+3*k,1);
    Fdsf(2,1)=-9810000;Fdsf(5,1)=-9810000;Fdsf(8,1)=-
9810000;Fdsf(11,1)=-9810000;
    Fdsf(3*4+1:3*k+3+3*4)=Fskid;


%% Combining DSF+skidbox and deck

Ktopside=zeros(3+3*k+3*d);
Ktopside(1:3*21,1:3*21)=Kdeck;
Ktopside(64:3+3*k+3*d,64:3+3*k+3*d)=Kdsf;
%connecting the deck to the DSF via DSU
```

```
KselementDSU=[AEDSU/LsDSU 0 0 -AEDSU/LsDSU 0 0;
    0 (12*EIdsu/(LsDSU^3)) 6*EIdsu/LsDSU^2 0 -12*EIdsu/LsDSU^3
6*EIdsu/LsDSU^2;
    0 6*EIdsu/LsDSU^2 4*EIdsu/LsDSU 0 -6*EIdsu/LsDSU^2
2*EIdsu/LsDSU;
    -AEDSU/LsDSU 0 0 AEDSU/LsDSU 0 0;
    0 -12*EIdsu/LsDSU^3 -6*EIdsu/LsDSU^2 0
(12*EIdsu/(LsDSU^3)) -6*EIdsu/LsDSU^2;
    0 6*EIdsu/LsDSU^2 2*EIdsu/LsDSU 0 -6*EIdsu/LsDSU^2
4*EIdsu/LsDSU];

    beta=-90;
T=[cosd(beta) sind(beta) 0 0 0 0;
  -sind(beta) cosd(beta) 0 0 0 0;
    0 0 1 0 0 0;
    0 0 0 cosd(beta) sind(beta) 0;
    0 0 0 -sind(beta) cosd(beta) 0;
    0 0 0 0 0 1];

KselementDSU_T=transpose(T)*KselementDSU*T;

for e=1:4

Ktopside(37+6*e:39+6*e,37+6*e:39+6*e)=Ktopside(37+6*e:39+6*e,3
7+6*e:39+6*e)+KselementDSU_T(1:3,1:3);
Ktopside(61+3*e:63+3*e,61+3*e:63+3*e)=Ktopside(61+3*e:63+3*e,6
1+3*e:63+3*e)+KselementDSU_T(4:6,4:6);
Ktopside(37+6*e:39+6*e,61+3*e:63+3*e)=Ktopside(37+6*e:39+6*e,6
1+3*e:63+3*e)+KselementDSU_T(1:3,4:6);
Ktopside(61+3*e:63+3*e,37+6*e:39+6*e)=Ktopside(61+3*e:63+3*e,3
7+6*e:39+6*e)+KselementDSU_T(4:6,1:3);
end
% Adding forces on the topside

Fdeck=zeros(3*21,1);
Fdeck_exc=[-1.3594e+07 -1.3594e+07 -1.4954e+07 -1.6313e+07 -
2.1751e+07 -2.1751e+07 -1.9032e+07 -1.3594e+07 -1.3594e+07 -
1.4954e+07 -1.6313e+07 -2.1751e+07 -2.1751e+07 -1.9032e+07 -
1.3594e+07 -1.3594e+07 -1.4954e+07 -1.6313e+07 -2.1751e+07 -
2.1751e+07 -1.9032e+07];

for i=1:21
Fdeck(-1+3*i)=Fdeck(-1+3*i)+Fdeck_exc(i);
end

Ftopside=[Fdeck;Fdsf];
```

```
% Adding connection between skidbox and barge
Ktopside(3*d+1:3+3*k+3*d,3*d+1:3+3*k+3*d)=Ktopside(3*d+1:3+3*k
+3*d,3*d+1:3+3*k+3*d)+diag(kcon_list);
%% Model quay


Kquay=zeros(3*q);

for i=1:q-1
Quay_element=[AE(i)/Lq(i) 0 0 -AE(i)/Lq(i) 0 0;
    0 (12*EIq(i)/(Lq(i)^3))+kquay(i) 6*EIq(i)/Lq(i)^2 0 -
12*EIq(i)/Lq(i)^3 6*EIq(i)/Lq(i)^2;
    0 6*EIq(i)/Lq(i)^2 4*EIq(i)/Lq(i) 0 -6*EIq(i)/Lq(i)^2
2*EIq(i)/Lq(i);
    -AE(i)/Lq(i) 0 0 AE(i)/Lq(i) 0 0;
    0 -12*EIq(i)/Lq(i)^3 -6*EIq(i)/Lq(i)^2 0
(12*EIq(i)/(Lq(i)^3))+kquay(i) -6*EIq(i)/Lq(i)^2;
    0 6*EIq(i)/Lq(i)^2 2*EIq(i)/Lq(i) 0 -6*EIq(i)/Lq(i)^2
4*EIq(i)/Lq(i)];
Kquay(-2+3*i:3*i+3,-2+3*i:3*i+3)=Kquay(-2+3*i:3*i+3,-
2+3*i:3*i+3)+Quay_element;

end

Fquay=zeros(3*q,1);

%% MODEL BARGE


   %Input
    Lb=1.25*ones(j,1);
    %hydrostatic force along the barge

    khydro=zeros(j,1);
    khydro(1:124)=1025*9.81*63;
    khydro(124:208)=1025*9.81*42;
    %%%%%%%%%%%%%%%%%%%%%%%%%%%%%%%%%%%%%%%%%%%%%%%%%%%%BALLAST
% if spring==1;
% ball=zeros(j+1,1);
% elseif spring==2;
% %  Ballast forces
% ball(1:17,1)=bal(1);
% ball(18:37,1)=bal(2);
% ball(38:57,1)=bal(3);
% ball(58:77,1)=bal(4);
% ball(78:97,1)=bal(5);
% ball(98:117,1)=bal(6);
% ball(118:137,1)=bal(7);
% ball(138:157,1)=bal(8);
% ball(158:177,1)=bal(9);
% ball(178:197,1)=bal(10);
```

```
% ball(198:209,1)=bal(11);
% else
%    ball(1:17,1)=Ball(1,2);
% ball(18:37,1)=Ball(2,2);
% ball(38:57,1)=Ball(3,2);
% ball(58:77,1)=Ball(4,2);
% ball(78:97,1)=Ball(5,2);
% ball(98:117,1)=Ball(6,2);
% ball(118:137,1)=Ball(7,2);
% ball(138:157,1)=Ball(8,2);
% ball(158:177,1)=Ball(9,2);
% ball(178:197,1)=Ball(10,2);
% ball(198:209,1)=Ball(11,2);
%
% end
%%%%%%%%%%%%%%%%%%%%%%%%%%%%%%%%%%%%%%%%%%BALLAST
    qb=W+Ballast(:,x)-cor;
%qb=W-cor;
%%%%%%%%%%%%%%%%%%%%%%%%%%%%%%%%%%%%%%%%%%%%%BAllast
    %Matrix forming
    Kbarge=zeros(3+3*j);
    Fbarge=zeros(3+3*j,1);
    Fbal=zeros(3+3*j,1);
    %Barge is modeled with the hydrostatic springs already in
place, these dont
    %change during the load-out phase.
    for i=1:j
    %Constructing stiffness matrix and fill in elements
    Kbelement=[AE(i)/Lb(i)+kx(i)  0  0 -AE(i)/Lb(i)  0  0;
    0  (12*EIb(i)/(Lb(i)^3))+khydro(i)*Lb(i)*0.5
6*EIb(i)/Lb(i)^2  0  -12*EIb(i)/Lb(i)^3  6*EIb(i)/Lb(i)^2;
    0  6*EIb(i)/Lb(i)^2  4*EIb(i)/Lb(i)  0  -6*EIb(i)/Lb(i)^2
2*EIb(i)/Lb(i);
    -AE(i)/Lb(i)  0  0  AE(i)/Lb(i)  0  0;
    0  -12*EIb(i)/Lb(i)^3  -6*EIb(i)/Lb(i)^2  0
(12*EIb(i)/(Lb(i)^3))+khydro(i)*Lb(i)*0.5  -6*EIb(i)/Lb(i)^2;
    0  6*EIb(i)/Lb(i)^2  2*EIb(i)/Lb(i)  0  -6*EIb(i)/Lb(i)^2
4*EIb(i)/Lb(i)];

    Kbarge(-2+3*i:3*i+3,-2+3*i:3*i+3)=Kbarge(-2+3*i:3*i+3,-
2+3*i:3*i+3)+Kbelement;


    %Constructing force vector and fill in elements

    %Felement=[-q(i)*L(i)/2; -q(i)*L(i)^2/12; -q(i)*L(i)/2;
q(i)*L(i)^2/12];
    Fbelement=[0; -qb(i)*Lb(i)/2; 0;0; -qb(i)*Lb(i)/2; 0];
    Fbarge(-2+3*i:3*i+3)=Fbarge(-2+3*i:3*i+3)+Fbelement;
    end
    % APPLY MOMENT AT DEADMAN ANCHOR AND AT SKIDBOX.
```

```
    %at skidbox
    if x<=61
    Fbarge(3:3:3*x)=-5.4540*10^6;
    else
        Fbarge(3*x-3*60:3:3*x)=-5.4540*10^6;
    end
%     %at deadman anchor
    Fbarge(119*3:3:131*3)=3.3610*10^7;

%%%%%%%%%%%%%%%%%%%%%%%%%%%%%%%%%%%%%%%%%%%%%%%%%%%%%%%%%%%%%%%%%%%%%%%BA
LLAST
%     %%%apply ballast
%   for i=1:j+1
%    Fbal(-1+3*i)=Fbal(-1+3*i)+ball(i);
%  end
% Fbal(2)=Fbal(2)*0.5;
% Fbal(626)=Fbal(626)*0.5;
% Fbarge=Fbarge+Fbal;
%
%%%%%%%%%%%%%%%%%%%%%%%%%%%%%%%%%%%%%%%%%%%%%%%%%%%%%%%%%%%%%%%%%%%%%%%%%
%%%%%BALLAST
    Db=Kbarge\Fbarge;
    BargeSelf=Db(2:3:3+3*j);
%% MODEL TOTAL SYSTEM
%
Ksys=zeros(6+3*(k+j)+3*l);
Ksys(1+q*3:3+3*k+3*l,1+q*3:3+3*k+3*l)=Ktopside;
Ksys(1:q*3,1:q*3)=Kquay;


%Model system over time, x represent number of connections
between barge
%and skidbox, model valid until step 6
if x<=61
kcon_con=kcon_list(3+3*k-(3*x-1):3+3*k);
%only not applicable for full contact so x=61 or 1 contact
correct with if
%loop
        if x==1 || x==k+1
            kcon_con(1)=kcon_con(1);
        else
        kcon_con(1)=kcon_con(1)*0.5;
        end

Kcon_upper=diag(-kcon_con,-3-3*k+3*x);
Kcon_upper2=zeros(3+3*k+3*l,3+3*j);
Kcon_upper2(1+3*l:3+3*k+3*l,1:3+3*k)=Kcon_upper2(1+3*l:3+3*k+3
*l,1:3+3*k)+Kcon_upper;
Kcon_lower2=transpose(Kcon_upper2);
Kcon_barge=diag(kcon_con);
Kbarge(1:3*x,1:3*x)=Kbarge(1:3*x,1:3*x)+Kcon_barge;
```

```
%connecting quay and DSF
Kcon_quay_upper=zeros(3*q,3+3*k);
diag_kcon_quay=diag(-kcon_list,-3*x);
Kcon_quay_upper=Kcon_quay_upper+diag_kcon_quay(1:3*q,1:3+3*k);
Kcon_quay_lower=transpose(Kcon_quay_upper);

%adding kcon to quay
Kcon_quay=zeros(3*q);
diagkquay=diag(kcon_list);
kconquay=diagkquay(1:3*q-3*x,1:3*q-3*x);
Kcon_quay(3*x+1:3*q,3*x+1:3*q)=Kcon_quay(3*x+1:3*q,3*x+1:3*q)+
kconquay;
Kquay=Kquay+Kcon_quay;


else
    Kcon_upper=diag(-kcon_list);
    Kcon_barge=diag(kcon_list);
    Kcon_upper2=zeros(3+3*k+3*l,3+3*j);
    %adding to total upper corner
    Kcon_upper2(1+3*l:3+3*k+3*l,-2+3*(x-60):3+3*k+3*(x-60)-
3)=Kcon_upper2(1+3*l:3+3*k+3*l,-2+3*(x-60):3+3*k+3*(x-60)-
3)+Kcon_upper;
    %transposing to lower left
    Kcon_lower2=transpose(Kcon_upper2);
    %Filling the interconnections into barge matrix diagonals
    Kbarge(-2+3*(x-60):3*(x-60)+3*k,-2+3*(x-60):3*(x-
60)+3*k)=Kbarge(-2+3*(x-60):3*(x-60)+3*k,-2+3*(x-60):3*(x-
60)+3*k)+Kcon_barge;
 %still fill in kqconquay otherwise it gives an error later
    Kcon_quay_upper=zeros(3*q,3+3*k);
    Kcon_quay_lower=transpose(Kcon_quay_upper);
end

%Filling the interaction matrices into the systemmatrix
Ksys(4+3*k+3*l:6+3*(k+j)+3*l,1:3+3*k+3*l)=Ksys(4+3*k+3*l:6+3*(
k+j)+3*l,1:3+3*k+3*l)+Kcon_lower2;
Ksys(1:3+3*k+3*l,4+3*k+3*l:6+3*(k+j)+3*l)=Ksys(1:3+3*k+3*l,4+3
*k+3*l:6+3*(k+j)+3*l)+Kcon_upper2;
Ksys(4+3*k+3*l:6+3*(k+j)+3*l,4+3*k+3*l:6+3*(k+j)+3*l)=Kbarge;

Ksys(1:3*q,3*(q+d)+1:3*l+3+3*k)=Ksys(1:3*q,3*(q+d)+1:3*l+3+3*k
)+Kcon_quay_upper;
Ksys(3*(q+d)+1:3*l+3+3*k,1:3*q)=Ksys(3*(q+d)+1:3*l+3+3*k,1:3*q
)+Kcon_quay_lower;
Ksys(1:3*q,1:3*q)=Ksys(1:3*q,1:3*q)+Kquay;


Fsys=[Fquay;Ftopside;Fbarge];
Dsys=Ksys\Fsys;
```

```
Ksysinv=inv(Ksys);
DsysBarge=Dsys(4+3*k+3*l:6+3*k+3*j+3*l);
DsysSkid=Dsys(1+3*l:3+3*k+3*l);
DsysQuay=Dsys(1:3*q);
DsysTopside=Dsys(1+3*q:3*q+3*d);



%% Calculate System Displacements

    w_barge=DsysBarge(2:3:3+3*j);

    theta_barge=DsysBarge(3:3:3+3*j);
    w_skid=DsysSkid(2:3:3+3*k);
    theta_skid=DsysSkid(3:3:3+3*k);
    Length_skid=(0:1.25:75)';
    Length_barge=(0:1.25:260)';
    w_quay=DsysQuay(2:3:3*q);
    theta_upperbar=DsysTopside(3*21+3:3:3*25);

%%%%%%%%%%%%%%%%%%%%%%%%%%%%%%%%%%%%%%%%%%%%%%%%%%%%%%%%%%%%BALLA
ST
% %%%Optimization
%
KoptBarge=Ksysinv(4+3*k+3*l:6+3*(k+j+l),4+3*k+3*l:6+3*(k+j+l))
;
% Kop=KoptBarge(2:3:3+3*j,2:3:3+3*j);
% Kop(:,1)=Kop(:,1).*0.5;
% Kop(:,209)=Kop(:,209).*0.5;
% Kopt(:,1)=sum(Kop(:,1:17),2);
% Kopt(:,2)=sum(Kop(:,18:37),2);
% Kopt(:,3)=sum(Kop(:,38:57),2);
% Kopt(:,4)=sum(Kop(:,58:77),2);
% Kopt(:,5)=sum(Kop(:,78:97),2);
% Kopt(:,6)=sum(Kop(:,98:117),2);
% Kopt(:,7)=sum(Kop(:,118:137),2);
% Kopt(:,8)=sum(Kop(:,138:157),2);
% Kopt(:,9)=sum(Kop(:,158:177),2);
% Kopt(:,10)=sum(Kop(:,178:197),2);
% Kopt(:,11)=sum(Kop(:,198:209),2);
%
% lb=[-5727944*1.25;-8852240*1.25;-9075466*1.25;-
9066618*1.25;-6236668*1.25;-9018353*1.25;-5930194*1.25;-
5919325*1.25;-5918118*1.25;-2166705*1.25;-4136913*1.25];
% ub=[0;0;0;0;0;0;0;0;0;0;0];
% A =[];
% b =[];
% Aeq =Kopt(1,:);
% beq =-w_barge(1);
% bal=lsqlin(Kopt,-w_barge,A,b,Aeq,beq,lb,ub);
% Ball(1:11,spring+1)=bal;
```

```
%%%%%%%%%%%%%%%%%%%%%%%%%%%%%%%%%%%%%%%%%%%%%%%%%%%%%%%%%BALLAS
T
%% ITEST
if x<=61
w_wood=w_skid(k+1-x+1:k+1)-w_barge(1:x);
kade=w_skid(1:k+1-x)-w_quay(x+1:q)<=0;
bak=w_wood<=0;
z(k+1-x+1:k+1,spring+1)=bak;
z(1:k+1-x,spring+1)=kade;
else
    w_wood=w_skid-w_barge((x-60):(x-60)+k);
    bak=w_wood<=0;
    z(1:k+1,spring+1)=bak;
end
%for
optimization%%%%%%%%%%%%%%%%%%%%%%%%%%%%%%%%%%%%%%%%%%%BALLAST
% z(:,2)=1;
   end
```

Appendix B: Topside configuration

The method for transforming the 3-D topside plus the deck support frame into a 2-D representation will be explained in this appendix. First let's take a look at the topside. As could be seen in chapter 4 the topside can be simplified into a 3 level framework. The side and front view of the topside will be shown again here, now with numbering added for the elements. The vertical member numbering is in red and the diagonal numbering is in purple.

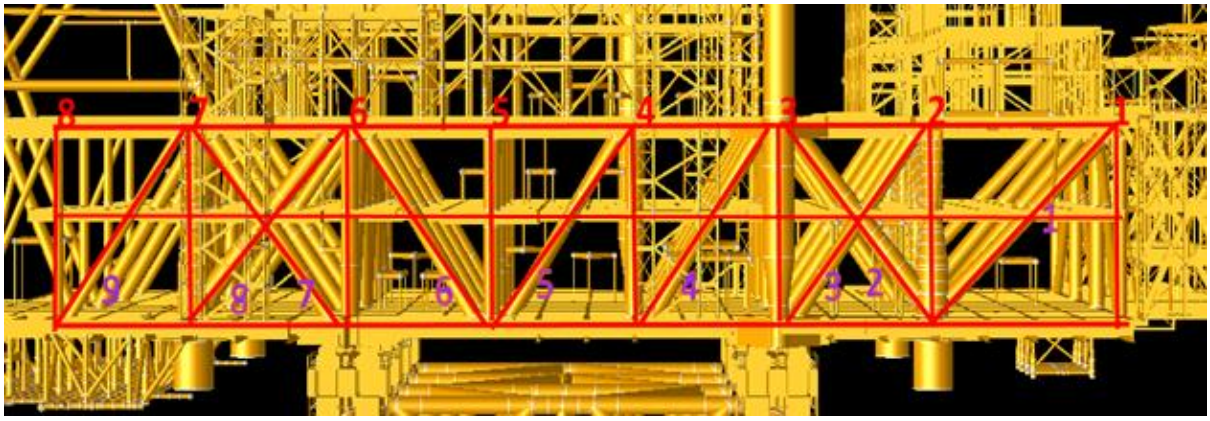

Figure A-1 Side view topside

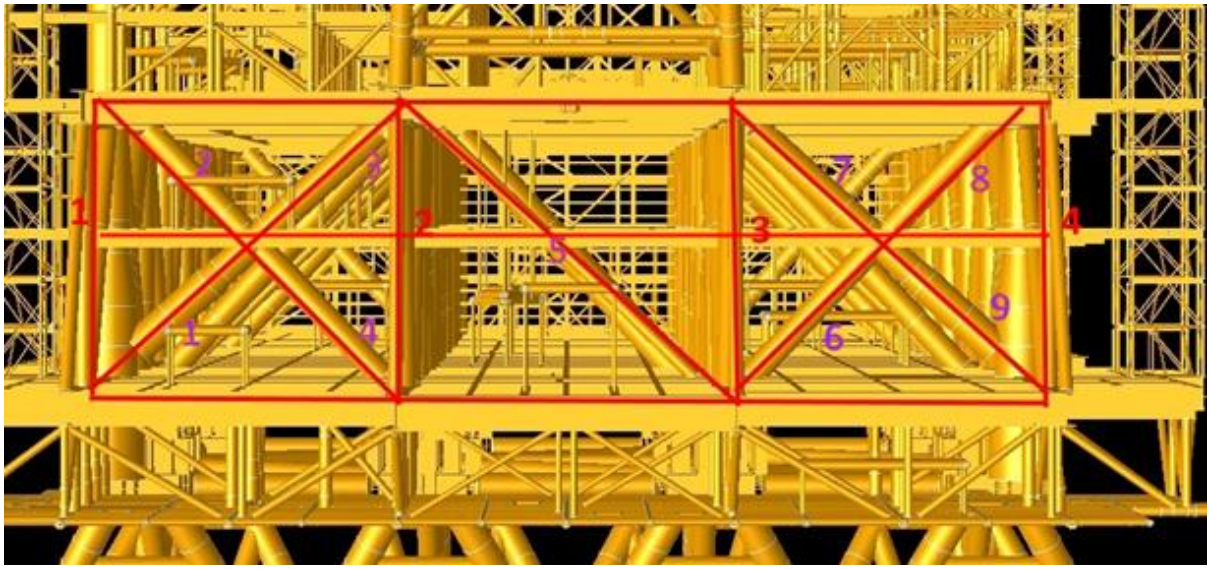

Figure A-2 Front view topside

The front view will be the 2-D projection of the topside which will be used in the model. So for example vertical member 1 of the front side needs to represent vertical members 1-8 and diagonal member 1-9 from the side view. The characteristics of each member in which we are interested, are the moment of inertia and the cross sectional area. The method chosen to make the front view projection an appropriate representation of the 3-D topside is the principle of superposition. So in the example of vertical member 1 in the front view, this means that the values for *EI* and *A* of vertical members 1-8 and diagonal members 1-9 in the side view are added to give the representation of vertical member 1 in the front view. This process is repeated for vertical members 2-4 in the front view and their respective corresponding members in the side view.

For the diagonal members in the front view the process will be the same. Their respective corresponding diagonal members are in the plane of vertical members 1-8 of the side view. For diagonal 2,4,6 and 8 there are only 2 corresponding members to be super positioned. These are in the plane of vertical member 2 and 7 of the side view.

The diagonal members in the front view are given the values seen in Table A-1. Each diagonal is represented by superposition of all the 7 layers deep diagonals since as can be seen in the side view the 8th layer doesn't have any diagonals.

Table A-1 Diagonal members front view

	side 1	side 2	side 3	side 4	side 5	side 6	side 7	Total I/A	EI/EA
Diagonal 1 I	72972399	1.67E+08	72972399	3151379	3151379	72972398.94	166906534	559033023	1.11807E+12
Diagonal 1 A	1479.69	2160.63	1479.69	289.6156	289.6156	1479.69014	2160.6303	9339.5623	1.86791E+11
Diagonal 2 I	0	64566986	0	0	0	0	64566986	129133972	2.58268E+11
Diagonal 2 A	0	1498.343	0	0	0	0	1498.3433	2996.6867	59933733849
Diagonal 3 I	72972399	1.53E+08	72972399	3151379	3151379	84335048.69	152935808	542454222	1.08491E+12
Diagonal 3 A	1479.69	2481.073	1479.69	289.6156	289.6156	1720.807376	2481.0728	10221.564	2.04431E+11
Diagonal 4 I	0	64566986	0	0	0	0	64566986	129133972	2.58268E+11
Diagonal 4 A	0	1498.343	0	0	0	0	1498.3433	2996.6867	59933733849
Diagonal 5 I	79407367	3151379	79407367	3151379	3151379	79407367.1	3151379.5	250827619	5.01655E+11
Diagonal 5 A	1479.69	289.6156	1479.69	289.6156	289.6156	1479.69014	289.61557	5597.5327	1.11951E+11
Diagonal 6 I	0	64566986	0	0	0	0	64566986	129133972	2.58268E+11
Diagonal 6 A	0	1498.343	0	0	0	0	1498.3433	2996.6867	59933733849
Diagonal 7 I	72972399	1.53E+08	72972399	3151379	3151379	72972398.94	152935808	531091572	1.06218E+12
Diagonal 7 A	1479.69	2481.073	1479.69	289.6156	289.6156	1479.69014	2481.0728	9980.4472	1.99609E+11
Diagonal 8 I	0	64566986	0	0	0	0	64566986	129133972	2.58268E+11
Diagonal 8 A	0	1498.343	0	0	0	0	1498.3433	2996.6867	59933733849
Diagonal 9 I	72972399	1.67E+08	84335049	3151379	3151379	84335048.69	166906534	581758323	1.16352E+12
Diagonal 9 A	1479.69	2160.63	1720.807	289.6156	289.6156	1720.807376	2160.6303	9821.7967	1.96436E+11

The vertical members in the front view are calculated in Table A-2, each vertical member in the front view is the superposition of all diagonals and vertical members behind it..

Table A-2

van heli naar flare	verti 1	verti 2	verti 3	verti 4	verti 5	verti 6	verti 7	verti 8
Vertical 1	23390527	1.67E+08	1.21E+08	78681482	78681482	120963065.9	166906534	17542895
Vertical 2	23390527	1.21E+08	1.21E+08	72972399	78681482	120963065.9	120963066	17542895
Vertical 3	23390527	1.21E+08	1.21E+08	72972399	78681482	120963065.9	120963066	17542895
Vertical 4	23390527	1.67E+08	1.21E+08	78681482	78681482	120963065.9	166906534	17542895
A vertical 1	772.8318	2160.63	1940.719	1600.445	1600.445	1940.718862	2160.6303	305.2
A vertical 2	772.8318	1940.719	1940.719	1479.69	1600.445	1940.718862	1940.7189	305.2
A vertical 3	772.8318	1940.719	1940.719	1479.69	1600.445	1940.718862	1940.7189	305.2
Avertical 4	772.8318	2160.63	1940.719	1600.445	1600.445	1940.718862	2160.6303	305.2

Diag 1	Diag 2	Diag 3	Diag 4	Diag 5	Diag 6	Diag 7	Diag 8	Diag 9	TOTAAL	EI/EA
50422071.22	1.21E+08	50422071	40744999	28887435	40744999	40744999	1.21E+08	20785393	1288713686	2.5774E+12
50422071.22	50422071	50422071	40744999	28887435	40744999	40744999	50422071	40744999	1069995284	2.14E+12
50422071.22	50422071	50422071	40744999	28887435	40744999	40744999	50422071	40744999	1069995284	2.14E+12
50422071.22	1.21E+08	50422071	40744999	28887435	40744999	40744999	1.21E+08	20785393	1288713686	2.5774E+12
1158.462291	1940.719	1158.462	929.9114	962.1128	929.9114	929.9114	1940.719	421.8	22853.6298	4.5707E+11
1158.462291	1158.462	1158.462	929.9114	962.1128	929.9114	929.9114	1158.462	929.9114	21236.6501	4.2473E+11
1158.462291	1158.462	1158.462	929.9114	962.1128	929.9114	929.9114	1158.462	929.9114	21236.6501	4.2473E+11
1158.462291	1940.719	1158.462	929.9114	962.1128	929.9114	929.9114	1940.719	421.8	22853.6298	4.5707E+11

For the 3 deck level the values for EI and EA are given in Table A-3. Each deck level is also assigned a number which represent its cell (numbering from left to right), so lower deck 1 refers to the element in the lowest deck in the left cell.

Table A-3

Lower deck 1 Inertia*E	1.99187E+11
Lower deck 1 Area*E	4.25102E+11
Lower deck 2 Inertia*E	1.99187E+11
Lower deck 2 Area*E	4.25102E+11
Lower deck 3 Inertia*E	1.99187E+11
Lower deck 3 Area*E	4.25102E+11
Intermediate deck 1 Inertia*E	5.91E+10
Intermediate deck 1 Area*E	2.5088E+11
Intermediate deck 2 Inertia*E	5.91E+10
Intermediate deck 2 Area*E	2.5088E+11
Intermediate deck 3 Inertia*E	5.91E+10
Intermediate deck 3 Area*E	2.5088E+11
Upper deck 1 Inertia*E	1.81079E+11
Upper deck 1 Area*E	4.0104E+11
Upper deck 2 Inertia*E	1.81079E+11
Upper deck 2 Area*E	4.0104E+11
Upper deck 3 Inertia*E	1.81079E+11
Upper deck 3 Area*E	4.0104E+11

Appendix C: Quayside foundation stiffness

For the calculation of the quayside foundation stiffness a rough estimate is used for the value of *EI*. A foundation thickness of 160 cm is used, a thickness also used at the 2e Maasvlakte [3]. There isn't much data available about the exact quayside characteristics, so assumptions had to be made.

First assumptions were made about the concrete which is used for the quayside foundation. Reinforced concrete is usually used in construction, however the percentage of rebar isn't known. An initial estimate formula which is used in civil engineering to determine the amount of rebar is used in this case to determine the *EI* of the foundation. The level of armament is determined from the values in other quaysides. The level of armament used in this quayside is 2.5%. This value is almost the maximum amount of rebar which can be applied in concrete since it has no use to use more rebar. The reason for this is that the concrete pressure zone will fail before the steel rebar fails, so there is no use for more steel rebar.

For the *E*-modulus a rough approach is used which is also used in civil engineering: [3]

$$E_{reinforced\ concrete} = E_{concrete} * V_{concrete\,\%} + E_{steel} * V_{steel\%} = 49.1\ GPa$$

An important issue is what are the dimensions of the quayside foundation beam in terms of width? This means how wide is the section that contributes to the stiffness of the beam. Here a conservative approach is chosen in that the width chosen for the quayside foundation beam is equal to the width of the skidbeams which transfer the loads into the quayside foundation. The width of each of the 2 skidbeams is 7.66 meters.

So now that the dimensions are known the moment of inertia can be calculated using the equation below:

$$EI_{foundation} = E_{reinforced\ concrete} * \left(\frac{1}{12}\right) * 2 * 7.66 * 1.6^3 = 2.57 * 10^{11}\ Nm^2$$